Field-Scale Evaluation of Drinking Water Biofiltration

by

Amina K. Stoddart

Submitted in partial fulfilment of the requirements
for the degree of Doctor of Philosophy

at

Dalhousie University
Halifax, Nova Scotia
March 2017

TABLE OF CONTENTS

LIST OF TABLES ..... **vii**

LIST OF FIGURES ..... **x**

ABSTRACT ..... **xvi**

LIST OF ABBREVIATIONS AND SYMBOLS ..... **xvii**

ACKNOWLEDGMENTS ..... **xxii**

CHAPTER 1 INTRODUCTION **1**

1.1 Introduction **1**

1.2 Research Questions **4**

1.3 Research Objectives **5**

1.4 Thesis Organization **5**

CHAPTER 2 FULL-SCALE PRE-CHLORINE REMOVAL: IMPACT ON FILTER PERFORMANCE AND WATER QUALITY **7**

2.1 INTRODUCTION **8**

2.2 MATERIALS AND METHODS **9**

2.2.1 Source water and plant description 9

2.2.2 Conversion to biofiltration 11

2.2.3 Filter operation and performance parameters 12

2.2.4 General water quality parameters 13

2.2.5 Biomass 13

2.2.6 Disinfection by-products 14

2.3 RESULTS & DISCUSSION 14

2.3.1 Raw water quality 14

2.3.2 Biomass 15

2.3.3 Filter performance 16

2.3.4 Natural organic matter removal 20

2.3.5 Disinfection by-product formation 23

2.4 CONCLUSIONS 27

CHAPTER 3 BIOMASS EVOLUTION IN FULL-SCALE ANTHRACITE-SAND DRINKING WATER FILTERS FOLLOWING CONVERSION TO BIOFILTRATION 28

3.1 INTRODUCTION 29

3.2 MATERIALS AND METHODS 31

3.2.1 Sample Site 31

3.2.2 Biofilm Biomass Sampling and Analysis 32

3.2.3 Planktonic Biomass Sampling and Analysis 33

3.2.4 Biofilm Biomass Growth Rate 33

3.2.5 Statistical Analysis 34

3.3 RESULTS & DISCUSSION 34

3.3.1 Biomass Accumulation with respect to Operational Day 34

3.3.2 Biomass Accumulation with Respect to Filter Run Time 41

3.3.3 Biomass Accumulation Scales 44

3.4 CONCLUSIONS 47

CHAPTER 4 WATER QUALITY AND FILTER PERFORMANCE OF NUTRIENT-, OXIDANT- AND MEDIA-ENHANCED DRINKING WATER BIOFILTERS 48

ABSTRACT 48

4.1 INTRODUCTION 50

4.2 MATERIALS AND METHODS 52

4.2.1 Pilot Plant and Source Water Description 52

4.2.2 Chemical Methods 56

4.2.3 Microbiological Techniques 57

4.2.4 Biofilter Operational Parameters 57

4.2.5 Statistical and Data Analysis 58

4.3 RESULTS & DISCUSSION 59

4.3.1 Water Quality 59

4.4 CONCLUSIONS 79

CHAPTER 5 BACTERIAL COMMUNITY STRUCTURE IN NUTRIENT- AND OXIDANT-ENHANCED DRINKING WATER BIOFILTRATION 81

5.1 INTRODUCTION 82

5.2 MATERIALS AND METHODS 84

5.2.1 Source Water 84

5.2.2 Full- and pilot-scale plant configuration and operation 85

5.2.3 Chemical Methods 88

5.2.4 Microbiological Techniques 89

5.2.5 Statistical Analysis 91

5.3 RESULTS & DISCUSSION 92

5.3.1 Water Quality 92

5.3.2 Microbial Community 94

5.4 CONCLUSIONS 106

CHAPTER 6 APPLICATION OF PHOTOELECTROCHEMICAL CHEMICAL OXYGEN DEMAND TO DRINKING WATER 108

6.1 ABSTRACT 108

6.2 INTRODUCTION 109

6.3 MATERIALS AND METHODS 110

6.3.1 Model Compound Preparation 110

6.3.2 Surface Water Collection 112

6.3.3 Determination of Organic Carbon and UV Absorbance 113

6.3.4 peCOD Analysis 113

6.3.5 Determination of Theoretical Oxygen Demand (ThOD) 114

6.4 RESULTS AND DISCUSSION 115

6.4.1 Correlation between peCOD and ThOD 115

6.4.2 Model Compounds 117

6.4.3 Surface and Treated Waters 119

6.4.4 peCOD as a Biofiltration Performance Indicator 126

6.5 CONCLUSIONS 129

CHAPTER 7 CONCLUSIONS AND RECOMMENDATIONS 130

7.1 Conclusions 130

7.1.1 Research Question 1: Conversion to Biofiltration 131

7.1.2 Research Question 2: Biofiltration Process Monitoring Tools 131

7.2 Recommendations 134

7.2.1 Conversion from Direct Filtration to Direct Biofiltration 134

7.2.2 Tools to Evaluate Biofiltration Performance 135

7.2.3 Tools to Enhance Biofiltration Performance 137

REFERENCES 138

APPENDIX A – Supplementary Figures 156

APPENDIX B – Copyright Permission Letters 167

Chapter 2 167

Chapter 3 168

Chapter 4 169

Chapter 6 170

LIST OF TABLES

Table 2.1 Quarterly mean raw water pH, turbidity and temperature 15

Table 2.2 Quarterly mean ATP concentration for filtration and biofiltration..... 16

Table 2.3 Average daily finished water production, filter run time, filter loading rate, UFRV and clean-bed head loss for warm and cold water conditions. Standard deviations are given in parentheses..... 17

Table 2.4 Quarterly raw and filtered water DOC and TOC means for filtration and biofiltration 22

Table 3.1 Fitted model parameters for start-of-filter-cycle biomass with respect to operational day..... 37

Table 3.2 Fitted parameters for in-filter cycle biomass concentration with respect to filter run time 42

Table 4.1 Biofilter investigation study phases..... 55

Table 4.2. Average influent and effluent nutrient concentrations. ± represents the standard deviation of the data 60

Table 4.3 Paired comparisons of cellular ATP concentrations of interstitial water sampled at a media depth of 150 mm following 24 hours of filter run time at at all raw water temperatures and raw water temperatures ≥15°C 63

Table 4.4 Comparison of enhancement strategies for TOC, DOC and SUVA removal following 24 hours of filter run time at all raw water temperatures and raw water temperatures ≥15°C 66

Table 4.5 Comparison of enhancement strategies for THMfp and HAAfp following 24 hours of filter run time 68

Table 4.6 Paired comparisons of filtered water turbidity following 20, 40 and 60 hours of filter run time at all raw water temperatures and raw water temperature ≥15°C 72

Table 4.7 Paired comparisons of filtered water head loss following 20, 40 and 60 hours of filter run time at raw water temperature ≥15°C 78

Table 5.1 Average raw water and biofilter influent TOC, DOC, UV_{254} and SUVA values. ± represents the standard deviation of two triplicate measures. 84

Table 5.2 Average hydraulic loading rate, average unit filter run volume (UFRV), average empty bed contact time (EBCT) and average terminal head loss for the four monitored filter cycles. The ± represents the 95% confidence interval with n = 4 87

Table 5.3 Average effluent TOC, DOC, UV_{254} and SUVA for full- and pilot-scale biofilters. ± represents the standard deviation of the data with n = 8 (TOC, DOC) and n = 6 (UV_{254}, SUVA) 93

Table 5.4 Average effluent THMfp and HAAfp for full- and pilot-scale biofilters. ± represents the standard deviation of the data with (n = 4) 93

Table 5.5 Average relative abundance at the genus level for the four sampling events. Genera were selected for this table if relative abundance was >5% in any given biofilter in at least one of the sampling events. Values in parentheses represent the range of the data. 102

Table 5.6 Average richness, diversity and evenness for the four sampling events. Error bars indicate the 95% confidence interval of the data. 104

Table 6.1 Model organic compound descriptions 111

Table 6.2 Treatment train descriptions for four surface water treatment plants in Halifax, Nova Scotia, Canada 112

Table 6.3 peCOD , TOC, DOC, UV_{254} and peCOD/TOC ratio for four surface water treatment trains. All values are average with $n = 3$. 120

Table 6.4 Average raw water, post-coagulation/flocculation and post-biofiltration TOC, DOC and peCOD concentration. +/- represents the standard deviation of the data..... 126

LIST OF FIGURES

Figure 2.1 Raw water temperature profile for the study duration..... 10

Figure 2.2 JD Kline Water Supply Plant schematic 11

Figure 2.3 Pre-chlorine doses (dose) and clearwell total chlorine concentrations (residual) 12

Figure 2.4 Finished water chlorine doses for 2012, 2013 and 2014 12

Figure 2.5 Turbidity percentile plot for filtration and biofiltration for warm water conditions. Error bars represent the 95% confidence intervals..... 18

Figure 2.6 Turbidity percentile plot for filtration and biofiltration for cold water conditions. Error bars represent the 95% confidence intervals..... 18

Figure 2.7 Head loss percentile plot for filtration and biofiltration for warm water conditions (August 2012 and August 2014). Error bars represent the 95% confidence intervals 20

Figure 2.8 Head loss percentile plot for filtration and biofiltration for cold water conditions (January 2013 and January 2014). Error bars represent the 95% confidence intervals 20

Figure 2.9 Finished water total THM concentration for filtration and biofiltration 24

Figure 2.10 Finished water total HAA concentration for filtration and biofiltration 25

Figure 2.11 Total THM percentage reductions for various locations in the distribution system 26

Figure 2.12 Total HAA percentage reductions for various locations in the distribution system 27

Figure 3.1 Natural log transformed biofilter biomass (ng ATP/cm^3 media) at the start (0 hours of filter run time) and end (58-80 hours of filter run time) of a filter cycle 36

Figure 3.2 Measured and fitted natural log-transformed start-of-filter-cycle biomass concentration (ng ATP/cm^3 media) with respect to operational day 37

Figure 3.3 Measured planktonic biomass concentration of raw water and biofilter effluent with respect to operational day 41

Figure 3.4 Measured and fitted natural log-transformed in-filter cycle biomass concentration (ng ATP/cm^3 media) 42

Figure 3.5 Planktonic biomass concentration of biofilter influent and biofilter effluents for a single filter cycle. Error bars represent the 95% confidence interval of the data 44

Figure 3.6 Schematic of biomass accumulation scales. μ represents the specific biomass growth rate 45

Figure 4.1 Pilot plant schematic for biofilter investigation 54

Figure 4.2 Cellular ATP concentration of interstitial water samples at a media depth of 150 mm following 24 hours of filter run time at all raw water temperatures..... 62

Figure 4.3 Paired comparisons of cellular ATP concentration of interstitial water sampled at a media depth of 150 mm following 24 hours of filter run time at raw water temperatures ≥15°C..... 62

Figure 4.4 Paired comparisons of biofilter effluent turbidity following 20, 40 and 60 hours of filter run time 70

Figure 4.5 Paired comparisons of filtered water turbidity following 20, 40 and 60 hours of filter run time at raw water temperature ≥15°C..... 71

Figure 4.6 Paired comparisons of biofilter head loss following 20, 40 and 60 hours of filter run time 76

Figure 4.7 Paired comparisons of biofilter head loss following 20, 40 and 60 hours of filter run time at a raw water temperature of ≥15°C 77

Figure 5.1 Full- and pilot-scale treatment train schematic 87

Figure 5.2 Average biomass concentration as measured by ATP for full- and pilot-scale biofilter effluents. Error bars represent the 95% confidence interval of the data with n = 4 95

Figure 5.3 Microbial community composition at the phylum level for full- and pilot-scale biofilters. Abundances represent the average of the four sampling events. Unassigned phyla and phyla with abundance < 1% in all samples were excluded. 97

Figure 5.4 Relative abundance of classes of *Proteobacteria* in the microbial communities of full- and pilot-scale biofilters averaged for sampling events in May, June, July and August. 98

Figure 5.5 Microbial community composition at the order level for full- and pilot-scale biofilters for the four sampling events. Unassigned orders and orders with abundance <1% in all samples were excluded. 99

Figure 5.6 Weighted Unifrac PCoA plot for examining the impact of different enhancement strategies and seasonal variation in full- and pilot-scale biofilters for the four sampling events 105

Figure 6.1 Relationship between ThOD and peCOD for reference model compounds. Error bars represent the 95% confidence interval of the data with n = 3 116

Figure 6.2 Relationship between ThOD and peCOD for carboxylic acid model compounds. Error bars represent the 95% confidence intervals with $n = 3$ 116

Figure 6.3 between ThOD and peCOD for amino acid model compounds. Error bars represent the 95% confidence intervals with $n = 3$ 117

Figure 6.4 Relationship between TOC and peCOD for reference compounds. Error bars represent the 95% confidence intervals with $n = 3$ 118

Figure 6.5 Relationship between TOC and peCOD for carboxylic model compounds. Error bars represent the 95% confidence intervals with $n = 3$ 119

Figure 6.6 Relationship between TOC and peCOD amino acid model compounds. Error bars represent the 95% confidence intervals with $n = 3$ 119

Figure 6.7 Comparison of Pockwock Lake peCOD, TOC and DOC during treatment. Error bars represent 95% confidence intervals with $n = 3$ 122

Figure 6.8 Comparison of Fletcher Lake peCOD, TOC and DOC during treatment. Error bars represent 95% confidence intervals with $n = 3$ 124

Figure 6.9 Relationship between SUVA and peCOD for four surface water sources pre-, during and post-treatment 125

Figure 6.10 TOC, DOC and peCOD percentage removals for coagulation/flocculation and biofiltration 127

Figure 6.11 Filter 1 (top) and filter 2 (bottom) total peCOD, dissolved peCOD, TOC and DOC effluent concentration with respect to filter run time. 128

Figure A.1 Residuals analysis of natural log-transformed end-of-filter-cycle biomass concentration (ng ATP/cm^3 media) against temperature. Dashed lines represent the 5th and 95th percentiles of the data. 156

Figure A.2 Residuals analysis of natural log-transformed start-of-filter-cycle biomass (ng ATP/cm^3 media) against operational day. Dashed lines represent the 5th and 95th percentiles of the data. 157

Figure A.3 Residuals analysis of natural log-transformed end-of-filter-cycle biomass concentration (ng ATP/cm^3 media) against operational day. Dashed lines represent the 5th and 95th percentiles of the data. 158

Figure A.4 Residuals analysis of natural log-transformed end-of-filter-cycle biomass (ng ATP/cm^3 media) against temperature. Dashed lines represent the 5th and 95th percentiles of the data. 159

Figure A.5 THMfp in ambient and P-enhanced biofilters over time. 160

Figure A.6 THMfp in ambient and ambient (GAC-Cap) biofilters over time (T≥15°C) 160

Figure A.7 ATP concentration in ambient, P-enhanced, PN-enhanced and PNOx-enhanced anthracite-sand biofilters at the start of a filter cycle and at 48 hours into a filter cycle at the surface of the media (0 mm) and 150 mm into the media. Error bars represent the standard deviation of triplicate measures. 161

Figure A.8 Microbial community composition at the phylum level of full- and pilot-scale biofilters for sampling events in May, June, July and August. Unassigned phyla and phyla with abundance <1% in all samples were excluded. 162

Figure A.9 Relative abundance of classes of *Proteobacteria* in the microbial communities of full- and pilot-scale biofilters for sampling events in May, June, July and August. 163

Figure A.10 Microbial community composition at the order level for full- and pilot-scale biofilters for sampling events in May, June, July and August. Unassigned orders and orders with abundance <1% in all samples were excluded. 164

Figure A.11 Observed OTUs, Chao1 Index, and ACE for full- and pilot-scale biofilters. Indicators were calculated using the R package, Phyloseq without rarefaction. 165

Figure A.12 Rarefaction curves for pilot-scale biofilters for a) observed OTUs, b) Chao1 index and c) phylogenic diversity. The rarefaction depth was set at 3440 sequences per sample. 166

ABSTRACT

Natural organic matter (NOM) is a complex mixture of organic material ubiquitous in natural waters. NOM can affect nearly all aspects of drinking water treatment. It can exert a demand on treatment chemicals, promote regrowth in distribution systems and can form genotoxic and/or carcinogenic disinfection by-products (DBPs) when exposed to disinfectant. Biofiltration is one treatment strategy that has potential to provide additional removal of NOM following coagulation. In biofiltration, bacteria indigenous to the source water form biofilms on filter media and use organic material as an energy source. This type of biological treatment within a filter has advantages over filtration with relatively biologically inert granular media because of its potential to provide additional NOM removal through biodegradation.

This thesis investigated conversion of full-scale anthracite-sand drinking water filters to biofilters through the removal of prechlorination. Results showed that filters operated in direct filtration mode could be converted in this way to reduce DBP formation in the plant effluent and distribution system without compromising water quality or filter performance. Biomass monitoring using adenosine triphosphate (ATP) showed that filter media biomass increased as a result of conversion. Further interpretation of the biomass data with a growth model demonstrated that consistency in biomass sampling within the context of the operational state of the filter or following significant process changes was critical information for long-term performance assessment. A concurrent pilot-scale investigation tested nutrient, oxidant and filter media enhancement strategies with the goal of improving NOM removal and further reducing DBP formation. Results showed that nutrient and oxidant addition could increase the filter biomass and alter the microbial community, but would not improve NOM removal or further reduce DBP formation potential.

Ultimately, despite reductions in DBP formation and increases in biofilter biomass, NOM removal across the biofilters remained unchanged with conversion and enhancements, posing a challenge for process monitoring. A novel method to measure oxygen demand was optimized for use in a drinking water matrix and used to evaluate NOM removal and transformation in the biofilters.

LIST OF ABBREVIATIONS AND SYMBOLS

°C	Degrees Celsius
®	Registered trademark
ACE	Abundance-based coverage estimator
AOC	Assimilable organic carbon
APHA	American Public Health Association
ATP	Adenosine triphosphate
AWWA	American Water Works Association
BAC	Biologically activated carbon
BAF	Biologically active filtration
BDCM	Bromodichloroacetic acid
BDOC	Biodegradable dissolved organic carbon
BOM	Biodegradable organic matter
BRP	Biological respiration potential
C:N:P	Carbon: nitrogen: phosphorus molar ratio
cm	Centimeter
COD	Chemical oxygen demand
DBAA	Dibromoacetic acid
DBCM	Dibromochloroacetic acid

DBP	Disinfection byproduct
DBPfp	Disinfection byproduct formation potential
DCAA	Dichloroacetic acid
DNA	Deoxyribonucleic acid
DO	Dissolved oxygen
DOC	Dissolved organic carbon
EBCT	Empty bed contact time
EPS	Extracellular polymeric substances
FDA	Fluorescein diacetate
FRT	Filter run time
g	Gram
GAC	Granular activated carbon
h	Hour
HAA	Haloacetic acid
HAAfp	Haloacetic acid formation potential
JDKWSP	JD Kline Water Supply Plant
KHP	Potassium hydrogen phthalate
L	Liter
LED	Light emitting diode

MAC	Maximum acceptable concentration
MBAA	Monobromacetic acid
MCAA	Monochloracetic acid
mg	Milligram
mg/L	milligram per litre
MIB	2-Methylisoborneol
min	Minute
MLD	Million liters per day
Mn	Manganese
N	Nitrogen
NDMA	Nitrosodimethylamine
NF	Nanofiltration
ng	Nanogram
nm	Nanometer
NOM	Natural organic matter
NTU	Nephelometric turbidity unit
OTU	Operational taxonomic unit
Ox	Oxidant
P	Phosphorus

PCoA	Principal coordinate analysis
peCOD	Photoelectrochemical chemical oxygen demand
pg	Picogram
PO_4-P	orthophosphate as phosphorus
ppm	Parts per million
R^2	Coefficient of determination
RLU	Relative light units
SEC	Size exclusion chromatography
SUVA	Specific ultraviolet absorbance at 254 nanometers
TCAA	Trichloracetic acid
THM	Trihalomethane
THMfp	Trihalomethane formation potential
ThOD	Theoretical oxygen demand
TOC	Total organic carbon
UF	Ultrafiltration
UFRV	Unit filter run volume
UV	Ultraviolet
UV_{254}	Ultraviolet absorbance at 254 nanometers
µA	Microampere

μC	Microcoulomb
μm	Micrometer
α	Significance level
σ	Standard deviation

ACKNOWLEDGMENTS

I would like to thank my supervisor, Dr. Graham Gagnon, for giving me this opportunity in the first place, for always countering my doubts with so much optimism and enthusiasm, and for being incredibly supportive of my overall professional development. I would also like to thank my supervisory committee, Dr. Jennie Rand and Dr. Su-Ling Brooks, for their valuable input throughout my research program.

The biggest thank you to Jessica Campbell for always going above and beyond to support this research. Thank you to the CWRS team, past and present: Heather Daurie, Elliot Wright, Brad Vickars, Ellen O'Hara, Dallys Serracin-Pitti, Amy McClintock, Matt Follett, Heather Granger, Megan Wood, Yamuna Vadasarukkai, Sarah Jayne Payne, John Bergese, Reese Williams, Lindsay Anderson and many, many others. Thank you to Jennie Rand and Alisha Knowles for being huge influences from the beginning.

My research program was supported with funding from the National Science and Engineering Research Council of Canada. Thank you to the partners of the NSERC/Halifax Water Industrial Research Chair in Water Quality and Treatment. Thank you so much Peter Flinn, and all of the staff at the JD Kline Water Supply Plant, for being so accommodating and making my time at Pockwock one of the best parts of my research program. Thank you Rob Menegotto for the opportunity to work so closely with you and your staff at MANTECH.

Thank you to my friends outside of the CWRS and family for the encouragement along the way. Most importantly, thank you Jordan—this wouldn't have been possible without you.

CHAPTER 1 INTRODUCTION

1.1 Introduction

Natural organic matter (NOM) is a complex mixture of organic material ubiquitous in natural waters. Sourced from both aquatic and terrestrial processes, NOM concentration and character varies both spatially and temporally in the environment (Krasner et al, 1996). Due to its complexity, NOM is typically quantified by its carbon content (i.e., total and dissolved organic carbon) and characterized by its bulk features such as hydrophobicity and molecular weight (Matilainen et al., 2011).

NOM can affect nearly all aspects of drinking water treatment. It can exert a demand on treatment chemicals, promote regrowth in distribution systems and can form genotoxic and/or carcinogenic disinfection by-products (DBPs) when exposed to disinfectant. To date, more than 600 DBPs have been identified in drinking water (Krasner et al., 2006). The most widely studied and regulated classes of DBPs are trihalomethanes (THMs) and haloacetic acids (HAAs).

Drinking water standards for THMs and HAAs are typically based on the sum of the individual compounds in each class. THMs refers to the total of chloroform, bromodichloromethane (BDCM), dibromochloromethane (DBCM) and bromoform, and HAAs typically refers to the total of monochloroacetic acid (MCAA), dichloroacetic acid (DCAA), trichlroacetic acid (TCAA), monobromoacetic acid (MBAA) and dibromoacetic acid (DBAA). Individual THM and HAA compounds typically occur in drinking water at the sub- to low-µg/L levels (i.e., MCAA, MBAA), low-µg/L levels (i.e., BDCM, DBCM, bromoform) or low- to mid-µg/L levels (chloroform, DCAA, CBAA, TCAA) (Richardson et al., 2007). The *Guidelines for Canadian Drinking Water Quality* currently indicate a maximum acceptable concentration (MAC) of 100 µg/L for THMs and 80 µg/L for HAAs "…based on a locational running annual average of a minimum of quarterly samples taken at the point in the distribution system with the highest potential [DBP] levels."

Many strategies are used to control THM and HAA formation in drinking water, including (1) the use of alternative disinfectants to replace chlorine, (2) the removal of THM and HAA precursors prior to disinfection and (3) the removal of THMs and HAAs after their formation. While the use of an alternative disinfectant (e.g., ozone, chloramines, chlorine dioxide) may reduce the formation of THMs and HAAs, it may promote the formation of other DBPs (e.g., bromate from ozone; nitrosodimethylamine (NDMA) from chloramines). In some cases, DBPs formed from alternative disinfectants may be more genotoxic than THMs and HAAs (Richardson et al., 2007). In addition, changeover from chlorine to chloramines has been associated with other adverse water quality outcomes such as increased potential for lead release from distribution systems (Switzer et al., 2006; Woszczynski et al. 2013).

The most common method to remove DBP precursors prior to disinfection is through conventional filtration (chemical coagulation-flocculation-sedimentation-filtration) (Jacangelo et al., 1995; Matilainen et al., 2010). To remove DBP precursors at these facilities, many utilities practice enhanced coagulation (i.e., coagulating at a higher coagulant dose than is required for turbidity/particle removal in order to maximize NOM removal) or optimized coagulation (i.e., coagulating at a pH and coagulant dose that controls multiple objectives including pathogens, turbidity, coagulant residuals and NOM) (Edzwald and Tobiason, 1999; Bell-Ajy et al., 2000). Enhanced or optimized coagulation has been shown to remove up to 30% more NOM than baseline coagulation conditions (Volk et al., 2000).

In general, coagulation removes hydrophobic and high molecular weight NOM to a greater extent than hydrophilic and low molecular weight NOM (White et al., 1997; Matilainen et al., 2010). In most waters, the hydrophobic fraction of NOM is the dominant precursor to both THM and HAA formation (Liang and Singer, 2003). However, in waters with a low hydrophobic content, the hydrophilic fraction may also represent an important precursor to DBP formation (Liang and Singer, 2003). In some waters, hydrophilic NOM may even have more reactivity toward DBP formation relative to other NOM fractions (Kwon et al., 2005). Other researchers have shown that the

reactivity of humic and nonhumic fractions is comparable when DBP formation is normalized to dissolved organic carbon (DOC) content (Owen et al., 1995).

Regardless of NOM fraction preference, even enhanced or optimized coagulation does not result in the removal of all NOM and NOM removal may be more challenging for specific treatment configurations. Treatment of low turbidity, low organic matter source water is often achieved using direct filtration (i.e., chemical coagulation-flocculation-filtration), which does not include a clarification step (e.g., sedimentation) prior to filtration. Without a clarification step, direct filtration plants may have less flexibility in design with respect to increasing coagulant doses, and managing the higher coagulant doses that may be required for adequate NOM removal may be a challenge. In cases where NOM removal achieved using enhanced or optimized coagulation is inadequate for control of DBP formation, additional treatment processes may be required.

Biofiltration is one treatment strategy that has potential to provide additional removal of NOM following coagulation. In biofiltration, bacteria indigenous to the source water form biofilms on filter media and use organic material as an energy source (Urfer et al., 1997). This type of biological treatment within a filter has advantages over filtration with relatively biologically inert granular media because of its potential to provide additional contaminant removal through biodegradation.

A typical barrier to having appreciable biological activity in granular media filters is prechlorination. Removal of prechlorination prior to filtration can initiate a passive and non-optimized biofiltration (i.e., passive biofiltration) process. In the case of targeting DBP formation, the benefit of removing prechlorination to initiate biofiltration may include a decrease in DBP formation as a result of less chlorine addition and biodegradation of DBP precursors.

Potential concerns for converting from filtration to passive biofiltration include poor particle removal and/or sloughing of biofilm resulting in elevated effluent turbidities, as well as rapid head loss development and/or underdrain clogging due to excessive biomass and extracellular polymeric substance (EPS) production. While there are full-scale

utilities that have converted filters to passive biofilters, water quality and filter performance information from these conversions is not typically disseminated (e.g. Water Research Foundation Project 4496).

The factors that affect NOM removal in biofilters have been extensively studied. Factors include NOM character, biomass concentration (Carlson and Amy, 1998), water temperature (Moll et al., 1999), empty bed contact time (EBCT), media type and backwash strategy (Urfer et al., 1997; Hozalski et al., 1999; Liu et al., 2001). In addition to these factors, more recently, nutrient availability has been studied as a factor that may impact biofiltration performance (Lauderdale et al., 2012; Lauderdale et al., 2014; Granger et al., 2014; Azzeh et al. 2014; McKie et al., 2015; Rahman et al., 2016). Recently, the desire to 'engineer' biofiltration processes by dosing nutrients and/or oxidants immediately prior to biofilters to enhance biological contaminant removal and improve hydraulic performance (i.e., engineered biofiltration) has governed drinking water biofiltration research.

Ultimately, biofiltration will be an important treatment process for water utilities to use to help manage drinking water quality standards, such as those for DBPs. Utilities will be increasingly interested in converting conventional filters to biofilters, increasing the need to understand the feasibility and potential unintended consequences of conversion. The recent shift from accepting biofiltration as a passive process to wanting to 'engineer' biofiltration will require a greater understanding of potential enhancement strategies, as well as the biofiltration microbiome itself. Additionally, as biofiltration becomes more widely used, a long-term challenge for the drinking water industry will be to develop monitoring tools to understand and improve process control for biofiltration.

1.2 Research Questions

This research was guided by the following research questions:

1. Can direct filters be converted to direct biofilters without negatively impacting filter performance?

2. What process monitoring tools can be used to understand and enhance biofiltration performance?

1.3 Research Objectives

Research questions were addressed through a series of objectives that focused on investigating conversion from direct filtration (chemical coagulation-flocculation-filtration) to direct biofiltration (chemical coagulation-flocculation-biofiltration) in a drinking water treatment plant. As part of this work, there was a need to address a knowledge gap surrounding process monitoring tools for optimizing biofiltration.

These objectives were as follows:

1. Determine if conversion from direct filtration to biofiltration can increase NOM removal and decrease DBP formation without negatively impacting filter performance;
2. Understand how converted biofilters acclimate biologically following conversion from direct filtration to biofiltration;
3. Investigate the use of nutrient, oxidant and media enhancement strategies to increase NOM removal and decrease DBP formation in biofilters;
4. Examine the effect of nutrient and oxidant enhancement strategies on the biomass quantity and microbial community structure in biofilters;
5. Assess the use of photoelectrochemical chemical oxygen demand as a drinking water treatment and biofiltration performance indicator.

1.4 Thesis Organization

Chapter 1 outlines the research rationale, research questions and research objectives.

Chapter 2 presents findings related to Objective 1, which involved examining water quality and filter performance at a full-scale drinking water treatment plant as it underwent conversion from direct filtration to direct biofiltration through removal or pre-

chlorination. A version of this work is published in *Journal American Water Works Association.*

Chapter 3 presents findings addressing Objective 2, which involved studying biomass acclimation at the same full-scale drinking water treatment plant as it underwent conversion from direct filtration to direct biofiltration through removal of pre-chlorination. A version of this work is published in *Journal American Water Works Association*.

Chapter 4 presents findings addressing Objective 3, which involved a pilot-scale investigation of the impact of nutrient and oxidant addition on biofilter effluent water quality and filter performance. A version of this work is in press at *Environmental Science: Water Research & Technology*.

Chapter 5 presents findings addressing Objective 4, which involved analyzing the biomass quantity and microbial community structure of full- and pilot-scale ambient biofilters and pilot-scale nutrient-, oxidant- and media-enhanced biofilters.

Chapter 6 presents findings related to Objective 5, which involved investigating the use of a novel chemical oxygen demand analyzer to understand NOM removal and transformation in drinking water treatment trains and biofiltration. A version of this work is published in *Journal American Water Works Association*.

Chapter 7 provides the conclusions and recommendations stemming from the overall research program.

CHAPTER 2 FULL-SCALE PRE-CHLORINE REMOVAL: IMPACT ON FILTER PERFORMANCE AND WATER QUALITY

ABSTRACT

Conversion from direct filtration to biofiltration in a full-scale drinking water treatment plant in Halifax, N.S., was assessed in terms of filter performance (e.g., turbidity, head loss) and water quality during a 48-month project. Conversion was achieved by removing pre-chlorination, with the overall objective of reducing disinfection by-product formation. As a result of pre-chlorine removal, it was hypothesized that the anthracite-sand filters would provide both particle removal and biological treatment in a single process step. When pre-chlorine was removed, adenosine triphosphate (ATP) concentrations on the filter media increased from ~50 to ~200–500 ng ATP/cm^3. Filter performance analysis revealed that conversion increased the filter effluent turbidity and reduced the filter head loss accumulation rate. Unit filter run volumes and filter run times were maintained. Water quality monitoring indicated that finished water disinfection by-product formation was reduced by ~10–20 µg/L for trihalomethanes and ~6–10 µg/L for haloacetic acids.[1]

---

[1]Note: A version of this chapter is published in *Journal American Water Works Association.*

Stoddart, A. K., & Gagnon, G. A. (2015). Full-Scale Pre-Chlorine Removal: Impact on Filter Performance and Water Quality. *Journal American Water Works Association*, 107 (12), E638-E647.

2.1 INTRODUCTION

Pre-chlorination is a common practice that many drinking water utilities use to provide disinfection, prevent biofilm growth in flocculation tanks and filters, enhance particle removal, increase filter run time, provide taste and odor control, and/or provide or assist in iron and manganese oxidation. However, chlorination before major treatment processes, such as coagulation/flocculation or filtration, can result in increased production of disinfection by-products (DBPs). DBP formation has been correlated with dissolved organic carbon (DOC), pH, temperature, and pre- and postfilter chlorination (McBean et al. 2010). However, in some cases, a shift from emphasizing pre-chlorination to post-chlorination has been shown to have the most impact on DBP formation as a result of the reduction in total organic carbon (TOC) and precursors in upstream treatment processes (McBean et al. 2010). Some utilities have successfully reduced trihalomethane (THM) formation by altering the pre-chlorination point to follow rather than precede major clarification steps (Blanck 1979, Harms & Looyenga 1977).

The main biological treatment processes for drinking water include slow sand filtration, riverbank filtration, rapid biofiltration (2–10 m/h) in direct filtration mode or following sedimentation, ozone-enhanced biofiltration, granular activated carbon biofiltration, and biological perchlorate/nitrate processes (Evans et al. 2010). Maintaining a disinfection residual in drinking water filters is one of the main distinctions between biofiltration and conventional filtration (Evans et al. 2010). Therefore, removal of pre-chlorination at a direct filtration drinking water treatment plant can be considered implementation of a passive and unoptimized rapid biofiltration process, assuming minimum nutrient and substrate requirements for biological growth are met. However, implementing biofiltration should be done with caution because, in some cases, biofiltration has been shown to result in higher effluent particle counts and reduced filter run times compared with pre-chlorinated filters (Goldgrabe et al. 1993). Other concerns when implementing biofiltration include potential operational issues such as bacteria and pathogen breakthrough (Evans et al. 2010).

The theoretical benefit of converting conventional filters to biofilters to reduce DBP formation can be twofold because pre- chlorination can increase DBP formation (e.g., McBean et al. 2010), and biodegradation can remove DBP precursors (e.g., Speitel et al. 1993). Furthermore, biofiltration has been applied to drinking water treatment to control many of the same contaminants as pre-chlorination, including taste and odor–causing compounds such as geosmin and 2-methylisoborneol (e.g., Elhadi et al. 2006) and manganese (e.g., Granger et al. 2014, Kohl & Dixon 2012, Mouchet 1992).

This study examined the removal of pre-chlorination and the subsequent shift to rapid biofiltration in the direct filtration mode at a direct filtration drinking water treatment plant in Nova Scotia, Canada. The goal of this study was to determine whether implementing biofiltration could reduce DBP formation and improve water quality (e.g., organic carbon removal) without negatively affecting filter operation (e.g., effluent turbidity, head loss, unit filter run volume [UFRV], filter run time). This full-scale analysis was carried out for 48 months (depending on the performance parameter) to consider temperature and seasonal water quality fluctuations.

2.2 MATERIALS AND METHODS

2.2.1 Source water and plant description

The JD Kline Water Supply Plant (JDKWSP) is a direct filtration drinking water treatment plant in Nova Scotia, Canada. Plant location results in a seasonal lake water temperature variation from ~1 to 23°C, with temperature maxima and minima occurring in August and January, respectively. Seasonal lake temperatures for the study duration are provided in Figure 2.1.

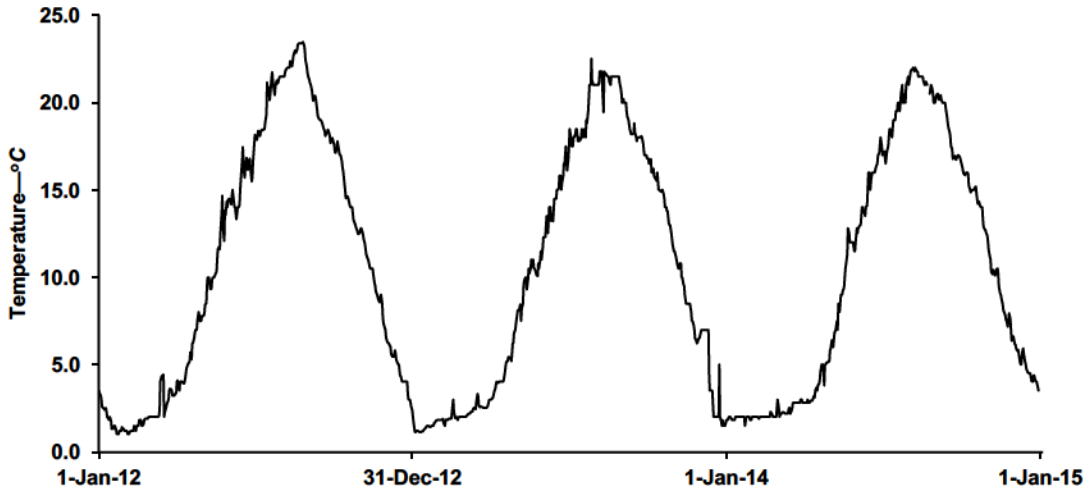

Figure 2.1 Raw water temperature profile for the study duration

The water treatment plant draws water from Pockwock Lake, which is characterized as a low-pH, low-turbidity, low-alkalinity, low-natural organic matter (NOM) source water (Vadasarukkai et al, 2011; Knowles et al, 2012). The exceptionally low pH (5.4-5.9) is a function of local geology, which provides limited buffering capacity (Ginn et al., 2007). Typical ammonia, total iron and total manganese concentrations for the study duration were <0.050 mg N/L, 0.054-0.061 mg/L and 0.035-0.045 mg/L, respectively (Halifax Water, 2013; Halifax Water, 2014). The water treatment plant has a design capacity of 227 ML/day but produced an average of 84 ± 4 ML/day over the filter performance study durations (August 2012 and 2013; January 2013 and 2014).

Surface water is drawn into the first of three pre-mix tanks where calcium hydroxide (lime) is added for pH adjustment, and potassium permanganate is added for oxidation of iron and manganese. Water then passes to the second premix tank, where additional mixing takes place, and then on to the final premix tank where carbon dioxide is used to adjust to the coagulation pH of 5.5-6, and aluminum sulfate is added for coagulation. In cold weather (typically late November to early June), cationic polymer is added (0.025 – 0.065 mg/L) as a flocculation aide. Rapid mix tanks are 4.0 m x 4.0 m x 5.8 m each (L x W x D) with a typical retention time of 1.1 minutes each. Water is then delivered to four identical flocculation trains where three-stage tapered hydraulic flocculation occurs.

More detailed information on flocculator flow characteristics is provided elsewhere (Vadasarukkai et al, 2011). Flocculation tanks are 5.0 m x 5.0 m x 7.8 m each (L x W x D) with a typical retention time of 22 minutes each. Water then passes directly to eight dual-media anthracite-sand (60 cm anthracite, 30 cm sand) filters (17.1 m x 8.5 m x 3.7 m; [L x W x D]). After filtration, water from filters 1, 3, 5 and 7 enters the west clearwell (4545 m^3), followed by a reservoir (13600 m^3) and then the east clearwell (4545 m^3). Water from filters 2, 4, 6 and 8 passes directly to the east clearwell. After the east clearwell, water enters a passive mixing chamber (356 m^3). At entrance of the passive mixing chamber, chlorine gas is added for disinfection (1.0-1.2 mg/L), sodium hydroxide is added for pH adjustment (pH 7.4), zinc-orthopolyphosphate is added for corrosion control (0.5 mg/L as PO_4), and hydrofluorosilicic acid is added for dental health. A schematic of this process is provided in Figure 2.2.

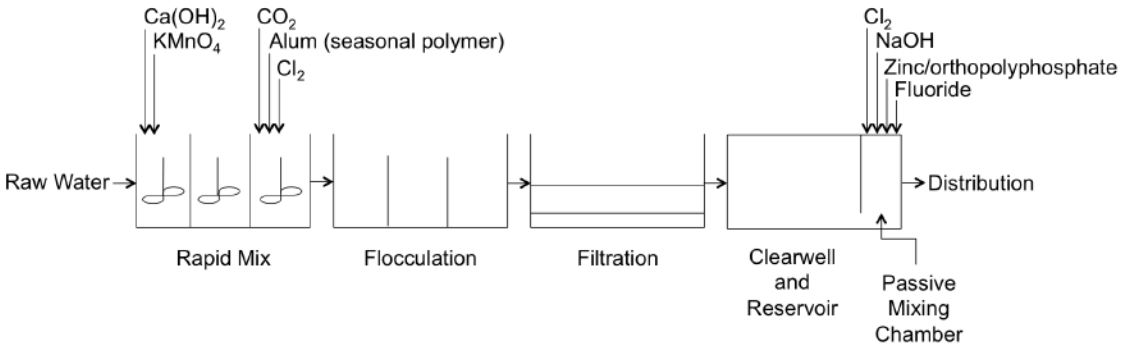

Figure 2.2 JD Kline Water Supply Plant schematic

2.2.2 Conversion to biofiltration

Prior to conversion to biofiltration in April 2013, chlorine was added in the third premix tank to maintain a post-filter total chlorine concentration of 0.05 mg/L. Operationally, this corresponded to a pre-chlorine dosage between approximately 0.5 and 1.8 mg/L from January 2012 to April 2013. Conversion to biofiltration occurred with a stepwise reduction in pre-chlorine dose over a 16-hour period beginning on April 3, 2013. Because JDKWSP uses water from the clearwell (total chlorine concentration target = 0.05 mg/L) for backwashing, removal of pre-chlorination also resulted in the removal of chlorinated

backwash. Historical pre-chlorine dosages between January 2012 to May 2013 and resulting post-filter total chlorine concentrations are provided in Figure 2.3. Historical finished water chlorine dose is provided in Figure 2.4.

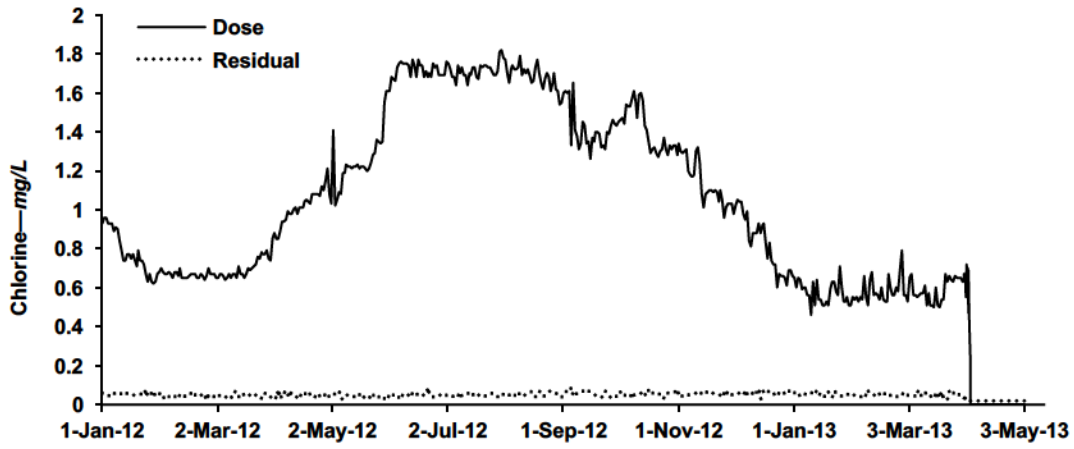

Figure 2.3 Pre-chlorine doses (dose) and clearwell total chlorine concentrations (residual)

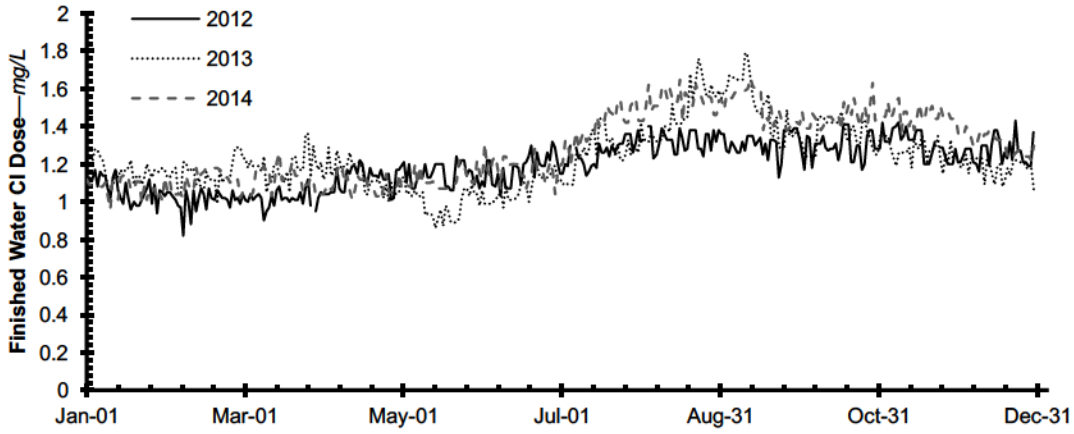

Figure 2.4 Finished water chlorine doses for 2012, 2013 and 2014

2.2.3 Filter operation and performance parameters

Per the operational criteria of the facility, filters were operated so they would not exceed an effluent turbidity of 0.2 NTU, a head loss of 2.15 m, or a filter run time of 80 hours.

Filter run time, UFRV, effluent turbidity, and head loss were used as performance indicators to assess the impact of pre-chlorine removal on filter performance. The JDKWSP has continuous monitoring for filter run time, effluent turbidity and head loss for all filters. It also has continuous particle count; however, only one filter had this capability, and it is not typically not used as an operational criterion at this facility. As a result, an analysis of these data was not conducted here. More information on particle count and size distribution at this facility is available elsewhere (O'Leary et al., 2003). Due to the large amount data generated, filter performance was assessed for warm and cold water conditions by averaging data from all filter runs occurring in August 2012 (n = 66) and August 2013 (n = 62) and all filter runs occurring in January 2013 (n = 56) and January 2014 (n = 66). These averages included all phases of the filter cycle (e.g., ripening, steady-state). This allowed for assessment of warm (22.5 ± 0.7°C for August 2012; 21.3 ± 0.5°C for August 2013) and cold (1.4 ± 0.3°C for January 2013; 1.9 ± 0.1°C January 2014) water conditions with and without pre-chlorination. As shown in Figure 2.1, these months also represented times when seasonal temperature plateaus occurred.

2.2.4 General water quality parameters

Total organic carbon (TOC) and DOC were monitored approximately weekly on raw, flocculated, and filtered water throughout the duration of the water quality study duration. TOC and DOC samples were collected headspace-free in baked (24 hours, 100°C) glass vials, acidified to pH < 2 with phosphoric acid, and analyzed using a TOC-V CPH analyzer (Shimadzu Corp, Kyoto, Japan).

2.2.5 Biomass

Biomass concentration was measured as adenosine triphosphate (ATP). ATP is a biochemical used by cells for energy storage and can thus be used as an indicator of the presence of active biomass (Evans et al, 2013a). Media samples were collected from the surface of the filter bed at the end of a filter cycle in sterile 50 mL falcon tubes. ATP was measured in triplicate on-site immediately after sampling using a commercially available

test kit (Deposit Surface Analysis, LuminUltra Technologies Ltd., Fredericton, Canada) following the manufacturer's instructions. In short, this method involved chemical removal of biofilm from a 1 g subsample of media followed by dilution of the resulting biofilm suspension, reaction with luciferase enzyme and quantification of the light emitted in relative light units (RLU) using a luminometer (PhotonMasterTM Luminometer, LuminUltra Technologies Ltd., Fredericton, Canada). To enable comparison among studies, media ATP concentrations were reported as mass ATP per unit volume of media (Pharand et al, 2014) using an anthracite density of 0.8 g/cm^3 after conversion from wet weight to dry weight using a correction factor. Correction factors were determined for each sample by weighing three subsamples before and after drying at 105°C for 24 hours. If no correction factor was available, an average correction factor of 0.60 (σ = 0.05) was used.

2.2.6 Disinfection by-products

Total trihalomethane (THM) and total haloacetic acids (HAA) concentrations were monitored approximately weekly on finished water. THMs and HAAs were detected using gas chromatography with electron capture (CP-3800 Gas Chromatograph, Varian, Inc., Walnut Creek, California) according to US EPA methods 551.1 and 552.2, respectively.

2.3 RESULTS & DISCUSSION

2.3.1 Raw water quality

Quarterly means with associated 95% confidence intervals for raw water pH, turbidity, and temperature are provided in Table 2.1. As shown in Table 2.1, raw water pH and turbidity were stable quarterly. Quarterly mean pH ranged from 5.29 to 5.89 over the study duration, whereas quarterly mean turbidity ranged from 0.27 to 0.54 NTU. Mean raw water temperature reached a minimum (~2°C) in the January-March quarters and a maximum (~20°C) in the July-September quarters; the April-June and October-December

quarters averaged 9-10°C. Overall, raw water pH and turbidity were stable over the study duration while temperature fluctuated seasonally. As a result, a quarterly analysis was used for subsequent ATP, DOC and TOC analysis.

Table 2.1 Quarterly mean raw water pH, turbidity and temperature

Year	Quarter	pH			Turbidity-*NTU*			Temperature-°C		
		Mean	95% CI	n	Mean	95% CI	n	Mean	95% CI	n
2012	Jan-Mar	5.29	0.03	91	0.42	0.01	91	2.1	0.2	91
	Apr-Jun	5.37	0.23	91	0.54	0.05	91	10.6	0.9	91
	Jul-Sep	5.63	0.21	91	0.48	0.04	92	20.5	0.4	92
	Oct-Dec	5.60	0.06	92	0.33	0.01	92	9.9	0.9	92
2013	Jan-Mar	5.51	0.05	90	0.27	0.01	90	1.9	0.1	90
	Apr-Jun	5.70	0.11	91	0.39	0.02	91	9.5	0.9	91
	Jul-Sep	5.82	0.06	92	0.42	0.01	92	19.6	0.3	92
	Oct-Dec	5.89	0.07	92	0.34	0.01	92	9.3	1.0	92
2014	Jan-Mar	5.44	0.02	90	0.33	0.00	90	2.2	0.1	90
	Apr-Jun	5.60	0.04	91	0.37	0.01	91	9.2	1.0	91
	Jul-Sep	5.85	0.06	92	0.40	0.01	92	19.6	0.4	90
	Oct-Dec	5.71	0.09	92	0.30	0.02	92	9.7	0.9	92

2.3.2 Biomass

Bioactivity was verified using ATP. ATP on granular activated carbon and sand media has been shown to correlate with total direct bacterial cell counts (Magic-Knezev and van der Kooij, 2004). It has also been used to assess when granular activated carbon (GAC) filters have become biologically active (i.e, conversion to biologically active carbon (BAF)) (Velten et al, 2011). As shown in Table 2.2, ATP concentrations increased by an order of magnitude when pre-chlorination was removed. Evans et al. (2013a) suggested that order of magnitude changes in ATP concentration over time indicate a significant change in the biological community within a biofilter. Although the increase also corresponded with an increase in raw water temperature, subsequent quarterly averages did not suggest that ATP concentrations were temperature-dependent. This finding was consistent with other full-scale findings in which ATP concentrations in anthracite-sand filters operated at 3-28°C did not show temperature dependence (Pharand et al. 2013).

Table 2.2 Quarterly mean ATP concentration for filtration and biofiltration

Year	Quarter	Mean—ng ATP/cm^3 media	95% CI	n
		Filtration		
2012/2013	-	56	31	2
		Biofiltration		
2013	**Apr-Jun***	288	93	18
	July-Sept	528	125	14
	Oct-Dec	429	202	11
2014	**Jan-Mar**	205	40	11
	Apr-Jun	305	59	16
	July-Sept	208	78	15
	Oct-Dec	353	98	5

*Quarter beginning after pre-chlorination removed

Subsequent quarterly mean ATP concentrations under biofiltration (non-chlorinated) conditions ranged from 205-528 ng ATP/cm^3 media. These values were in the operating range of 10^2-10^3 ng ATP/cm^3 media identified for acclimated biofilters by Pharand et al. (2014), indicating a comparable level of active biomass was attained.

2.3.3 Filter performance

Filter performance was assessed using daily finished water production, filter run time, filter loading rate, unit filter volume (UFRV), effluent turbidity and head loss. As summarized in Table 2.3, all biofiltration averages for daily finished water production, filter run time, filter loading rate, UFRV and clean-bed head loss fell within the standard deviation of filtration averages. This indicated that removal of pre-chlorination, and subsequent conversion to biofiltration, did not affect these parameters. Furthermore, there was no evidence that water temperature/season had an impact on production, filter run time, UFRV or clean-bed head loss, since all cold water averages for these parameters fell within the standard deviation of warm water averages.

Table 2.3 Average daily finished water production, filter run time, filter loading rate, UFRV and clean-bed head loss for warm and cold water conditions. Standard deviations are given in parentheses

Filter Parameter	Warm Water		Cold Water	
	Filtration Aug 2012	Biofiltration Aug 2013*	Filtration Jan 2013	Biofiltration Jan 2014*
Daily Finished Water Production-*ML*	84 (4)	82 (5)	86 (3)	83 (4)
Filter Run Time—*h*	66 (8)	68 (5)	71 (3)	68 (5)
Filter Loading Rate—*m/h*	3.3 (0.3)	3.7 (0.2)	3.6 (0.1)	3.7 (0.2)
UFRV—m^3/m^2	215 (24)	253 (18)	257 (13)	250 (15)
Clean-bed Head Loss –*m*	0.08 (0.09)	0.05 (0.04)	0.08 (0.05)	0.05 (0.05)

*Seven of eight filters in operation

Biofiltration—non-chlorinated

Filtration—pre-chlorinated

UFRV—unit filter run volume

Percentile plots showing the 10th, 50th, 75th, 90th, 95th and 98th percentiles were used to assess filter effluent turbidity. Per the *Canadian Drinking Water Guidelines* (Health Canada, 2014), direct filtration plants should achieve turbidity ≤0.3 NTU in at least 95% of measurements either per filter cycle or per month. As shown in Figure 2.5, this was achieved with filtration and biofiltration under both warm and cold water conditions. These guidelines also stipulate that filters should be designed and operated to reduce turbidity as low as reasonably achievable and strive to achieve a treated water turbidity of <0.1 NTU from individual filters.

As shown in Figure 2.5 and Figure 2.6, effluent turbidity increased with removal of pre-chlorine and subsequent conversion to biofiltration under both warm (Figure 2.5) and cold (Figure 2.6) water conditions. This is inconsistent with a pilot-scale study where no discernable difference in filtered water turbidity from pre-chlorinated anthracite-sand filters and anthracite-sand biofilters was identified (Goldgrabe et al, 1993). Before biofiltration, 95th percentile effluent turbidities were <0.1 NTU under both warm and cold water conditions. With biofiltration, 95th percentile effluent turbidities were <0.1 NTU at 0.081 NTU under warm water conditions, but slightly above 0.1 NTU at 0.107 NTU for cold water conditions. This is somewhat inconsistent with a full-scale study where

biological anthracite-sand filters always maintained turbidity <0.1 NTU, regardless of temperature (Emelko et al, 2006).

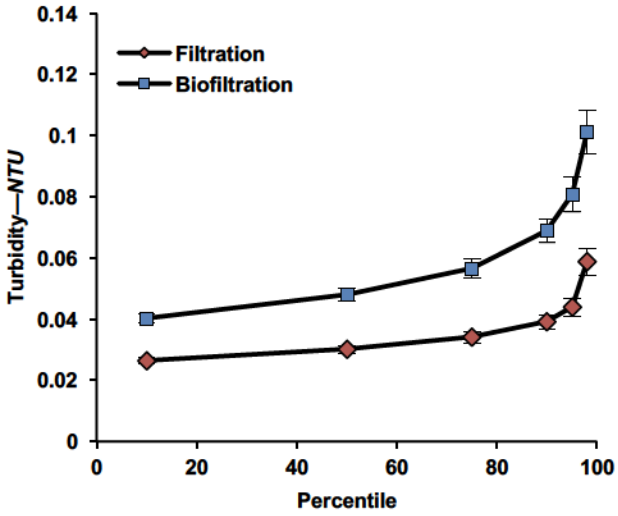

Figure 2.5 Turbidity percentile plot for filtration and biofiltration for warm water conditions. Error bars represent the 95% confidence intervals

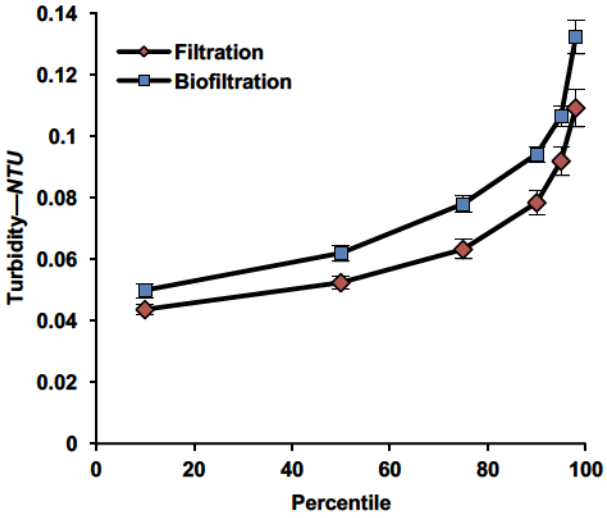

Figure 2.6 Turbidity percentile plot for filtration and biofiltration for cold water conditions. Error bars represent the 95% confidence intervals

Also shown in Figure 2.5 and Figure 2.6 is that cold water conditions resulted in higher effluent turbidity concentrations than warm water conditions for both filtration and biofiltration at all percentiles. However, since this occurred for both filtration and

biofiltration, it was likely the result of a reduction in coagulation and flocculation efficiency at low temperatures, which can be particularly marked for aluminum sulfate coagulation in low turbidity waters (Morris and Knocke, 1984). While polymer is added at this facility to mitigate this effect, it evidently does not completely overcome this challenge.

It was initially hypothesized that implementing biofiltration would increase head loss by decreasing filter porosity through biofilm growth on media (Goldgrabe et al, 1993) and that biofiltration warm water head loss would be greater than biofiltration cold water head loss as a result of higher activity levels and substrate loading in warmer months. As shown in Figure 2.7 and Figure 2.8, only the latter was true for this analysis. Percentile plots for head loss showed that average head loss decreased with conversion to biofiltration under both warm and cold water conditions. As expected, biofiltration head loss was higher under warm water conditions than under cold water conditions. DOC percent removal across the filter, raw water temperature and biofilm ATP concentrations for the corresponding July-September quarter (1.9%, 19.6°C and 528 ng ATP/cm^3, respectively) where higher than corresponding quarterly averages for the January-March quarter (0.4%, 2.2°C and 205 ng ATP/cm^3, respectively) possibly supporting this observation.

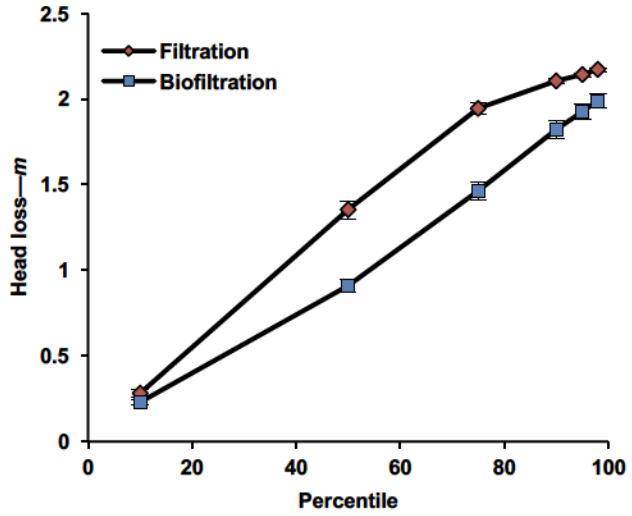

Figure 2.7 Head loss percentile plot for filtration and biofiltration for warm water conditions (August 2012 and August 2014). Error bars represent the 95% confidence intervals

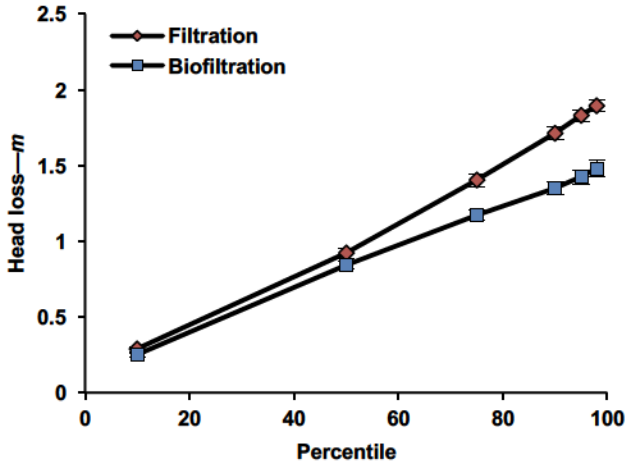

Figure 2.8 Head loss percentile plot for filtration and biofiltration for cold water conditions (January 2013 and January 2014). Error bars represent the 95% confidence intervals

2.3.4 Natural organic matter removal

Quarterly means for raw and filtered water TOC and DOC, as well as DOC percentage removals for filtration (pre-chlorinated) and biofiltration (non-chlorinated) are provided

in Table 2.4. Biofiltration performed similarly to filtration in terms of TOC and DOC removals. There was no statistical difference (p>0.05) in quarterly filtered water TOC and DOC means from 2012 to 2014, with the exception of the January-March quarter. However, quarterly means for raw water TOC and DOC were also consistent from 2012 to 2014 (p>0.05), with the exception of the January-March quarter. This indicated that raw water quality was consistent over the study duration with the exception of an increase in average raw water TOC and DOC in the 2014 January-March quarter. Since all other quarters showed consistent TOC and DOC removal performance between filtration and biofiltration, it was assumed that the increase in filtered water TOC and DOC in the 2014 January-March quarter was associated with the increase in raw water TOC and DOC and not attributable to implementing biofiltration.

As shown in Table 2.4, average quarterly DOC percent removals across the biofilter were limited at 0.7-4.6%, whereas DOC removals for the entire treatment train were much higher at 32-36%, indicating that the majority of the DOC removal was the result of the coagulation/flocculation processes. Notably, average quarterly DOC percent removals across the filter were higher for the July-September and October-December quarters (1.3-4.6%) than for the January-March and April-June quarters (0.4-0.7%). As shown in Table 2.1, average temperature was 19.6°C for both corresponding July-September quarters and 9.3-9.7°C for the corresponding October-December quarters. These temperatures were much higher than the corresponding January-March quarter (2.2°C); however, the April-June quarter had a similar average temperature to the October-December quarters at 9.2°C. With the exception of the 2013 July-September and October-December quarters, ATP concentrations were not discernibly higher for quarters that experienced higher DOC percent removals across the filter.

Table 2.4 Quarterly raw and filtered water DOC and TOC means for filtration and biofiltration

Year	Quarter	Raw Water						Filtered Water						Average Percent Removal	
		TOC			DOC			TOC			DOC			DOC	
		Mean	95% CI	n	Mean	95% CI	n	Mean	95% CI	n	Mean	95% CI	n	Filter	Total
Filtration															
2012	Apr-Jun	3.10	0.06	10	3.02	0.06	10	-	-	-	-	-	-	-	-
	Jul-Sep	2.76	0.22	10	2.76	0.19	10	1.96	0.46	2	1.82	0.01	2	-	-
	Oct-Dec	2.93	0.12	8	2.95	0.10	8	1.95	0.08	7	2.01	0.14	7	-	32
2013	Jan-Mar	3.08	0.07	5	3.06	0.07	5	1.98	0.13	5	1.98	0.10	5	-	35
Biofiltration															
2013	Apr-Jun	3.02	0.12	10	2.98	0.08	10	1.92	0.07	10	1.97	0.11	10	-	34
	Jul-Sep	2.92	0.10	8	2.85	0.06	8	1.94	0.08	9	1.92	0.07	9	1.9	33
	Oct-Dec	2.91	0.15	9	2.90	0.14	9	1.85	0.05	9	1.85	0.04	9	3.2	36
2014	Jan-Mar	3.33	0.05	18	3.26	0.06	17	2.18	0.05	18	2.16	0.03	17	0.4	34
	Apr-Jun	3.07	0.10	16	2.99	0.10	16	1.90	0.10	16	1.91	0.09	16	0.7	36
	Jul-Sep	2.85	0.06	16	2.94	0.09	16	1.94	0.16	16	1.89	0.06	16	4.6	35
	Oct-Dec	2.93	0.20	7	2.86	0.24	7	1.96	0.08	6	1.95	0.17	7	1.3	32

Ultimately, although biofiltration did not compromise the effluent TOC and DOC typically achieved in the process, it also did not significantly improve overall removals. This was an interesting result because it was anticipated that the increase in active biomass (as measured through ATP) would correspond to an increase in DOC removal. However, despite ATP concentrations reaching levels consistent with acclimated biofilters, biofiltration did not result in an improvement in filtered water TOC or DOC over filtration. This is consistent with a recent finding in which, using data from several pilot and full-scale studies, no correlation between ATP concentrations and DOC removal was identified (Pharand et al, 2014). However, as described later in Chapter 6, additional data from this facility indicate that a 0.26 mg/L DOC reduction across the biofilter can correspond to a 1.5 mg/L removal of oxidizable organic matter (as measured through photoelectrochemical chemical oxygen demand) across the filter. As a result, it is hypothesized that more biological transformation of NOM may occur than is detectable by DOC. If reactions break down NOM but do not fully oxidize NOM compounds to carbon dioxide, then DOC (as measured though combustion) may not respond to this biological NOM transformation.

2.3.5 Disinfection by-product formation

Despite the lack of significant improvement in TOC and DOC with biofiltration, removing pre-chlorination resulted in reduced total THMs and total HAAs levels in finished water. Figure 2.9 and Figure 2.10 show seasonal trends in finished water total THM and total HAA concentrations before and after biofiltration was implemented.

As shown in Figure 2.9, total THM for finished water before biofiltration peaked in mid to late summer (August-September) in 2011 and 2012 at 54 and 55 µg/L, respectively. After removal of pre-chlorination, the late summer total THM finished water peak was ~24 µg/L in August 2013. Similarly, lows for finished water total THMs occurred in February 2012 and March 2013 and measured 24 and 16 µg/L, respectively. In contrast, February/March lows after implementation of biofiltration were <10 µg/L. As shown in Figure 2.10, finished water total HAAs peaked in the spring months with peak finished

water total HAA concentrations reaching 41, 45 and 45 µg/L in June 2011, June 2012 and March 2013, respectively. Following conversion to biofiltration, there was a decrease in finished water total HAAs throughout the month of April and May; this was followed by a steady concentration increase in June and July to a peak value of 30 µg/L in early August 2013 followed by another peak of 35 µg/L in March 2014. Total HAA finished water peaks with biofiltration were 6-10 µg/L less than peaks measured during filtration. One exception was a post-biofiltration finished water total HAA recording of 40 µg/L on May 27, 2014. This also corresponded to an elevated total THM concentration for the same finished water sample, likely indicating an abnormally high DBP precursor concentration or potential sample contamination for this date.

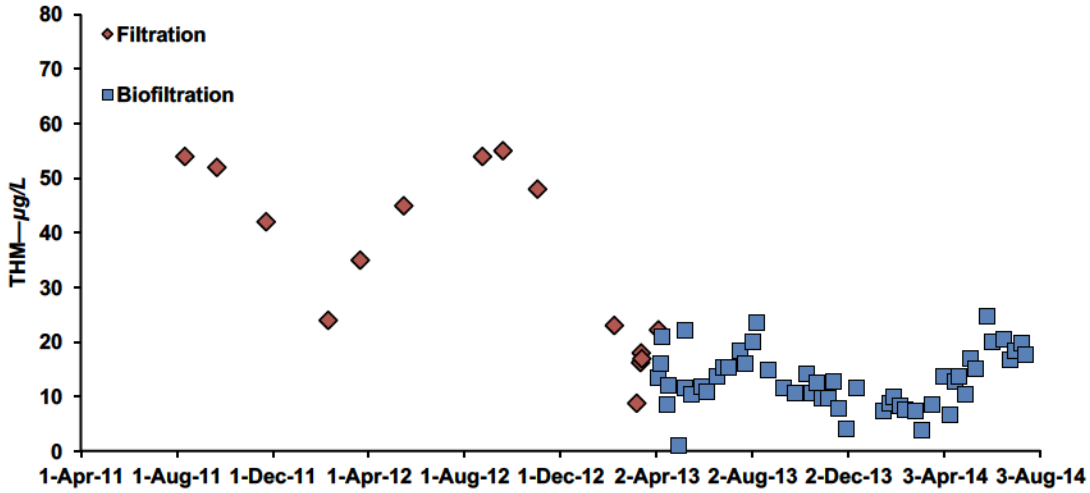

Figure 2.9 Finished water total THM concentration for filtration and biofiltration

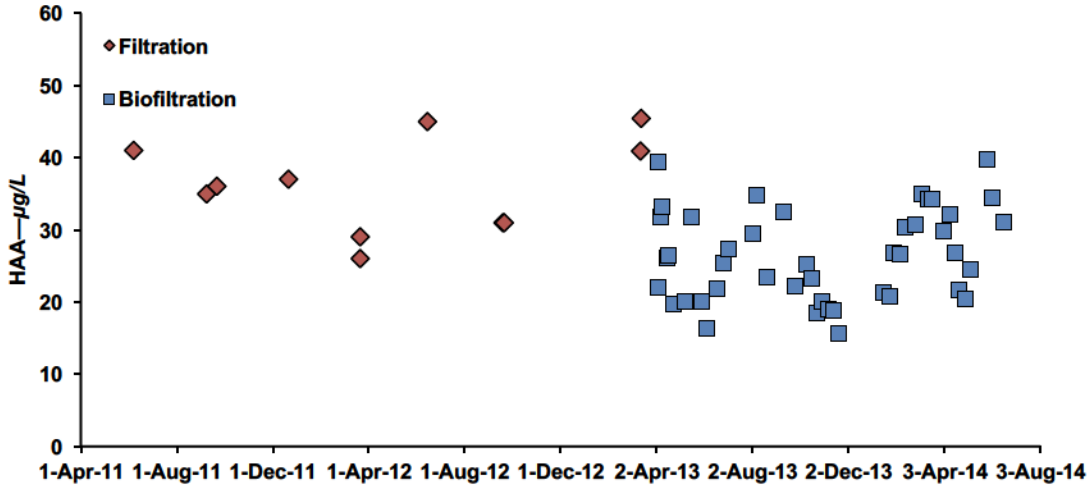

Figure 2.10 Finished water total HAA concentration for filtration and biofiltration

As shown in Figure 2.11 and Figure 2.12, total THM and total HAA concentrations were also measured at various locations in the distribution system. Percentage reductions in distribution system total THM and total HAA concentration were calculated using the following equation:

$$\%\ Reduction = \frac{\bar{x}_{Filtration} - \bar{y}_{Biofiltration}}{\bar{x}_{Filtration}} \qquad \text{(Equation 1.1)}$$

Where,

$\bar{x}_{Filtration}$ is the mean monthly DBP concentration with pre-chlorination (May/June 2011 – Feb/Mar 2013)

$\bar{y}_{Biofiltration}$ is the mean monthly DBP concentration without pre-chlorination (May/June 2013 – Feb/Mar 2015)

As shown in Figure 2.11, conversion to biofiltration resulted in a reduction in total THM formation. On average, distribution system total THM concentration was reduced by 29%. The highest overall reduction was observed in November at 47%, followed by August (39%), May (27%), and February (1%). As shown in Figure 2.12, conversion resulted in an average distribution system total HAA reduction of 15%. The highest

overall total HAA percent reduction was observed in December (34%), followed by September (16%) and June (15%). May had a negative average percent reduction of 5%, indicating an average increase in distribution system total HAA concentration for that month. Despite this increase, in general, conversion resulted in reduced DBP formation in the distribution system, mirroring results obtained in finished water measured at the plant effluent, and indicating that DBP formation was reduced as a result of conversion and not merely delayed. The limited reduction in total THM concentration for February and the increase in total HAA concentration for March indicate seasonality in DBP production. More advanced characterization of NOM using high performance size exclusion chromatography with combined resin fractionation (e.g., Kent et al., 2014) and/or organic carbon detection (e.g., McKie et al. 2015) is required to better understand seasonal fluctuation and chlorine reactivity of precursor material at this particular site.

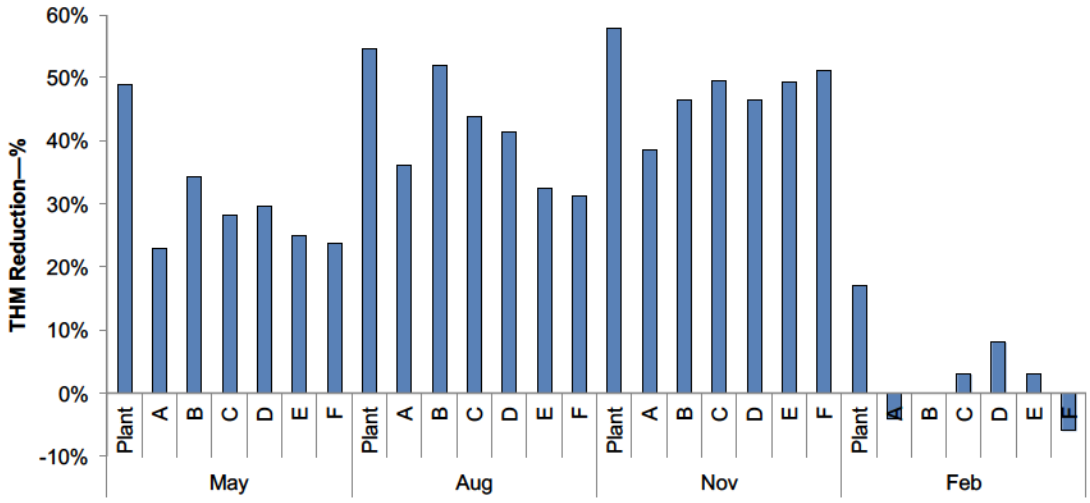

Figure 2.11 Total THM percentage reductions for various locations in the distribution system

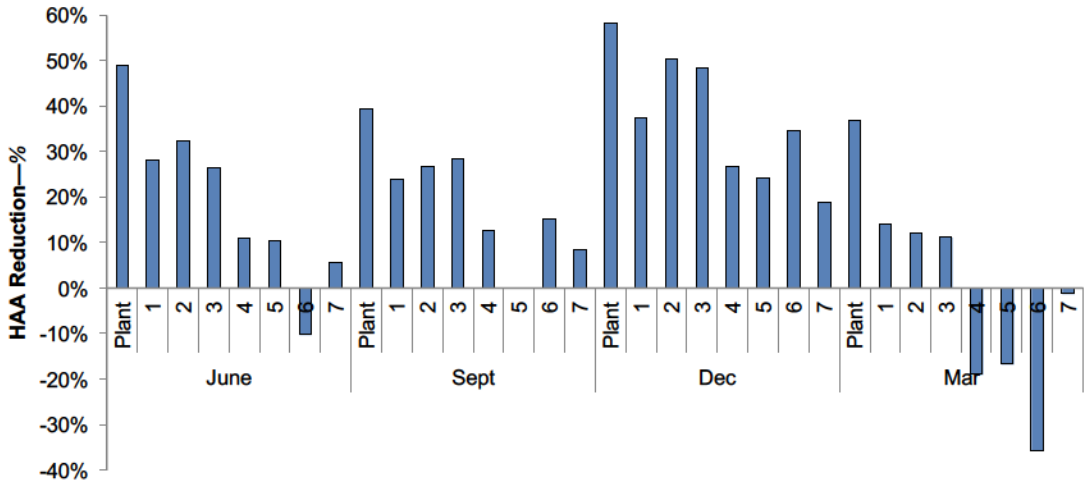

Figure 2.12 Total HAA percentage reductions for various locations in the distribution system

2.4 CONCLUSIONS

Conversion from filtration (pre-chlorinated) to biofiltration (non-chlorinated) at a direct filtration drinking water treatment plant was assessed in terms of filter performance and water quality. ATP analysis showed that when pre-chlorine was removed active biomass on the filter media increased to levels consistent with other acclimated drinking water biofilters. Filter performance analysis revealed that conversion resulted in an increase in filter effluent turbidity and a reduction in filter head loss, but that unit filter run volumes and filter run times were maintained. Despite increases in effluent turbidity, biofiltration was able to meet the *Canadian Drinking Water Guidelines* of ≤0.3 NTU. Water quality monitoring indicated that effluent TOC and DOC were not improved, potentially due to the substantial removal of TOC and DOC in the existing process and the non-optimized nature of the implemented biofiltration process. Despite this, DBPs were reduced by ~10-20 µg/L for trihalomethanes and ~6-10 µg/L for haloacetic acids. Communication of case study data from similar conversions is needed to further understand the parameters that make this type of conversion successful.

CHAPTER 3 BIOMASS EVOLUTION IN FULL-SCALE ANTHRACITE-SAND DRINKING WATER FILTERS FOLLOWING CONVERSION TO BIOFILTRATION

ABSTRACT

This study investigated biomass concentrations, as measured by adenosine triphosphate (ATP), in full-scale, anthracite-sand biofilters as they acclimated to conversion from direct filtration to biofiltration. Results showed that there were three scales of biofilter biomass accumulation: an accumulation period within each filter cycle, and an accumulation period associated with adapting to chlorine-free conditions for both biomass measured at the start of the filter cycle and biomass measured at the end of the filter cycle. Both start- and end-of-cycle biomass reached steady-state after 220 days of operation. Start-of-filter-cycle biomass accumulated at a rate of 0.008 d^{-1} and reached a steady state concentration of 59 ng ATP/cm^3 media. End-of-filter cycle biomass reached an apparent steady-state concentration of 267 ng ATP/cm^3 media. Biomass measured over a single filter cycle had an accumulation pattern similar to start-of-filter-cycle biomass but accumulated more rapidly (1.96-4.46 d^{-1}).[2]

---

[2] Note: A version of this chapter is published in *Journal American Water Works Association.*

Stoddart, A. K., Schmidt, J. J. & Gagnon, G. A. (2016). Biomass Evolution in Full-Scale Anthracite-Sand Drinking Water Filters Following Conversion to Biofiltration. *Journal American Water Works Association,* 108(12), E615-E623.

3.1 INTRODUCTION

Drinking water biofilters can remove dissolved contaminants and suspended solids through multiple mechanisms including adsorption, particle capture and biodegradation. The use of biofiltration in drinking water treatment can provide benefits over conventional filtration by providing contact time for biodegradation. Biofiltration can improve drinking water quality by improving biological stability in distribution systems, reducing disinfection byproduct precursors (e.g., Speitel et al., 1993), removing taste and odor causing compounds (e.g., Elhadi et al., 2006) and controlling manganese (e.g. Mouchet, 1992; Kohl & Dixon, 2012; Granger et al., 2014). Given these advantages, there is potential benefit and interest in converting conventional drinking water filters to biofilters.

There is an on-going need for monitoring tools in biofiltration design to improve filter operation metrics and ensure process optimization (Evans et al., 2013a). One such metric that is being considered for biomass concentration is the measurement of adenosine triphosphate (ATP). As a routine measurement, ATP is gaining popularity as a biofiltration monitoring tool for its ease of use through commercially available test kits and rapid (5- to 10-min) analysis time (Evans et al., 2013b). ATP is also a favorable biomass indicator in terms of precision, accuracy, span, representativeness and selectivity/specificity (Evans et al., 2013b). ATP is produced through metabolism of substrate (i.e., electron donors such as organic matter) and its presence and abundance can be used to indicate the presence and abundance of active/viable biomass (Berney et al., 2008).

ATP can be monitored in aqueous or bulk water (i.e., raw water, filter influents and filter effluents) (Hammes et al., 2010; Lautenschlager et al., 2014) to estimate planktonic or bulk water biomass, as well as on granular media such as anthracite (Pharand et al., 2015), sand (Magic-Knezev and van der Kooij, 2004; Lautenschlager et al., 2014) and granular activated carbon (GAC) (Magic-Knezev and van der Kooij, 2004; Velten et al., 2007; Velten et al., 2011) to estimate biofilm biomass. ATP has been shown to correlate

reasonably well ($R^2 = 0.69$) with total cell concentration (i.e., as measured using flow cytometry) in distributed drinking water (Siebel et al., 2008) and correlate significantly ($p < 0.05$) with total direct bacterial cell counts for biomass detached from drinking water biofilter media (Magic-Knezev and van der Kooij, 2004). As a result, planktonic or bulk water ATP measurements on filter influents can give an indication of biomass loading to biofilters, while measurements in the filter effluents can provide an estimate of detached biomass due to biofilm sloughing (Velten et al., 2011; Lautenschlager et al., 2014).

Ideally, ATP concentration could be related to biofilter performance parameters (e.g., substrate removal, head loss) to provide rapid indication of biofilter performance in terms of organic matter and micropollutant removal, to diagnose biofilter effluent water quality deterioration or to understand filter clogging. At present, results relating biofilm ATP to filter performance are mixed. Increased media ATP concentrations (resulting from nutrient enhancement with PO_4-P) in pilot and bench-scale biofilters have been related to increased dissolved organic carbon (DOC) removals in pilot-scale drinking water biofilters (Lauderdale et al., 2012; Granger et al., 2014). In granular activated carbon (GAC) filters undergoing conversion to biologically activated carbon (BAC) biofiltration, biofilters reached steady-state with respect to DOC removal at the same time as biomass steady-state, as measured by ATP, was reached (Velten et al., 2011). In contrast, other analyses have found that biomass concentration in the top media layer in drinking water biofilters, as measured by phospholipids, ATP and/or FDA hydrolysis, is not directly related to biodegradable organic matter (BOM) (Emelko et al., 2006) or dissolved organic carbon (DOC) removal (Pharand et al., 2014; Pharand et al., 2015) in pilot- or full-scale biofilters.

The purpose of this study was to examine biomass accumulation in the top media layer (~10 cm) of full-scale anthracite-sand drinking water biofilters during conversion from filtration to biofiltration. It was hypothesized that biomass concentrations measured at the start and end of a filter cycle would differ considerably, pointing to the need for more careful consideration of biomass sampling protocols. Ultimately, the objective of this study was to monitor the bulk and biofilm ATP concentrations in full-scale anthracite-

sand biofilters to assess how they acclimated biologically to chlorine-free conditions to determine (1) how biomass concentrations changed under these conditions, (2) how long it would take for filters to reach biomass steady-state and (3) when, during a filter cycle, ATP samples should be taken for an effective monitoring plan. The sampling program was carried out for 20 months to include the impact of temperature and potential seasonal fluctuations in water quality.

3.2 MATERIALS AND METHODS

3.2.1 Sample Site

Sampling was conducted at a municipal water treatment facility in Halifax, Canada. The treatment train at the facility underwent conversion from direct filtration (i.e., no clarification step prior to filtration) to direct biofiltration through removal of pre-chlorination during the study. The pre-mix process at the facility involved addition of lime for pH adjustment and alkalinity, addition of potassium permanganate for iron and manganese control, followed by pH adjustment with carbon dioxide and coagulation with aluminum sulfate. Flocculation occurred via three-stage hydraulic mixing and biofiltration occurred through eight dual media anthracite-sand filters (600 cm of anthracite, 300 cm of sand). Prior to conversion, pre-chlorine was added during the pre-mix process to provide a post-filter chlorine residual of 0.05 mg/L. Filter effluent was also used for backwashing, and therefore, removal of pre-chlorination also resulted in the removal of chlorinated (~0.05 mg/L) backwash. The facility source water is Pockwock Lake. Pockwock Lake is characterized by low turbidity (~0.4 NTU), low pH (~5.5), low alkalinity (< 1 mg/L) and low organic carbon (~2.5 mg DOC/L; ~2.5 mg TOC/L) content (Knowles et al., 2012; Vadasarukkai et al., 2011). Plant siting resulted in a large seasonal temperature fluctuation (~1-23°C) during the study; however, raw water pH, turbidity and total and dissolved organic carbon concentrations remained stable seasonally (Chapter 2). Coagulation and flocculation treatment steps remained unchanged over the study duration. Subsequently, water quality entering the biofilters was also stable throughout the study duration. Average biofilter influent TOC and DOC concentrations

were 2.9 ± 0.3 mg/L and 2.0 ± 0.2 mg/L, respectively. Further details of the treatment process and water quality during conversion are provided in Chapter 2.

3.2.2 Biofilm Biomass Sampling and Analysis

To understand how biomass accumulated following conversion to biofiltration, media samples were collected directly before (end of filter cycle) and after (start of filter cycle) backwash for a period of 20 months. To further understand how biomass accumulated over the course of a single filter cycle, media samples were collected at the beginning (i.e., directly after backwash at 0 hours of filter run time), in the interim (12 min, 30 min, 1 h, 2 h, 3 h, 5 h, 6 h, 8 h, 22 h, 24 h, 29 h and 47 h of filter run time) and at the end (53 h of filter run time) of a filter cycle in two paired biofilters. This within filter cycle monitoring was conducted following the initial 20 month monitoring period.

Filter media samples were taken from the surface (top ~10 cm) of the filter bed using a sampling pole fitted with a wide mouth polypropylene bottle. Samples were taken at approximately the same location in each filter. Samples were homogenized and transferred to sterile 50 mL falcon tubes. Biomass was measured on-site immediately after sampling using a 1 g (wet weight) subsample. Biomass concentration was assessed using ATP. ATP concentrations were determined as described previously in Chapter 2 using a commercial ATP kit (DSA test kit, LuminUltra Technologies Inc, Fredericton, Canada) according to the manufacturer's instructions. In short, this method involved chemical removal of biofilm from media, followed by dilution of resulting biofilm suspension, reaction with luciferase enzyme and quantification of the light emitted in relative light units (RLU) using a luminometer (PhotonMasterTM Luminometer, LuminUltra Technologies Ltd., Fredericton, Canada). ATP concentration was measured in triplicate and reported as mass ATP per unit volume of filter media (Pharand et al., 2014). RLUs were converted to ATP concentrations and expressed in ng ATP/cm^3 media using an anthracite density of 0.8 g/cm^3. Media wet weight was converted to dry weight concentration using a correction factor. Correction factors were determined in triplicate by weighing subsamples before and after drying at 105°C for approximately 24 hours.

3.2.3 Planktonic Biomass Sampling and Analysis

Bulk water biofilter influent and effluent biomass samples were collected in 50 mL sterile falcon tubes from continuously running sample ports. Planktonic biomass was quantified by ATP. ATP was measured on-site immediately after sampling using a commercial ATP test kit (QGA test kit, LuminUltra Technologies Inc, Fredericton, Canada) according to the manufacturer's instructions. A 50 mL sample volume was used for the analyses.

3.2.4 Biofilm Biomass Growth Rate

Biomass accumulation was modeled using a first order differential equation developed by Baranyi and Roberts (1994). Biomass specific accumulation rates (μ_{max}) were calculated from biomass concentration, as measured by ATP, using the equation given in Equation 1:

$$y(t) = y_0 + \mu_{max}t - \frac{1}{m}\ln\left(1 + \frac{e^{m\mu_{max}t} - 1}{e^{m(y_{max} - y_0)}}\right) \qquad \text{(Equation 2.1)}$$

where,

$y(t)$ is the natural logarithm of the cell concentration at $t=t$

y_0 is the natural logarithm of the cell concentration at $t=t_0$

μ_{max} is the maximum specific growth rate

y_{max} is the natural logarithm of the maximum cell concentration

m is a curvature parameter

In the current study, the biomass specific growth rate from Baranyi and Roberts (1994) was referred to as a biomass specific accumulation rate since it was used to describe both the growth that occurred with respect to operational time for start-of-filter-cycle biomass, and the accumulation (assumed to include biomass growth as well as biomass collection from filtered floc material) of biomass in a single filter cycle.

Model results were generated using ComBase DMFit web edition (ComBase, 2015). ATP concentration has been shown to correlate well ($R^2 = 0.69$) with total cell concentration (i.e., as measured using flow cytometry) in distributed drinking water (Siebel et al., 2008), as well as total direct bacterial cell counts in drinking water biofilters (Magic-Knezev and van der Kooij, 2004). Therefore, ATP concentration was used in place of cell concentration for the model.

3.2.5 Statistical Analysis

Linear regression was used to determine if direct relationships existed between parameters. Regression significance for start-of-filter-cycle biomass and temperature, start-of-filter-cycle biomass and operational day, end-of-filter-cycle biomass and temperature, and end-of-filter-cycle biomass and operational day was assessed using the p-value at a significance level of 0.05, as well as qualitative visual analyses of residuals. Natural log transformed biomass was used for these analyses in order to determine specific rates. The p-values and residuals for these regressions were calculated using the Analysis Toolpak in Microsoft Excel. Comparison between steady-state start and end-of-filter-cycle biomass was conducted using a two-tailed, paired Student t-test with a significance level of 0.05. The start of steady-state was defined as the time at which the start-of-filter-cycle biomass concentration was within 3% of y_{max}. Confidence intervals for fitted parameters (i.e., y_0, μ_{max}, y_{max}) were determined from standard errors generated in ComBase DMfit (ComBase, 2015). All confidence intervals represent the 95% confidence interval.

3.3 RESULTS & DISCUSSION

3.3.1 Biomass Accumulation with respect to Operational Day

To understand how the converted filters acclimated to chlorine-free conditions, media biomass concentration was measured at the start of a filter cycle (i.e., immediately after backwash at 0 hours of filter run time) and at the end of a filter cycle (i.e., at 58-80 hours

of filter run time). Samples taken at the start of the filter cycle represented the attached biomass that was not removed during the backwash. Samples taken at the end of the filter cycle included both attached biomass and biomass accumulated from growth and physical removal of flocculated material incurred over an individual filter cycle.

3.3.1.1 Start of Filter Cycle

Despite the dynamic process of backwashing, removal of pre-chlorine and subsequent conversion to biofiltration resulted in a gradual increase in start-of-filter-cycle biomass with respect to operational day (Figure 3.1). This increase in biomass concentration was not directly correlated to temperature. Regression analysis confirmed no linear correlation between natural log-transformed start-of-filter-cycle ATP concentration and temperature ($R^2 = <0.01$, $p = 0.84$) (residuals plot provided in Supplemental Figure A.1). Further regression analysis confirmed a weak but significant linear correlation between start-of-filter-cycle ATP concentration and operational day ($R^2 = 0.49$, $p = <0.01$) (residuals plot provided in Supplemental Figure A.2).

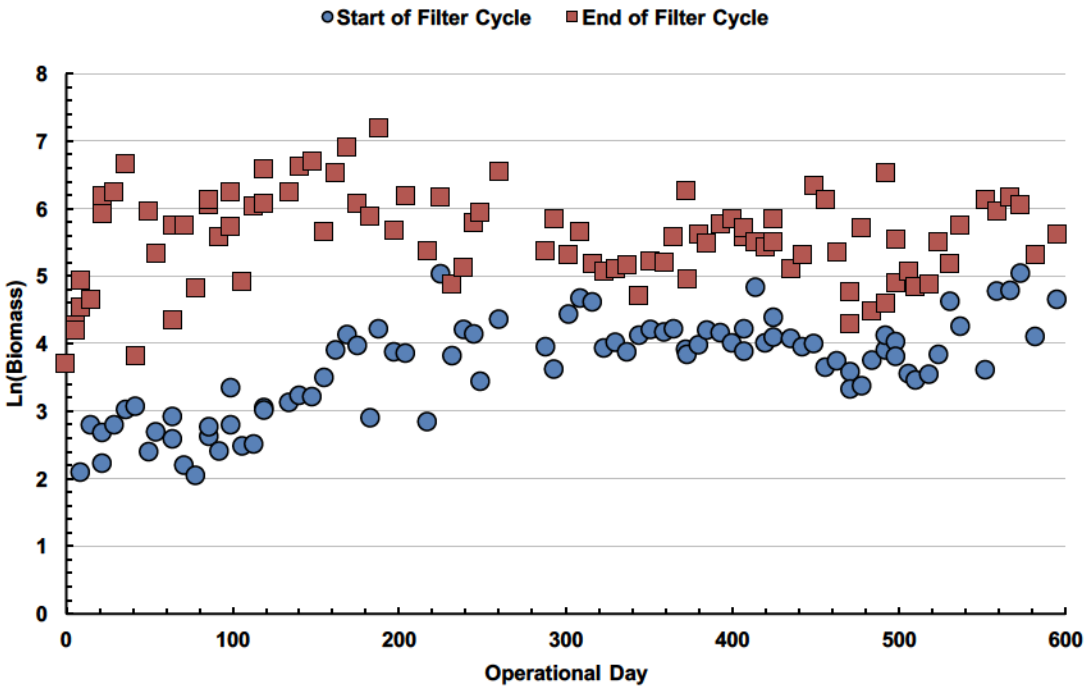

Figure 3.1 Natural log transformed biofilter biomass (ng ATP/cm^3 media) at the start (0 hours of filter run time) and end (58-80 hours of filter run time) of a filter cycle

Linear interpretations (i.e., y_t-$y_0/\Delta t$) can be used to determine the specific growth rate (μ_{max}) of biomass in drinking water biofilters by excluding the steady-state (Velten at al., 2011), and/or the lag phase, if applicable. However, manual exclusion requires subjective determination of inflections points; consequently, the sigmoidal Baranyi and Roberts model was applied to improve parameter estimation. The measured biomass concentrations and fitted model are provided in Figure 3.2. Fitted model parameters are provided in Table 3.1.

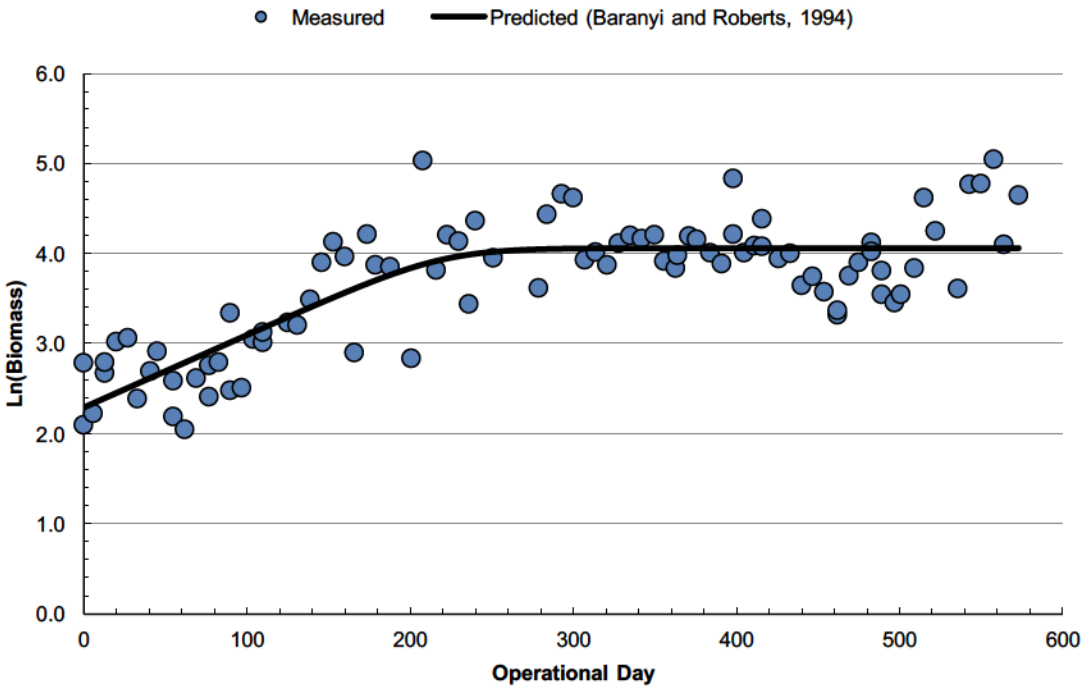

Figure 3.2 Measured and fitted natural log-transformed start-of-filter-cycle biomass concentration (ng ATP/cm^3 media) with respect to operational day

Table 3.1 Fitted model parameters for start-of-filter-cycle biomass with respect to operational day

Parameter	Per Operational Day
r^2	0.66
y_0	2.29 ± 0.26
μ_{max}	0.008 ± 0.003 d^{-1}
y_{max}	4.07 ± 0.12

A biomass specific accumulation rate of 0.008 ± 0.003 d^{-1} for start-of-filter-cycle biomass was calculated using the model. Comparatively, Velten et al. (2011) reported a much higher biomass specific growth rate of 0.0984 d^{-1} in the top 10 cm of ozonated pilot-scale GAC biofilters over a 200-day period. While the biofilter described by Velten et al. (2011) was operated at a consistently lower temperature (7.05 ± 0.7°C) and lower

influent DOC concentration (1.1 ± 0.04 mg/L) than the current study, the impact of backwashing was not considered and filter operation time without backwash neared 200 days. This infrequent backwashing strategy is not feasible for biofilters that must also perform particle removal through rapid filtration. As a result, the biomass accumulation rate described herein may provide an indication of the biomass accumulation rate expected during conversion from rapid filtration to rapid biofiltration.

The initial natural logarithm of the start-of-filter-cycle biomass concentration (y_0) obtained from the model was 2.29. The fitted maximum natural logarithm of the biomass concentration (y_{max}) was 4.07. These values corresponded to 9.9 ng ATP/cm^3 media and 59 ng ATP/cm^3 media, for initial and maximum biomass concentration, respectively. These concentrations fell outside the typical range of ATP concentrations (i.e., 100-1000 ng ATP/cm^3 media) identified for drinking water biofilters (Pharand et al., 2014). In that work, Pharand et al. (2015) sampled biomass during an individual filter cycle, as opposed to concentrated sampling at the start of a filter cycle. The current study highlighted that determining ATP concentration at the start of a filter cycle and within a filter cycle was important for understanding the range of expected ATP concentrations in biofiltration.

Ultimately, the use of the Baranyi and Roberts model allowed for a systematic analysis of initial biomass concentration, maximum biomass concentration and biomass accumulation rate with respect to operational day. This systematic approach facilitated the analysis of the data by eliminating the need to subjectively interpret minimum (y_0) and maximum (y_{max}) biomass concentration and accumulation rate (μ_{max}). The model can also detect a lag phase if applicable. Accurate and systematic determination of these parameters is also beneficial to elucidate start-up expectations for conversion from rapid filtration to rapid biofiltration, and potentially for commissioning of new rapid biofilters with virgin media.

3.3.1.2 End of Filter Cycle

No direct linear correlation between natural log-transformed end-of-filter-cycle ATP concentration and operational day ($R^2 = 0.007$, $p = 0.428$) was detected (Supplemental

Figure A.3). Additionally, consistent with natural log transformed start-of-filter-cycle ATP concentration, regression analysis confirmed that there was no direct linear correlation between natural log-transformed end-of-filter-cycle biomass concentration and temperature ($R^2 = 0.057$, $p = 0.021$) (Supplemental Figure A.4). This stability in ATP concentration, despite temperature fluctuations, is consistent with previously reported ATP concentrations in full-scale drinking water biofilters (Pharand et al., 2014; Pharand et al., 2015).

End-of-filter-cycle biomass concentration always exceeded start-of-filter-cycle biomass concentration (Figure 3.1). End-of-filter-cycle ATP concentration increased from an initial concentration of 40 ng ATP/cm^3 media to a maximum concentration of 1326 ng ATP/cm^3 media at approximately day 190 before decreasing to an apparent steady-state concentration of approximately 267 ng ATP/cm^3 media at approximate operational day 220 (Figure 3.1). This type of biofilm incubation trend (i.e., with a maximum concentration followed by a decline in concentration before reaching a steady-state) has been reported using various biomass indicators, including ATP concentration (van der Kooij et al., 1995; van der Kooij et al., 2003; Velten et al., 2007; Waines et al., 2011), production of CO_2 as a result of mineralization of saturated C-glucose (Servais et al., 1994) and phospholipid extraction (i.e., nmol PO_4/g carbon) paired with fluorescein diacetate (FDA) testing (Seredyńska-Sobecka et al., 2006).

Previous research has suggested that the rapid initial biomass peak is due to the assimilation of adsorbed substrate by attached microorganisms (van der Kooij et al., 2003; Velten et al., 2007). As anthracite media is not recognized for its adsorptive capacity, substrate could be available to the biomass as hydrophilic organic material that was not adsorbed to alum floc during coagulation. Chapter 6 will demonstrate that total organic carbon and DOC had the same concentration following biofiltration at this plant, which indicates that organic material enmeshed in floc material was physically removed. Also evident from Chapter 6, the photoelectrochemical chemical oxygen demand (peCOD) concentration was decreased following coagulation/flocculation (adsorption) and then further decreased through biofiltation (biodegradation). For Atlantic Canada

surface water, hydrophilic acids are significant contributors to haloacetic acid (HAA) formation (Kent et al., 2014) and during biofilter operation at this facility the degradation of HAA precursors was evident (Chapter 2). Thus, it was hypothesized that once pre-chlorination was removed and biofilm growth was no longer suppressed, biofilm began to accumulate and consume the available substrate, contributing to a rapid initial biomass accumulation. Balance was eventually achieved between biofilm processes of attachment, growth, detachment and decay as the filter continued its operation.

3.3.1.3 Planktonic Biomass

Planktonic biomass concentrations for raw water and biofilter effluent are provided in Figure 3.3. Raw water ATP averaged 58 ± 6 pg ATP/mL during the study duration with no apparent seasonal temperature related trend. This observation was confirmed by linear regression ($R^2 < 0.01$, $p = 0.570$) and indicated that there was similar biomass loading to the filters despite seasonal temperature fluctuations. Biofilter effluent ATP increased with the removal of pre-chlorine from an initial concentration of 2 pg/mL with pre-chlorine to an average concentration of 13 ± 1 pg ATP/mL without pre-chlorine. This increase in effluent ATP concentration occurred rapidly, with effluent ATP concentrations reaching the 10-20 pg/mL level within 6 hours of pre-chlorine removal and approximately 22 hours after stepwise pre-chlorine dosage reductions began. Biofilter effluent ATP concentrations were measured at various times during the different individual filter cycles (i.e. 0.5-69 hours of filter run time) to determine this average effluent ATP concentration. Biofilter effluent ATP concentration was independent of filter run time ($R^2 < 0.01$, $p = 0.885$) and raw water temperature ($R^2 < 0.01$, $p = 0.604$).

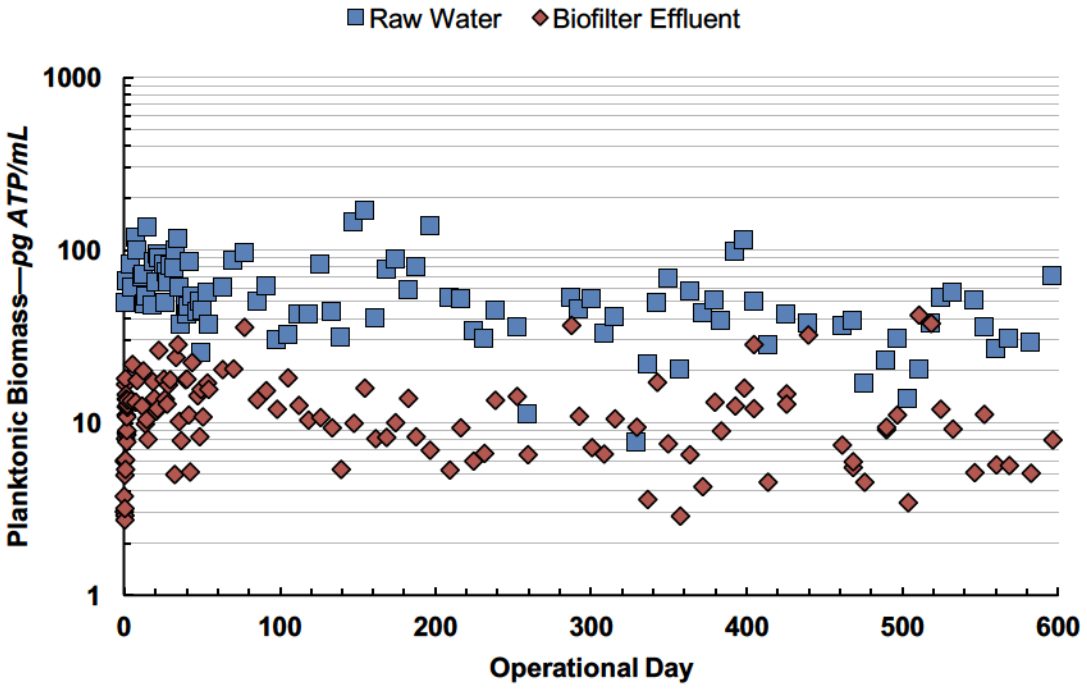

Figure 3.3 Measured planktonic biomass concentration of raw water and biofilter effluent with respect to operational day

3.3.2 Biomass Accumulation with Respect to Filter Run Time

To further understand how biomass accumulated over the course of a single filter cycle, media biomass was sampled at the beginning, in the interim and at the end of a filter cycle in two paired biofilters (Figure 3.4). The data was interpreted using the Baranyi and Roberts model (Baranyi and Roberts, 1994). Fitted model parameters are provided in Table 3.2.

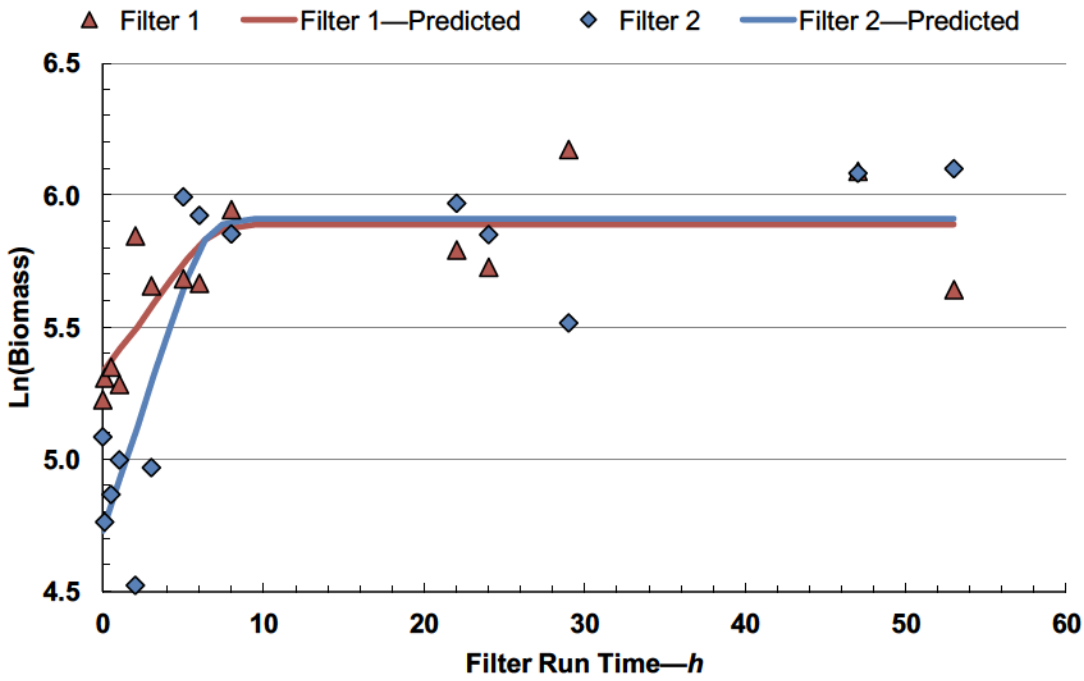

Figure 3.4 Measured and fitted natural log-transformed in-filter cycle biomass concentration (ng ATP/cm^3 media)

Table 3.2 Fitted parameters for in-filter cycle biomass concentration with respect to filter run time

Parameter	Per Filter Cycle	
	Filter 1	Filter 2
r^2	0.58	0.74
y_0	5.33 ± 0.19	4.73 ± 0.30
μ_{max}	1.96 ± 1.68 d^{-1}	4.46 ± 2.80 d^{-1}
y_{max}	5.89 ± 0.16	5.91 ± 0.24

Fitted initial natural log biomass concentrations (y_0) were 5.33 ± 0.19 and 4.73 ± 0.30 for Filter 1 and Filter 2, respectively (Table 3.2). These initial biomass concentrations were statistically different from each other and statistically higher than the fitted maximum biomass concentration (y_{max} = 4.07 ± 0.12) found for start-of-filter-cycle biomass. However, these concentrations were not entirely unprecedented given the range of start-

of-filter-cycle initial natural log biomass concentrations (y_0) found over the study period (Figure 3.1). Despite different initial biomass concentrations (y_0), Filter 1 and Filter 2 had the same fitted maximum natural log biomass concentration (y_{max}) at 5.89 ± 0.16 and 5.91 ± 0.24, respectively. This finding indicated that the filter media may have reached a maximum biomass concentration associated with the surface area or that the biofilm experienced restricted substrate diffusion in this media layer, potentially as a result of suspended solids removal.

A biomass specific accumulation rate of 1.96 ± 1.68 d^{-1} and 4.46 ± 2.80 d^{-1} was calculated for Filter 1 and Filter 2, respectively. Within-filter accumulation rates were 3 orders of magnitude greater than the accumulation rate determined for start-of-filter-cycle biomass (i.e., 0.008 d^{-1}). Within-filter cycle accumulation rates were also 2 orders of magnitude greater than growth rates reported by Velten et al. (2011) for an ozone-GAC pilot-scale biofilter. The raw water temperature and influent DOC concentration were higher for the current study at 20.6 ± 0.3°C and 2.17 ± 0.10 mg/L, respectively, compared to 7.05 ± 0.7°C and 1.1 ± 0.04 mg/L for the Velten et al. (2011) study. Additionally, the biofilter influent in the Velten et al. (2011) study was treated with ozone following the initial colonization period, reportedly effectively eliminating biomass accumulation due to attachment of planktonic bacteria and ensuring that the determined accumulation rate was attributed only to growth and not deposition/attachment of planktonic bacteria from the filter influent.

To assess the impact of biomass deposition/attachment versus growth, planktonic biomass was also measured in biofilter influent and individual biofilter effluents in the paired biofilters during the within-filter cycle analysis. Concentrations are provided in Figure 3.5. Influent and effluent biomass concentrations were stable over the course of the filter cycle. Biofilter influent averaged 179 ± 16.5 pg ATP/mL (n = 5). Biofilter effluent averaged 22 ± 4.9 pg ATP/mL (n = 5) and 20 ± 4.1 pg ATP/mL (n = 5) for Filter 1 and Filter 2, respectively. Despite continuous loading of planktonic biomass to the biofilters and continuous sloughing or release of planktonic biomass from the biofilters

for the duration of the filter cycle, the model showed that the within filter cycle biomass reached steady state in both filters after 8 hours of filter run time (Figure 3.4).

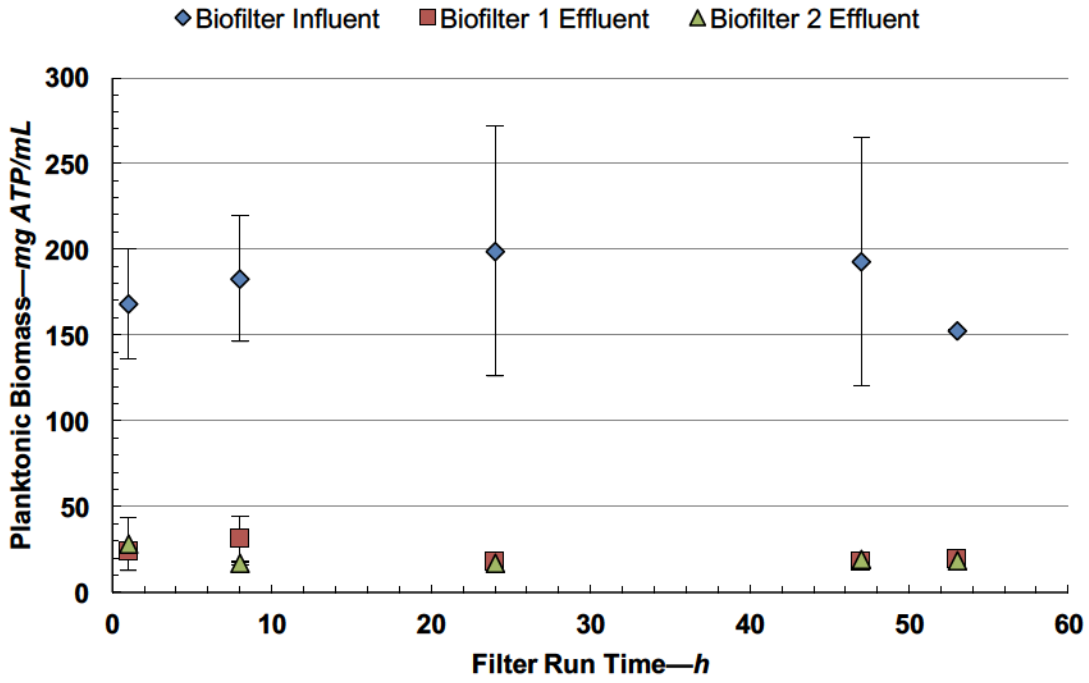

Figure 3.5 Planktonic biomass concentration of biofilter influent and biofilter effluents for a single filter cycle. Error bars represent the 95% confidence interval of the data

3.3.3 Biomass Accumulation Scales

Start-of-filter-cycle and end-of-filter-cycle ATP concentration analysis revealed three scales of biomass accumulation; one for the biomass measured at the start of the filter cycle, one for the biomass measured at the end of the filter cycle and one for the biomass accumulated during a single filter cycle. A generalized schematic of these three scales is shown in Figure 3.6.

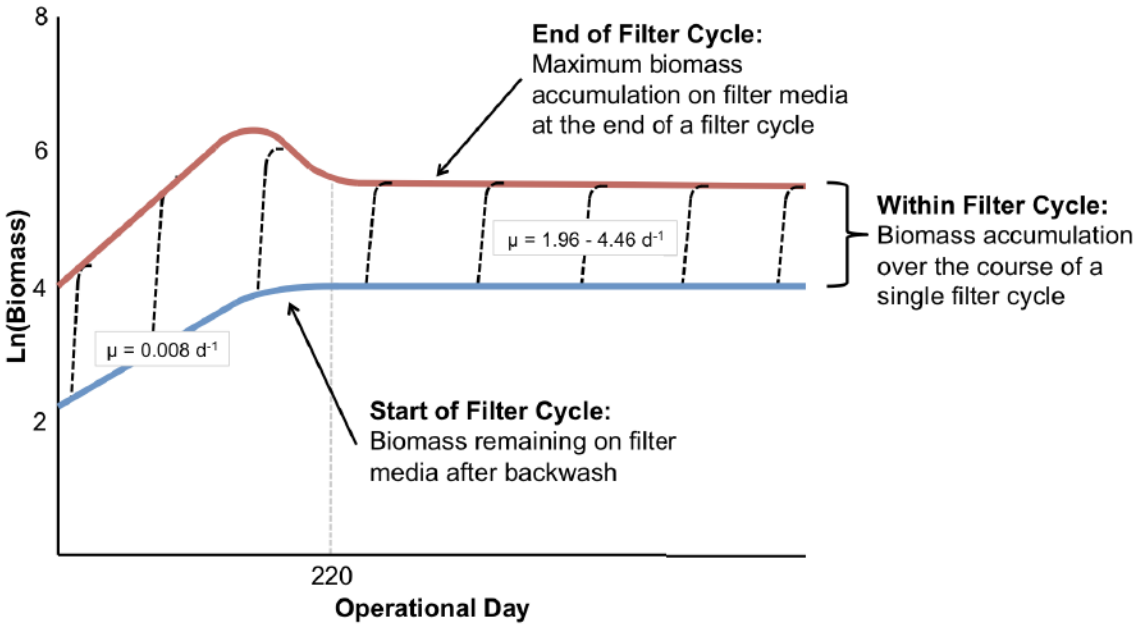

Figure 3.6 Schematic of biomass accumulation scales. μ represents the specific biomass growth rate

Following conversion to biofiltration through removal of pre-chlorination and prior to reaching a steady-state, start-of-filter-cycle biomass increased with operation time, indicating that biomass fixed to the media surface was increasing. During this same period, end-of-filter-cycle biomass accumulation followed a predictable trend also found in other studies with an increase in concentration to a maximum, followed by a decrease in concentration before reaching steady-state. Despite differences in accumulation pattern, end-of-filter-cycle and start-of-filter-cycle biomass reached steady state at approximately the same time (i.e., after 220 days of operation) (Figure 3.1). Once reached, the start-of-filter-cycle and end-of-filter-cycle steady-state biomass concentrations was maintained despite seasonal temperature fluctuations from 1.5 - 22.0°C (average = 10.1°C), reiterating the independence of ATP concentration on temperature for these biofilters.

The start-of-filter-cycle and end-of-filter-cycle biomass concentrations did not converge at the same steady-state ATP concentration. At steady-state, ATP concentrations decreased from approximately the same quantity (i.e., 59 ng ATP/cm^3 media) with each

backwash and increased over the course of a filter cycle to approximately the same quantity (i.e., 267 ng ATP/cm^3 media). Essentially, once steady-state was reached, all biomass gained over the course of the filter cycle was lost during backwash. This difference in steady-state start and end-of-filter-cycle ATP concentration was statistically significant ($p < 0.01$). Previous studies investigating the impact of backwash on biomass concentrations have found that biomass concentrations (as measured by the phospholipid method) before and after backwash were not reduced by non-chlorinated backwash (Miltner et al., 1995) or air scour (Emelko et al., 2006). While air scour also does not result in significant reduction in biomass concentration after backwash, biomass concentrations are lower in biofilters backwashed with air scour than in those backwashed with non-chlorinated water alone (Ahmad et al., 1998; Emelko et al., 2006). Ahmad et al (1998) found that higher biomass concentrations (as inferred by effluent heterotrophic plate counts) in non-air scoured biofilters did not correspond to an increase in substrate (i.e. AOC) removal. However, chlorinated backwash has been shown to reduce biomass concentration and substrate removal over filters backwashed with non-chlorinated water (Miltner et al., 1995; Ahmad et al., 1998), as well as cause temporary loss of substrate control (Miltner et al., 1995). Air scour and chlorinated backwash were not part of the backwashing protocol used in the current study, indicating that statistically significant reductions in biomass concentration as a result of backwash can occur without air scour or chlorination of backwash water.

Knowledge and consideration of biomass concentration and accumulation rates in biofilters may be important when attempting to correlate biomass concentrations to substrate removal and for biofilter optimization. More research is needed to determine if the accumulation phase of the biomass within a biofilter contributes to contaminant removal. Future research may help elucidate conditions that have led to conflicting findings in the literature related to the role that biomass concentration plays in substrate removal. For example, some studies have found that biomass concentration on filter media does not directly correlate to BOM (Emelko et al., 2006) or DOC removal (Pharand et al., 2014; Chapter 2), while other findings indicate that incomplete or limited

removal of biomass from filter media during backwash is beneficial to substrate removal performance (Miltner et al. 1995; Hozalski and Bouwer, 1998).

3.4 CONCLUSIONS

Biomass accumulation was measured by adenosine triphosphate (ATP) in full-scale drinking water filters as they acclimated to the removal of pre-chlorination and the subsequent conversion from filtration to biofiltration. This study showed that biomass was sensitive to time of sampling. Three scales of biomass accumulation were observed; Biomass measured at the start and end of the filter cycle increased with respect to operational day and biomass measured over the course of a single filter cycle increased with respect to filter run time. This points to the need for biomass sampling consistency within the context of the operational state of the filter (e.g., filter run time) or following significant process changes (e.g., removal of pre-chlorination).

The biomass data were interpreted using a growth model commonly used in predictive microbiology. The use of the growth model allowed for systematic and objective determination of biomass specific accumulation rate and initial and maximum biomass concentrations. The start-of-filter-cycle biomass concentration increased from 9.9 ng ATP/cm^3 media to a steady-state concentration of 59 ng ATP/ cm^3 media at a biomass specific accumulation rate of 0.008 d^{-1}. Biomass measured at the end of each filter cycle could not be interpreted using the growth model but followed a predictable pattern prior to reaching an apparent steady-state of 267 ng ATP/cm^3 media. Biomass accumulation within a single filter cycle followed a similar trend to that of biomass measured at the start of the filter cycle but accumulated more rapidly (1.96-4.46 d^{-1}). Determining typical biofilter biomass concentrations and accumulation rates is important when attempting to correlate biomass concentration to biofilter performance. The use of ATP for biomass monitoring has potential to address the ongoing need for monitoring tools in biofiltration design, operation and optimization.

CHAPTER 4 WATER QUALITY AND FILTER PERFORMANCE OF NUTRIENT-, OXIDANT- AND MEDIA-ENHANCED DRINKING WATER BIOFILTERS

ABSTRACT

Nutrient, oxidant and media enhancement strategies were applied to pilot-scale biofilters with the objective of enhancing biodegradation to improve effluent water quality (e.g., TOC, DOC, SUVA, THMfp, HAAfp) and filter performance (e.g., effluent turbidity and head loss). While some statistically significant ($\alpha = 0.05$) differences in DOC removal and DBPfp were identified as a result of specific enhancement strategies, enhancement strategies did not result in improvements in water quality (as measured by TOC, DOC, SUVA and DBPfp) that could be considered of practical operational importance. Water quality improvements were either operationally inconsistent, small in magnitude and/or within the deviation that would be expected from the biofilters when operated under equivalent ambient (i.e., not enhanced) conditions. With respect to filter performance, enhancement strategies also occasionally resulted in a statistically significant difference in effluent turbidity and head loss. However, when identified, statistically significant mean differences in effluent turbidity were deemed not meaningful given the instrument accuracy (i.e., ±0.02 NTU), the relatively small magnitude of the mean differences, or the magnitude of the mean difference observed between biofilters operated under equivalent ambient conditions. With respect to head loss, statistically significant mean differences in head loss that were also considered meaningful given the magnitude of the deviation between ambient biofilters and the accuracy of the pressure transmitters, were largely consistent with the literature; however, the magnitude of the mean differences that showed improvement to head loss were small (10-18 cm), and likely would not be

sufficient to substantially extended filter run times to have any practical operational importance.[3]

[3] Note: A version of this chapter is published in *Environmental Science: Water Research & Technology.*

Stoddart, A. K., & Gagnon, G. A. (2017). Water Quality and Filter Performance of Nutrient-, Oxidant- and Media-Enhanced Drinking Water Biofilters. *Environmental Science: Water Research & Technology.* 10.1039/C6EW00293E

4.1 INTRODUCTION

Biofiltration performance can be influenced by a number of factors including time since start-up, water temperature, substrate loading, empty bed contact time (EBCT), backwashing protocol, and filter media type (Huck et al., 2000). These influencing factors can be controlled to various degrees (Huck et al., 2000). Of course, time since start-up, water temperature and substrate loading are largely uncontrollable. Other factors, such as EBCT and backwashing protocol, may be more difficult to control than they seem, especially in biofilters that have been converted from conventional filters and are also required to provide particle removal and reach finished water turbidity requirements (i.e., <0.1 NTU). In addition to these established influencing factors, recently, the impact of nutrient limitation on biofiltration performance has been investigated (Lauderdale et al., 2012).

While carbon is traditionally considered the limiting factor for biofilm growth in drinking water treatment and distribution, in some waters where there is a low availability of phosphorus, phosphorus can be the limiting nutrient (Lehtola et al., 2002). In these water sources, researchers have shown that phosphorus can increase biofilm production (Lehtola et al., 2002, Hozalski et al., 2005, Fang et al., 2009). With respect to biofiltration, it has been hypothesized that since phosphorus is efficiently removed during chemical coagulation, that the addition of phosphorus prior to a biofilter could improve biofilter operation (Juhna and Rubulis, 2004; Lauderdale et al., 2012). For example, Lauderdale et al. (2012) found nutrient enhancement effective at reducing terminal head loss in biofilters, as well as improving DOC removal. However, results of nutrient enhancement in biofiltration has been mixed and more investigations are required to understand the broad applicability of this enhancement strategy as other studies have found phosphorus addition ineffective at improving natural organic matter (NOM) removal (Vahala et al., 1998, Juhna and Rubulis, 2004).

In addition to phosphorus enhancement alone, some studies have investigated combined phosphorus and nitrogen addition, often with the objective of avoiding nutrient limitation

given a specific carbon:nitrogen:phosphorus (C:N:P) molar ratio of 100:10:1 (Lauderdale et al., 2012). This molar ratio is considered a balanced nutrient ratio for bacteria (Lauderdale et al., 2012). McLean et al. (1996) found that nutrient addition of nitrate and phosphate did not significantly improve biodegradable dissolved organic carbon (BDOC) removal, but that nutrient addition with ammonium and phosphate led to near statistically significant ($p = 0.052$) improvement in BDOC removal over the reference filter and was attributed to the greater bioavailability of ammonium as compared to nitrate. Conversely, Azzeh et al. (2015) and McKie et al. (2015) found that addition of nitrogen (as ammonium chloride) and phosphorus (as phosphoric acid) did not enhance biofilter performance.

Hydrogen peroxide residuals may be present in biofilter influents as a result of addition or formation during ozonation (Urfer and Huck, 1997). Despite its oxidation capacity, Urfer and Huck (1997) found that low levels of hydrogen peroxide residuals (i.e., ~1 mg/L) did not inhibit the biodegradation of select BOM compounds in pilot-scale biofilters. Recently, the addition of hydrogen peroxide to drinking water biofilters as a means to increase the oxidative action of biofilter microorganisms and control extracellular polymeric substances (EPS) to improve hydraulic performance has been investigated (Lauderdale et al. 2012; Azzeh et al., 2015). Operationally, Lauderdale et al. (2012) demonstrated that addition of hydrogen peroxide at low concentrations (i.e., 1 mg/L) to pilot-scale biofilters decreased terminal head loss by up to 60% while maintaining MIB, Mn and DOC treatment performance. It was postulated that the decrease in terminal head loss was the result of the oxidation of EPS since hydrogen peroxide addition also reduced EPS concentration as compared to the control (Lauderdale et al., 2012).

Many studies have also investigated the use of different filter media to enhance biofiltration. GAC often outperforms anthracite media for BOM removal, particularly under more challenging biofiltration conditions such as at low temperatures or chlorinated backwash (LeChevallier et al., 1992; Emelko et al., 2006). GAC also typically supports a greater amount of biomass than anthracite media (Wang et al., 1995;

Liu et al., 2001), which is often attributed to its adsorptive nature and greater porosity and surface area. In some cases, greater removal of BOM in GAC biofilters has been shown to coincide with higher biomass concentrations (Wang et al., 1995).

The objective of this study was to assess the impact of nutrient (i.e., nitrogen and phosphorus), oxidant (i.e., hydrogen peroxide) and media (i.e., GAC) enhancement strategies on effluent water quality and operational performance of pilot-scale biofilters. Nutrients were added to achieve a C:N:P molar ratio of 100:10:1. The study was carried out over a period of more than 24 months and involved monitoring general water quality parameters (i.e., TOC, DOC, specific UV absorbance at 254 nm [SUVA], DBPfp) and operational performance parameters (i.e., turbidity, head loss). While nutrient and/or oxidant addition has improved water quality and biofilter hydraulic performance in some investigations, broad applicability and improvement has yet to be demonstrated.

4.2 MATERIALS AND METHODS

4.2.1 Pilot Plant and Source Water Description

Pilot-scale biofiltration studies were conducted using source water from Pockwock Lake in Halifax, Canada. Source water quality for the study duration is described in detail in Chapter 2. Raw water turbidity and pH were stable during the study duration with quarterly averages between 0.30-0.50 NTU for turbidity and 5.3-5.9 for pH (Chapter 2). Raw water temperature varied seasonally with quarterly averages between 2 and 20°C (Chapter 2). Quarterly average raw water TOC and DOC concentration ranged from 2.8 to 3.3 mg/L and the fraction of DOC removed from coagulated raw water using biofiltration has been reported to be low for this source water (Chapter 2).

The pilot plant was operated to emulate the full-scale treatment process at the study site, which is also described in detail in Chapter 2. The pilot plant (Intuitech Inc., Salt Lake City, Utah) was comprised of two identical and parallel treatment trains. A schematic of the treatment trains is provided in Figure 4.1. Raw water from Pockwock Lake entered the first of three pre-mix tanks where mechanical mixing occurred. Lime was added in

the first pre-mix tank to adjust the pH for oxidization with potassium permanganate ($KMnO_4$). Carbon dioxide (to reduce the pH to the coagulation target which ranged from approximately 5.5-6.0) and coagulant (aluminum sulfate; 0.7-0.9 mg/L as aluminum) were added in the final pre-mix tank. Each pre-mix tank had a detention time of approximately 1 minute. Coagulation was followed by 3-stage flocculation at G-values of 30 s^{-1}, 20 s^{-1}, 10 s^{-1}, respectively. Flocculation stage detention times ranged from 16-19 minutes per flocculation basin. Flocculated water then entered the biofiltration skid. As shown in Figure 4.1, each skid housed 3 biofilters; two anthracite-sand biofilters (600 mm of anthracite over 300 mm of sand), which emulated the full-scale filter media configuration, and one anthracite-sand biofilter equipped with a granular activated carbon cap (150 mm of GAC over 450 mm of anthracite and 300 of mm sand). Media effective sizes were 0.89 mm (anthracite) and 0.52 mm (sand). Media uniformity coefficients were 1.67 mm (anthracite) and 1.53 mm (sand). GAC was 12X40 mesh. Filter loading rate was 4.4 m/h for an EBCT of 12.5 minutes. The pilot biofilters were equipped with continuous monitoring for filtration performance and operational parameters including effluent turbidity, particle count, head loss, filter run time and flow. In agreement with full-scale plant operational criteria, filters were equipped with automatic shut-offs and operated to not exceed an effluent turbidity of 0.2 NTU, a head loss of 2.15 m or a filter run time of 80 hours. These operational criteria typically resulted to two filter runs per week per biofilter. Filters were backwashed with filter effluent. Backwash consisted of an air scour phase, a combined air scour and water wash phase, and three water wash phases. Previous research at this facility demonstrated that parallel pilot plant trains could produce reasonably equivalent water quality to each other and to the full-scale water treatment plant (Knowles et al., 2012).

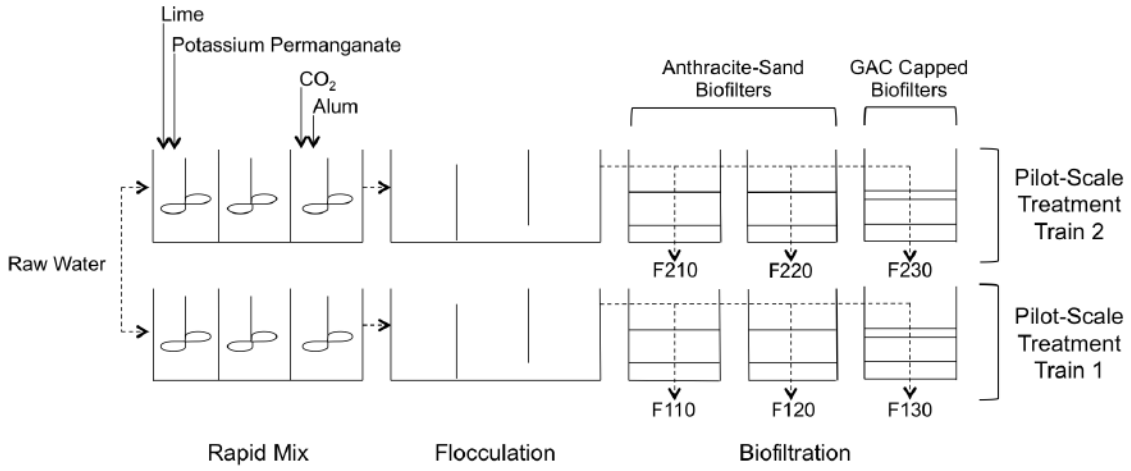

Figure 4.1 Pilot plant schematic for biofilter investigation

Study phases and durations are described in Table 4.1. Nutrients were dosed to achieve nutrient balance according to a C:N:P molar ratio of 100:10:1. Given a typical biofilter influent TOC concentration of approximately 3 mg/L, nitrogen and phosphorus were dosed at target concentrations of 0.351 mg NH_4-N/L and 0.078 mg PO_4^{3-}-P/L, respectively. Hydrogen peroxide was dosed at a target concentration of 0.4 mg/L.

Table 4.1 Biofilter investigation study phases

Treatment 1		Treatment 2		Phase Duration[a]—Days	Temperature—°C		
Enhancement Strategy	Biofilter No.	Enhancement Strategy	Biofilter No.		Mean ± SD	Min	Max
Ambient[b]	F210	Ambient	F220	487	12.2 ± 7.2	1.1	23.5
Ambient	F210	P	F220	355	11.0 ± 7.7	1.5	23.5
Ambient	F210	NP	F110	596	9.2 ± 7.0	1.1	22.5
Ambient	F210	NPOx	F120	596	9.2 ± 7.0	1.1	22.5
P	F220	NP	F110	232	7.5 ± 6.7	1.5	21.8
P	F220	NPOx	F120	232	7.5 ± 6.7	1.5	21.8
NP	F110	NPOx	F120	596	9.2 ± 7.0	1.1	22.5
Ambient	F210	Ambient (GAC cap)	F230	596	9.2 ± 7.0	1.1	22.5
NPOx	F120	NPOx (GAC cap)	F130	596	9.2 ± 7.0	1.1	22.5

[a]Excluding acclimation period (minimum of 8 weeks)

[b]All biofilter media configuration was 600 mm anthracite over 300 mm sand unless otherwise stated

Ambient—No enhancement strategy applied

N—Nitrogen enhancement with ammonium chloride addition at a target dose of 0.351 NH_4-N mg/L for a C:N molar ratio of 100:10

P—Phosphorus enhancement with phosphoric acid addition at a target dose of 0.078 mg PO_4-P/L for a C:P molar ratio of 100:1

Ox—Oxidant enhancement with hydrogen peroxide addition at a target dose of 0.4 mg/L

GAC Cap—150 mm of GAC over 450 mm anthracite and 300 mm of sand

4.2.2 Chemical Methods

Nitrogen (N), Phosphorus (P) and oxidant (Ox) enhancement was achieved using stock solutions prepared from ammonium chloride (NH_4Cl), concentrated phosphoric acid, and commercial grade 3% H_2O_2 dosed using peristaltic pumps. Enhancements were dosed in-line as water passed from the last flocculation tank to each biofilter. Nutrient and oxidant concentration were verified through sample ports located 150 mm above the media surface in each biofilter to ensure proper dosing. Nutrient concentrations were also measured in the biofilter effluents.

Total nitrogen concentration was determined using a Shimadzu Total Nitrogen unit (Shimadzu Corporation, Kyoto, Japan) measuring unit mounted on a Shimadzu TOC-V CPH (Shimadzu Corporation, Kyoto, Japan). Orthophosphate-phosphorus concentration was measured spectrophotometrically using a DR4000 (Hach, Loveland, CO) for on-site dose monitoring. Total phosphorus concentration was also monitored using inductively coupled plasma mass spectrometry (XSeries 2 ICPMS, Thermo Fisher Scientific, Inc., Waltham, MA) for reporting purposes. Hydrogen peroxide concentration was measured spectrophotometrically using a hydrogen peroxide test kit (Hach, Loveland, CO) according to the manufacturer's instructions.

The biodegradable dissolved organic carbon (BDOC) concentration of flocculated water was monitored approximately bi-monthly for the first year of filter operation. BDOC tests were performed following a procedure described by Servais et al. (1989) using organic carbon free glassware. BDOC was determined as the difference between the initial DOC at the time of preparation and the DOC after incubation at room temperature for 28 days.

Water quality samples were collected at a specific time (i.e., after 24 hours of filter run time) during each filter run to account for potential dynamic processes within each filter cycle. TOC and DOC samples were collected headspace free in baked (24 hours, 100°C) glass vials, acidified to pH <2 with phosphoric acid and stored at 4°C pending analysis using a TOC-V CPH analyzer (Shimadzu Corp, Kyoto, Japan). DOC samples were

filtered through 0.45 µm filter membranes prior to collection. SUVA was determined by dividing average DOC concentration by the average UV absorbance at 254 nm (UV_{254}). UV_{254} was measured in triplicate using a spectrophotometer (DR4000, Hach, Loveland, CO) after filtration through 0.45 µm filter membranes. Trihalomethane (THM) and total haloacetic acid (HAA) formation potential were determined using uniform formation conditions as described by Summers et al. (1996). THMs and HAAs resulting from this procedure were detected using gas chromatography with electron capture (CP-3800 Gas Chromatograph, Varian, Inc., Walnut Creek, California) according to US EPA methods 551.1 and 552.2, respectively.

4.2.3 Microbiological Techniques

Interstitial water from the biofilters was was analyzed for adenosine triphosphate (ATP) concentration. Interstitial water was collected from sample ports located at a media depth of 150 mm following 24 hours of filter run time. Samples were collected in sterile, 50 mL falcon tubes and measured on-site, immediately after sampling using a commercial ATP test kit (Quench Gone Aqueous, LuminUltra Technologies Ltd., Fredericton, Canada) and luminometer (PhotonMasterTM Luminometer, LuminUltra Technologies Ltd., Fredericton, Canada) according to the manufacturer's instructions. A 50 mL sample volume was used. This measurement was used to provide a non-invasive indication of the biomass response to enhancement strategies. This technique does not quantify biomass attached to filter media and can only quantify planktonic biomass, detached biomass and any growth associated with these two fractions.

4.2.4 Biofilter Operational Parameters

Filtered water turbidity and head loss were measured continuously during biofilter operation. Filtered water turbidity was measured continuously using inline turbidimeters (1720E low-range turbiditmeter, Hach, Loveland, USA). The reported accuracy of the turbidimeters was ±0.02 NTU. Head loss was measured continuously in each biofilter using pressure transmitters (WIKA ECO-1 pressure transmitter, Lawrenceville, USA).

The reported accuracy of the pressure transmitters was ≤1.0% (including non-linearity, hysteresis, zero point and full scale error) of an ideal span of 0 to 1 bar (i.e., 0 to 10 m).

Filter runs were not assessed based on the entire turbidity and head loss profile for each filter cycle since, while the majority of filter cycles were operated until the turbidity, head loss or filter run time limit was reached, not all filter cycles could be reasonably operated this way without 24-hour attendance. Therefore, for comparison purposes, turbidity and head loss measures were assessed following 20, 40 and 60 hours of filter run time. While 24 hours of filter run time was used for assessing water quality parameters, it was not used when assessing filter performance and operational parameters because flow changes as a result of sampling events for water quality parameters were found to briefly influence the inline turbidity measurements made at the 24-hour time point. To avoid this influence, the time of 20 hours was selected.

4.2.5 Statistical and Data Analysis

Any changes to enhancement strategy were followed by an 8-week conditioning phase. Any water quality or filter performance data gathered during conditioning phases was excluded from the analysis. The conditioning phase for GAC-capped biofilters was extended past this 8-week time frame to nearly 8 months, at which point the adsorptive capacity of the GAC was assumed to be exhausted.

Paired two-tailed t-tests were used to assess statistical significance between biofilter performance using a procedure similar to Knowles et al. (2012). The use of a 95% confidence interval can be too stringent for some parameter comparisons between parallel pilot trains, particularly for online parameters (Andrew et al., 2005). For this reason, alternate acceptable limits of difference can be established for parallel treatment train pilot plant configurations (Knowles et al., 2012; Andrews et al., 2005; Anderson et al., 1993). As a result, water quality and filter performance parameters in the current study were also compared against the mean difference measured between the two ambient

condition biofilters as a means to take into account the actual expected level of equivalence between parallel treatment trains.

4.3 RESULTS & DISCUSSION

4.3.1 Water Quality

4.3.1.1 Nutrient Enhancement

Average influent and effluent nutrient concentrations are provided in Table 4.2. Results showed that, on average, nitrogen and phosphorus dosing was within <10% of the target dose of 0.351 mg NH_4-N/L and 0.078 mg PO_4-P/L. Average phosphorus concentration was consistently lower in the biofilter effluents than in the influents. This reduction could be associated with microbial assimilation and/or adsorption to alum floc. Due to the direct filtration configuration, alum flocs were not removed through a clarification process (e.g., sedimentation) prior to biofiltration, potentially allowing for adsorption of supplemented phosphorus to this flocculated material (Lauderdale et al., 2014). Minimal reduction in nitrogen concentration across the biofilters was observed, indicating that discernible microbial assimilation of nitrogen did not occur. Flocculated water BDOC concentration ranged between 0.07 and 0.30 mg/L (average = 0.17 ± 0.09 mg/L), which corresponded to between 4 and 16% of the biofilter influent DOC concentration. This implied that, following coagulation/flocculation, only a small portion of the DOC typically remained amenable to biodegradation. Furthermore, the pilot plant did not have an oxidation step prior to filtration and it is expected that the amount of easily biodegradable organic matter (e.g., carboxylic acids) would be very low. As previously discussed, the C:N:P ratio used to determine the required nutrient doses was based on the typical TOC concentration (i.e., ~3 mg/L) of the biofilter influent. Given the portion of TOC that was actually bioavailable, very little nitrogen was required.

Table 4.2. Average influent and effluent nutrient concentrations. ± represents the standard deviation of the data

Biofilter		Total Phosphorus—*mg/L*		Total Nitrogen—*mg/L*	
		Influent	Effluent	Influent	Effluent
Anthracite	F210	NA	NA	NA	NA
	F220	0.085 ± 0.044	0.071 ± 0.089	NA	NA
	F110	0.080 ± 0.046	0.046 ± 0.062	0.322 ± 0.041	0.322 ± 0.150
	F120	0.087 ± 0.048	0.040 ± 0.047	0.353 ± 0.079	0.335 ± 0.078
GAC-Cap	F230	NA	NA	NA	NA
	F130	0.081 ± 0.040	0.048 ± 0.054	0.352 ± 0.094	0.338 ± 0.084

4.3.1.2 Adenosine Triphosphate

Planktonic cellular ATP concentrations from interstitial water sampled at a media depth of 150 mm typically ranged between 1000 and 3000 pg ATP/mL (Figure 4.2, Figure 4.3). Mean planktonic cellular ATP concentration differed by 8 pg/mL for the ambient biofilter comparison when all raw water temperatures were considered and 115 pg/mL when only temperatures ≥15°C were considered.

In comparison to the ambient biofilter, the mean planktonic cellular ATP concentration was typically higher for the biofilters that had nutrient and oxidant strategies applied (Table 4.2). However, only NPOx enhancement resulted in a statistically significant increase (p-value < 0.01) over the ambient condition (Table 4.3). NP and NPOx enhancement also typically increased the average planktonic cellular ATP concentration as compared to the P-enhanced biofilter. However only the NPOx enhancement strategy (across the entire temperature range) was statistically (p-value < 0.05) greater than the P-enhanced biofilter.

Several studies have observed increases in biomass quantity and/or activity as a result of nutrient addition (Sang et al., 2003; Lauderdale et al., 2012; Granger et al., 2014). It is possible that no impact on planktonic ATP concentrations were seen with nutrient enhancement alone because the microbial community was already adapted to a low

nutrient environment, given the low nitrogen and phosphorus concentrations in the source water (Rahman et al., 2016). Additionally, the sampling strategy in the current study only quantified planktonic ATP concentration within the biofilters and did not measure the ATP concentrations of any biofilm adhered to the filter media. Increases in planktonic cellular ATP concentrations with NPOx enhancement could be the result of several factors. It is possible that hydrogen peroxide oxidized NOM making it more bioavailable and able to support more biomass and/or that hydrogen peroxide reduced the formation of biofilms (Christensen et al., 1990) causing planktonic biomass to increase through biofilm detachment.

Media enhancement with a GAC cap under ambient conditions resulted in a statistically significant decrease in planktonic cellular ATP concentration when temperatures ≥15°C were considered. This indicated that there was less planktonic bacteria in the interstitial water after passing through a GAC-cap than after passing through an equivalent depth of anthracite, and potentially suggesting that an increase in biofilm formation and/or a decrease in biofilm detachment occurred at higher temperatures as a result of media enhancement. Under NPOx-enhanced conditions, media enhancement increased planktonic cellular ATP concentration, potentially reiterating the ability of GAC to support more biomass and the role of oxidant in the destruction of biofilms, however, the increase was not statistically significant. Measurement of attached biomass would be required to confirm these hypotheses.

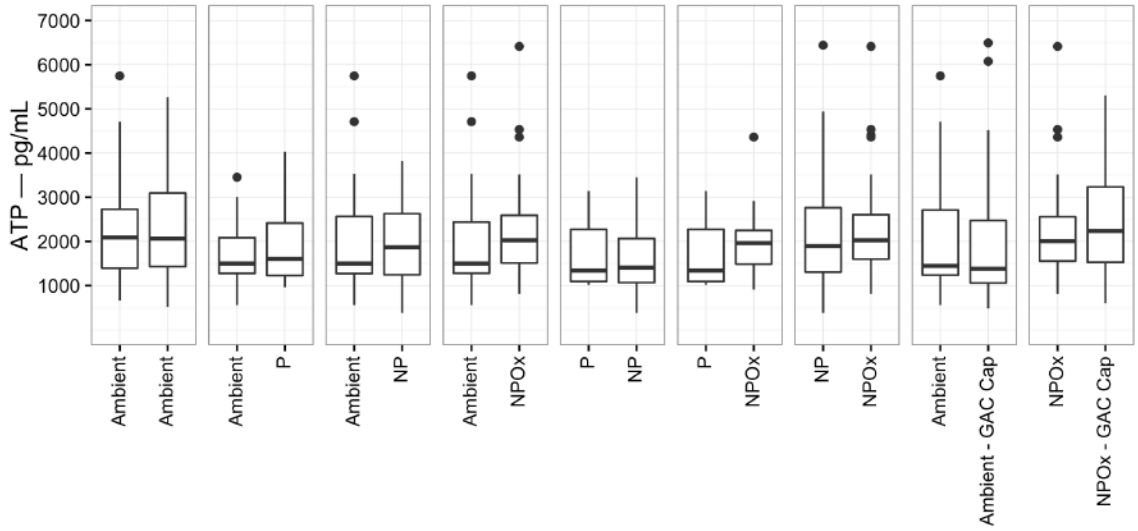

Figure 4.2 Cellular ATP concentration of interstitial water samples at a media depth of 150 mm following 24 hours of filter run time at all raw water temperatures

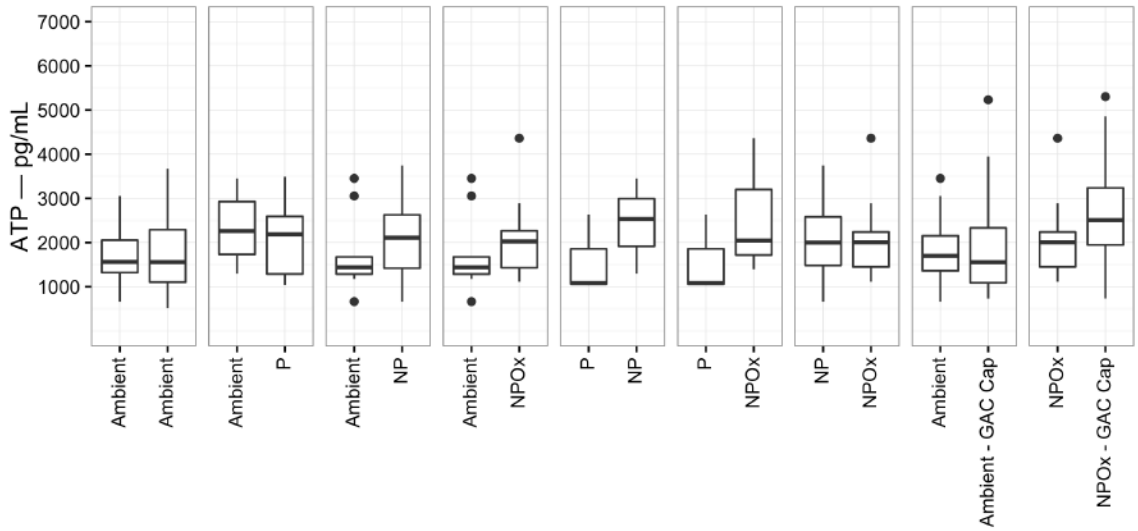

Figure 4.3 Paired comparisons of cellular ATP concentration of interstitial water sampled at a media depth of 150 mm following 24 hours of filter run time at raw water temperatures ≥15°C

Table 4.3 Paired comparisons of cellular ATP concentrations of interstitial water sampled at a media depth of 150 mm following 24 hours of filter run time at at all raw water temperatures and raw water temperatures ≥15°C

Treatment 1	Treatment 2	Cellular ATP			Cellular ATP (at T ≥ 15°C)		
		Mean Difference —pg/mL	n	p-value	Mean Difference —pg/mL	n	p-value
Ambient	Ambient	-8	21	0.972	-115	11	0.628
Ambient	P	-134	23	0.276	226	6	0.392
Ambient	NP	-150	39	0.301	-424	11	0.098
Ambient	NPOx	-301	37	**0.005**	-415	11	**0.005**
P	NP	58	14	0.760	-844	3	0.135
P	NPOx	-372	14	**0.036**	-1015	3	0.124
NP	NPOx	-108	39	0.439	5	12	0.984
Ambient	Ambient (GAC cap)	-7	35	0.959	365	11	**0.022**
NPOx	NPOx (GAC cap)	-278	38	0.106	-620	12	0.056

Mean differences were determined as Treatment 1 – Treatment 2

4.3.1.3 NOM removal

DOC removal across the pilot-scale biofilters was limited and similar to removals achieved by the full-scale treatment process. As described in Chapter 2, quarterly DOC percent removal across the full-scale biofilters ranged from 0.4-4.6%. NOM removed at the pilot-scale under ambient conditions ranged from 0.66-2.77 mg/L for TOC and -0.45-0.31 mg/L for DOC, resulting in an average study duration percentage removal of 40% for TOC and 0.2% for DOC. On a mass basis, the average DOC removal across the ambient biofilter was 6 µg/L, which was much less than was predicted to be biologically available based on average BDOC concentration (i.e., 0.17 mg/L). As with the full-scale plant at this location (Chapter 2), TOC removal across the biofilters at the pilot-scale was much greater than DOC removal as a result of particle removal associated with the direct filtration design of the treatment train.

In general, nutrient, oxidant and media enhancement did not impact effluent TOC, DOC or SUVA concentrations. Some statistically significant differences were observed for DOC (Table 4.4) as a result of enhancement strategies, however the observed mean

differences were small (i.e., ≤ 0.07 mg/l) and likely not of practical importance, especially given that a mean difference of up to 0.03 mg/L was observed for biofilters operated under equivalent conditions (i.e., the comparison between ambient condition biofilters at temperatures ≥ 15°C). In addition, using the same pilot-plant as the current study, Knowles et al. (2012) found that the magnitude of the TOC and DOC differences between the three pairs of pilot filters (Figure 4.1)ranged from 0.01-0.064 mg/L for TOC and 0.021-0.059 mg/L for DOC when operated under equivalent conditions. Given the magnitude of these differences, the significant results identified in the current study for the DOC parameter are likely not meaningful given measurement error.

This finding is in contrast with other studies where a statistically significant improvement in DOC (Lauderdale et al., 2012), TOC (Granger et al., 2014; Sang et al., 2003) and or BDOC (Sang et al., 2003) removal was observed with nutrient enhancement. For example, Lauderdale et al. (2012) found that, on average, nutrient enhancement of GAC biofilters at a C:N:P ratio of 100:10:2 removed 75% more DOC than the control with an average of 0.75 mg/L of DOC removed in the enhanced biofilter and 0.40 mg/L removed in the control biofilter. In this study, pilot-scale biofilters were packed entirely with GAC and temperatures were typically higher than the current study, ranging from 11-30°C. Additionally, this study was relatively short-term, with DOC removal data generated over a period of 2 weeks. Rahman et al. (2016) found that DOC removal was improved by P enhancement for the first month of supplementation; however, following this one month period, DOC removal dropped back to the same level as the control. Other studies have also found that nutrient enhancement was not effective at improving DOC (McKie et al., 2015; Azzeh et al., 2015; Lauderdale et al., 2014) and TOC (Vahala et al., 1998) removal. For example, Azzeh et al., (2015) found that nutrient enhancement of pilot-scale biofilters at C:N:P ratios of 100:30:2, 100:40:2 and 100:40:20 did not improve DOC removal and that, at a C:N:P ratio of 100:40:20, biopolymer removal decreased by 25%, prompting the conclusion that nutrient surpluses beyond 100:10:1 might be counter-productive.

It is possible that more DOC removal could be achieved with a more substantial GAC cap. Exhausted GAC is generally reported to out-perform anthracite for NOM removal, particularly at low temperatures (Emelko et al., 2006; Coffey et al., 1995; Liu et al., 2001) and in the presence of chlorinated backwash (Liu et al. 2001). This improved performance is typically attributed to the higher surface area and greater porosity of GAC as compared to anthracite. When only temperatures ≥15°C were considered, the effect of media enhancement on DOC removal was still positive but no longer statistically significant, suggesting that GAC may only reasonably be expected to provide additional DOC removal over anthracite for a fraction of the year (i.e., raw water temperatures are <15°C from mid-October to mid-June).

Table 4.4 Comparison of enhancement strategies for TOC, DOC and SUVA removal following 24 hours of filter run time at all raw water temperatures and raw water temperatures ≥15°C

Treatment 1	Treatment 2	Mean Difference —*mg/L*	n	p-value	Mean Difference —*mg/L*	n	p-value	Mean Difference —*L/mg-m*	n	p-value
		TOC			DOC			SUVA		
Ambient	Ambient	0.00	42	0.672	0.01	38	0.566	-0.03	36	0.296
Ambient	P	-0.02	28	0.426	0.04	29	0.060	0.00	23	0.878
Ambient	NP	0.04	40	0.072	0.05	39	**0.017**	0.03	40	0.296
Ambient	NPOx	0.02	41	0.272	0.02	39	0.206	0.03	34	0.489
P	NP	0.04	14	0.066	0.02	16	0.687	-0.02	11	0.581
P	NPOx	0.04	15	0.067	-0.01	16	0.768	0.01	12	0.734
NP	NPOx	0.00	44	0.806	-0.02	39	0.069	0.00	33	0.838
Ambient	Ambient (GAC cap)	0.02	37	0.646	0.04	37	**0.022**	-0.05	33	0.420
NPOx	NPOx (GAC cap)	0.02	46	0.164	0.03	40	**0.010**	0.01	33	0.534
		TOC (at T ≥ 15°C)			DOC (at T ≥ 15°C)			SUVA (at T ≥ 15°C)		
Ambient	Ambient	0.01	19	0.557	0.03	17	0.333	-0.07	15	0.180
Ambient	P	-0.03	16	0.374	0.07	18	**0.044**	-0.04	11	0.175
Ambient	NP	0.04	13	0.408	0.06	13	0.065	-0.06	10	0.214
Ambient	NPOx	0.01	14	0.724	0.01	13	0.740	-0.09	9	0.102
P	NP	0.05	5	0.262	-0.05	6	0.460	-0.07	3	0.191
P	NPOx	0.03	5	0.398	-0.10	6	0.125	-0.02	3	0.658
NP	NPOx	0.00	15	0.970	-0.04	14	**0.044**	-0.02	10	0.577
Ambient	Ambient (GAC cap)	0.03	13	0.059	0.06	13	0.111	-0.07	10	0.297
NPOx	NPOx (GAC cap)	0.02	17	0.277	0.04	14	0.243	0.01	11	0.736

Mean differences were determined as Treatment 1 – Treatment 2

4.3.1.4 Disinfection Byproduct Formation Potential

As shown in Table 4.5, nutrient, oxidant and media enhancement strategies resulted in reductions or increases in average HAAfp up to 2 µg/L when all raw water temperatures were considered and up to 5 µg/L when only raw water temperatures ≥15°C were considered. For the comparison between biofilters receiving NPOx enhancement, media enhancement resulted in a statistically significant reduction in HAAfp; however, the mean difference for this comparison was 2 µg/L. For THMfp, on average, nutrient and oxidant enhancement (i.e., P, NP and NPOx-enhancement) resulted in a small reduction in THMfp as compared to the ambient biofilter. However, this reduction was only statistically significant when the ambient and P-enhanced biofilters were compared. Large reductions in THMfp in the P-enhanced biofilter as compared to the ambient biofilter followed a non-systematic pattern, were highly inconsistent over time and only observed in 5 of the 15 sampling events (Supplementary Figure A.5), indicating that the reductions of THMfp may have been related to unidentifiable experimental error and further validation of the findings is required. The comparison between the ambient biofilter and the ambient media-enhanced biofilter at temperatures ≥15°C showed a similar result (Supplementary Figure A.6). Notably, biofilter comparisons that showed a statistically significant improvement in DOC removal (i.e., ambient vs. NP-enhanced, ambient vs. ambient media-enhanced, and NPOx-enhanced vs. NPOx and media enhanced) did not correspond with a statistically significant reduction in THMfp or HAAfp.

These findings support findings from a previous investigation where it was also found that nutrient enhancement (at C:N:P ratios of 100:30:2, 100:40:2 and 100:40:20) of pilot-scale biofilters did not improve THM or HAA precursor removal (Azzeh et al., 2015). Additionally, Azzeh et al. (2015) found that hydrogen peroxide dosed at 0.1 or 0.5 mg/L did not influence THM or HAA formation potentials in pilot-scale biofilters, but that a higher dose of 1 mg/L was effective at reducing THM and HAA formation potentials, possibly indicating that the oxidant enhancement dose used in the current study (i.e., 0.4 mg/L) was not sufficient to influence DBPfp (Table 4.5).

Table 4.5 Comparison of enhancement strategies for THMfp and HAAfp following 24 hours of filter run time

Treatment 1	Treatment 2	Mean Difference —µg/L	n	p	Mean Difference —µg/L	n	p
		THMfp			HAAfp		
Ambient	Ambient	0	22	0.935	0	22	0.862
Ambient	P	12	15	**0.021**	1	14	0.456
Ambient	NP	5	39	0.180	0	29	0.849
Ambient	NPOx	2	39	0.517	-1	31	0.301
P	NP	5	13	0.635	0	11	0.944
P	NPOx	-6	14	0.213	-2	14	0.419
NP	NPOx	-4	41	0.326	-1	30	0.230
Ambient	Ambient (GAC cap)	6	38	0.127	1	31	0.419
NPOx	NPOx (GAC cap)	0	40	0.998	-1	33	0.471
		THMfp (at T ≥ 15°C)			HAAfp (at T ≥ 15°C)		
Ambient	Ambient	-1	9	0.804	0	4	0.949
Ambient	P	14	4	0.218	1	4	0.554
Ambient	NP	1	13	0.806	-5	6	0.170
Ambient	NPOx	3	14	0.408	-5	8	0.110
P	NP	-8	3	0.259	NA	NA	NA
P	NPOx	-8	4	0.233	-3	4	0.281
NP	NPOx	3	14	0.304	-2	5	0.119
Ambient	Ambient (GAC cap)	14	14	**0.004**	-1	8	0.443
NPOx	NPOx (GAC cap)	1	15	0.822	2	8	**0.014**

Mean differences were determined as Treatment 1 – Treatment 2

4.3.1.5 Effluent Turbidity and Head Loss Development

Effluent turbidity was evaluated at 20, 40 and 60 hours of filter run time at all temperatures (Figure 4.4) and at temperatures ≥ 15°C (Figure 4.5). Effluent turbidities were typically higher when all temperatures were considered than when only temperatures ≥15°C were considered. This was likely the result of a reduction in coagulation and flocculation efficiency at low temperature which was also observed in the full-scale plant at this location (Chapter 2).

As shown in Table 4.6, enhancement strategies occasionally resulted in a statistically significant impact on 20, 40 and 60 hour effluent turbidity. However, a statistically significant difference between biofilters operated under equivalent ambient conditions was also identified for 40 and 60 hour effluent turbidity when all temperatures were considered. This indicated that a 95% confidence interval was too stringent to assess for a meaningful difference in effluent turbidity between biofilters as a result of enhancement strategy.

As shown in Table 4.6, significant mean differences for effluent turbidity ranged between 0.007 and 0.043 NTU. Mean differences at the lower bound of this range were likely not meaningful given the reported accuracy of the online turbiditmeters used in the study (i.e., ± 0.02 NTU). Similarly, the larger mean differences at the upper bound of this range were likely not meaningful given the level of equivalence that can reasonably be expected from the parallel pilot trains. For example, using the same pilot plant as the current study, Knowles et al. (2012) found that the magnitude of the turbidity differences between the three pairs of pilot filters (i.e., F110 and F210, F120 and F220 and F130 and F230; Figure 4.1) ranged from 0.008-0.044 NTU, when operated under equivalent conditions. Given the magnitude of the significant mean differences, the significant results identified in the current study for the turbidity parameter were likely not the result of the various enhancement strategies. The turbidity results of this study were consistent with other findings (Lauderdale et al., 2012; Lauderdale et al., 2014). For example, Lauderdale et al. (2012) did not observe significant changes in turbidity breakthrough in pilot-scale biofilters as a result of nutrient enhancement at a target C:N:P ratio of 100:10:1 or oxidant enhancement with hydrogen peroxide at a target dose of 1 mg/L.

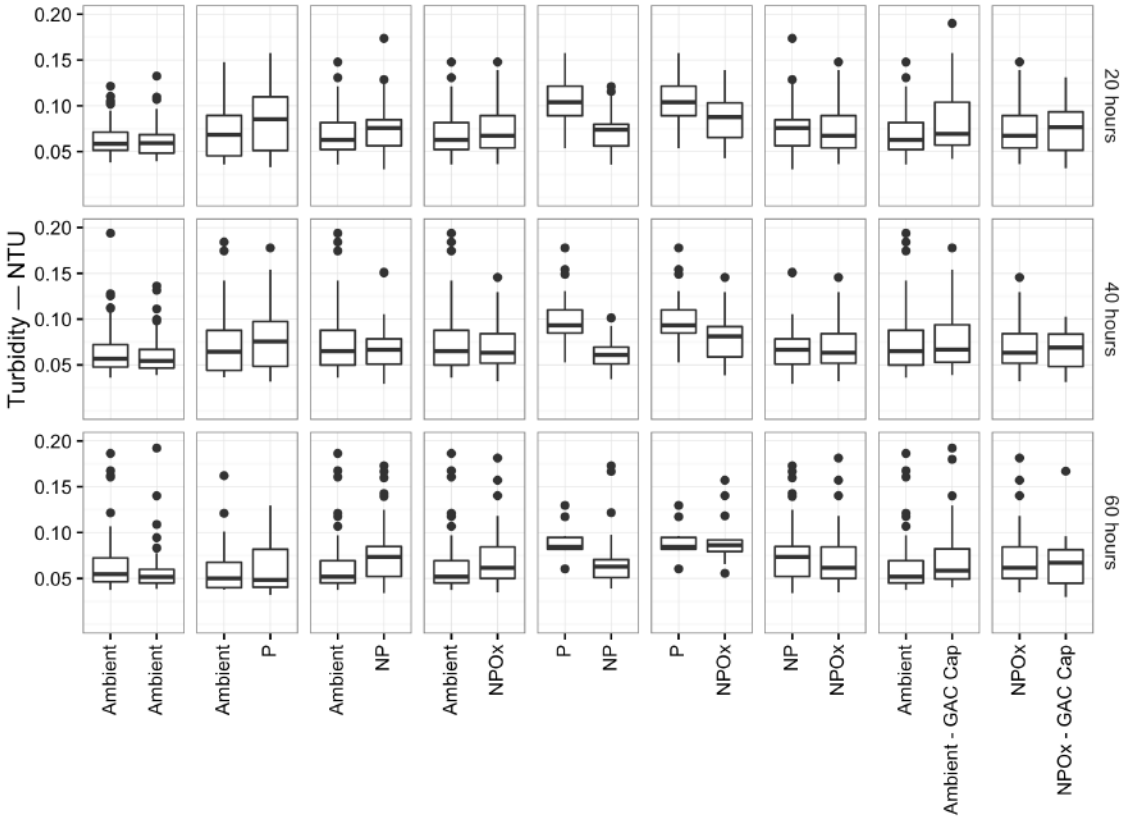

Figure 4.4 Paired comparisons of biofilter effluent turbidity following 20, 40 and 60 hours of filter run time

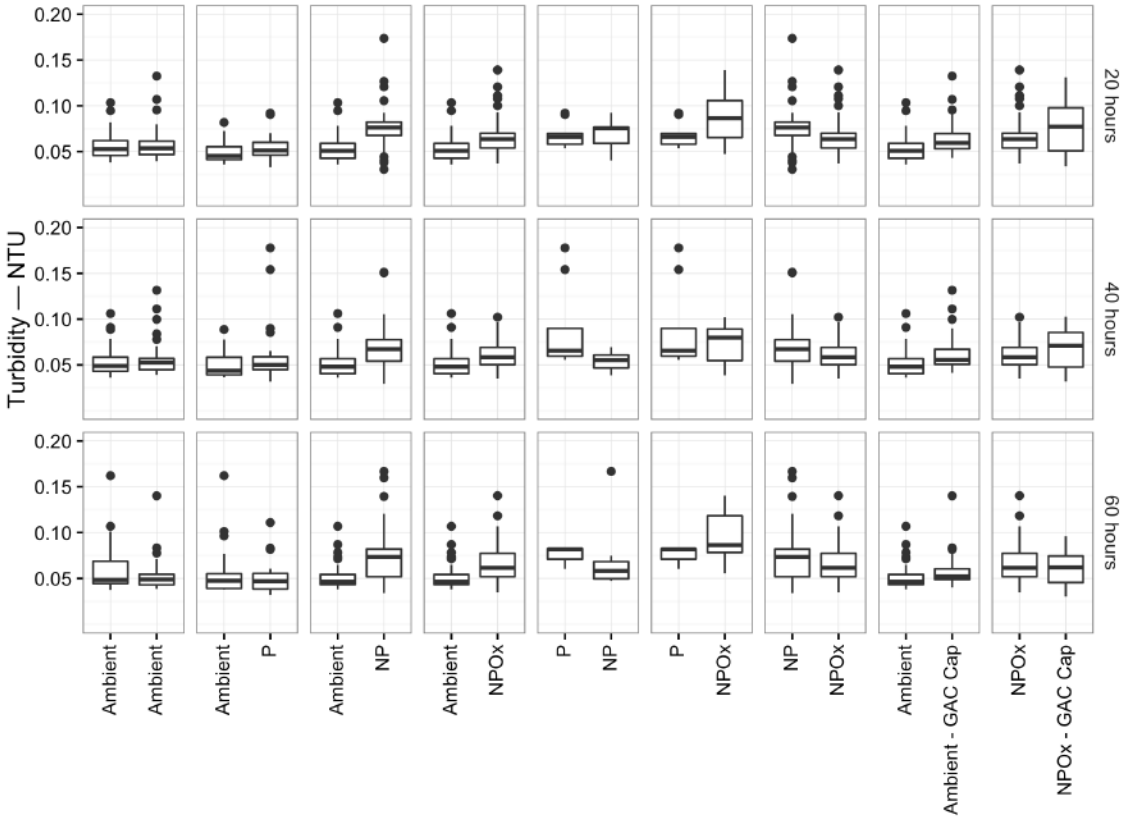

Figure 4.5 Paired comparisons of filtered water turbidity following 20, 40 and 60 hours of filter run time at raw water temperature ≥15°C

Table 4.6 Paired comparisons of filtered water turbidity following 20, 40 and 60 hours of filter run time at all raw water temperatures and raw water temperature ≥15°C

Treatment 1	Treatment 2	Filter Run Time	Turbidity			Turbidity (at T ≥ 15°C)		
			Mean Difference*	n	p	Mean Difference*	n	p
		—h	*—NTU*			*—NTU*		
Ambient	Ambient	20	0.001	97	0.330	-0.002	48	0.229
		40	0.007	88	**0.004**	-0.002	46	0.151
		60	0.010	59	**0.014**	0.007	37	0.116
Ambient	P	20	-0.011	77	**0.000**	-0.005	34	0.103
		40	0.001	63	0.670	-0.002	30	0.537
		60	0.001	27	0.863	0.000	21	1.000
Ambient	NP	20	0.005	108	0.115	-0.025	35	**0.000**
		40	0.004	77	0.344	-0.020	29	**0.000**
		60	-0.010	32	0.188	-0.028	19	**0.001**
Ambient	NPOx	20	-0.003	102	0.208	-0.011	34	**0.005**
		40	0.003	72	0.294	-0.007	29	0.116
		60	-0.002	28	0.768	-0.011	17	0.013
P	NP	20	0.030	42	**0.000**	0.001	9	0.884
		40	0.036	33	**0.000**	0.043	8	**0.018**
		60	0.023	4	**0.018**	NA	NA	NA
P	NPOx	20	0.015	40	**0.000**	-0.004	9	0.447
		40	0.017	32	**0.002**	0.028	8	0.156
		60	-0.007	3	0.184	NA	NA	NA
NP	NPOx	20	-0.002	122	0.498	0.003	47	0.616
		40	-0.005	101	0.104	0.003	43	0.579
		60	-0.005	46	0.292	-0.005	24	0.455
Ambient	Ambient (GAC cap)	20	-0.010	126	**0.000**	-0.012	37	**0.000**
		40	0.002	100	0.517	-0.009	34	**0.000**
		60	0.000	42	0.962	-0.005	24	0.202
NPOx	NPOx (GAC cap)	20	-0.002	121	0.409	-0.007	48	**0.025**
		40	0.001	104	0.475	-0.006	46	0.061
		60	0.005	44	0.147	0.008	21	0.141

Mean differences were determined as Treatment 1 – Treatment 2

Head loss was also evaluated at 20, 40 and 60 hours of filter run time at all temperatures (Figure 4.6) and at temperatures ≥ 15°C (Figure 4.7). As shown in Table 4.7, enhancement strategies frequently resulted in a statistically significant impact on 20, 40 and 60 hour head loss, especially when NPOx enhancement and NPOx and media enhancement were applied. However, a statistically significant difference between biofilters operated under equivalent ambient conditions was also identified for the comparison between ambient biofilter head loss at all time points for all temperatures and for temperatures ≥15°C, indicating that a 95% confidence interval was too stringent to assess for a meaningful difference in head loss between biofilters as a result of enhancement strategy.

Using the mean differences identified in the comparison between the two ambient biofilters (i.e., 0.02 – 0.07 m) and the reported accuracy of the pressure transmitters (i.e., ≤ 0.1 m) as a reference point for meaningful difference, meaningful differences for the NPOx-enhanced biofilter as compared to the ambient biofilter and the NPOx and media-enhanced biofilter as compared to the NPOx-enhanced bifilter were identified. Meaningful mean differences were also identified for the P and NP-enhanced comparison and the P and NPOx-enhanced comparison following 60 hours of filter run time, however, sample sizes were too small to have confidence in the result (i.e., n=2-4).

Focusing on the comparison between the ambient biofilter and the NPOx-enhanced biofilter at all temperatures, NPOx enhancement resulted in a statistically significant 27%, 7% and 9% reduction in average head loss at 20, 40 and 60 hours of filter run time, respectively. These percent reductions were similar to those reported in other studies as a result of nutrient enhancement but lower than those reported as a result of oxidant enhancement (Lauderdale et al., 2012; Lauderdale et al., 2014; Azzeh et al., 2015).

In nutrient enhancement studies, Lauderdale et al. (2012) found that nutrient enhancement at a target C:N:P ratio of 100:10:2 decreased biofilter terminal head loss by 15% as compared to a control. In a subsequent study involving pilot plants in Dallas and Tampa Bay, Lauderdale et al. (2014) found that nutrient enhancement at a target C:N:P

ratio of 100:10:1 did not provide expected improvement to hydraulic performance (i.e., head loss). This result was attributed to the biofilter influent pH and ferric hydroxide floc carryover impacting the bioavailability of the supplemented phosphorus and the use of liquid ammonium sulfate as the NH_4-N source. When liquid ammonium sulfate was not used and pH was adjusted to inhibit phosphorus adsorption to floc carryover, nutrient enhancement (C:N:P of 100:>10:>1) resulted in an 18 (Dallas) and 35% (Tampa Bay) decrease in terminal head loss as compared to the controls. The presence of floc carryover on the bioavailability of phosphorus could also explain why nutrient enhancement alone did not statistically improve hydraulic performance in the current study. Due to the direct filtration design of the treatment process, all floc material was carried over to the biofilters. Influent pH to the biofilters was equivalent to the target coagulation pH which typically ranged between 5.5 and 6.0. This pH range is amenable to phosphorus adsorption to alum floc (Kim et al., 2002).

In initial oxidant enhancement studies with hydrogen peroxide at a dose of 1 mg/L under ambient nutrient conditions (C:N:P ratio of 100:3:0), Lauderdale et al. (2012) found that oxidant enhancement decreased terminal head loss by up to 60% as compared to a control. In subsequent oxidant enhancement studies in Dallas and Tampa Bay, Lauderdale at al. (2014) found that a hydrogen peroxide at a dose of 0.1 mg/L reduced terminal head loss by up to 33% compared to the control at one location and by up to 25% compared to the control with a dose of 1.0 mg/L at the other location. Similarly, Azzeh et al. (2015) found that oxidant enhancement at 0.5 and 1 mg/L of H_2O_2 resulted in a statistically significant ($\alpha = 0.05$) reduction in head loss of 48 and 40% over a control. Combined with the results in the current study, these results indicate the importance of determining a matrix specific oxidant dose. It is possible that additional improvement in hydraulic performance could have been realized in the current study if the oxidant dose had been optimized.

Focusing on the comparison between the NPOx-enhanced biofilter and NPOx- and media-enhanced biofilter at all temperatures, media enhancement resulted in a statistically significant 111%, 23% and 16% increase in average head loss at 20, 40 and

60 hours of filter run time, respectively. However, overall, while statistically significant and typically consistent with findings by others, the observed increases and reductions in head loss as a result of enhancements were limited, given the accuracy of the pressure transmitters used and the level of equivalence between parallel treatment trains. Any observed reductions in head loss would likely be insufficient to warrant application of these enhancement strategies in the full-scale plant at this location.

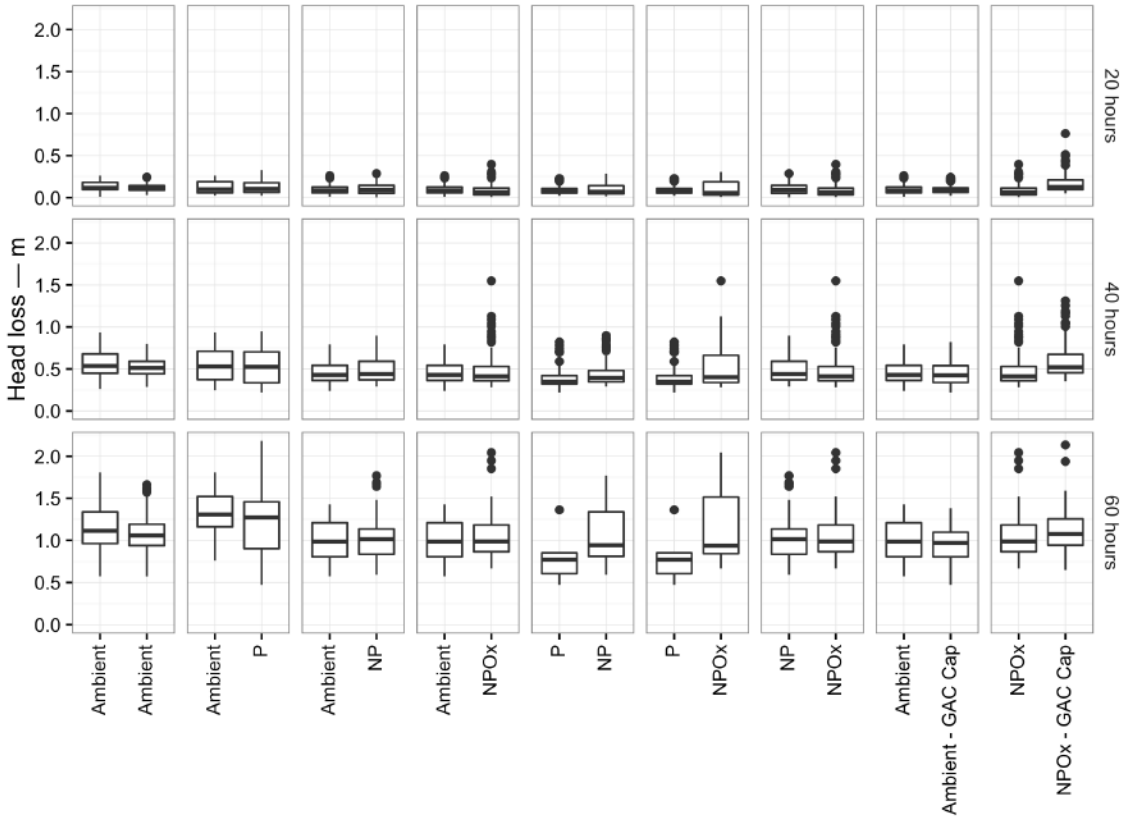

Figure 4.6 Paired comparisons of biofilter head loss following 20, 40 and 60 hours of filter run time

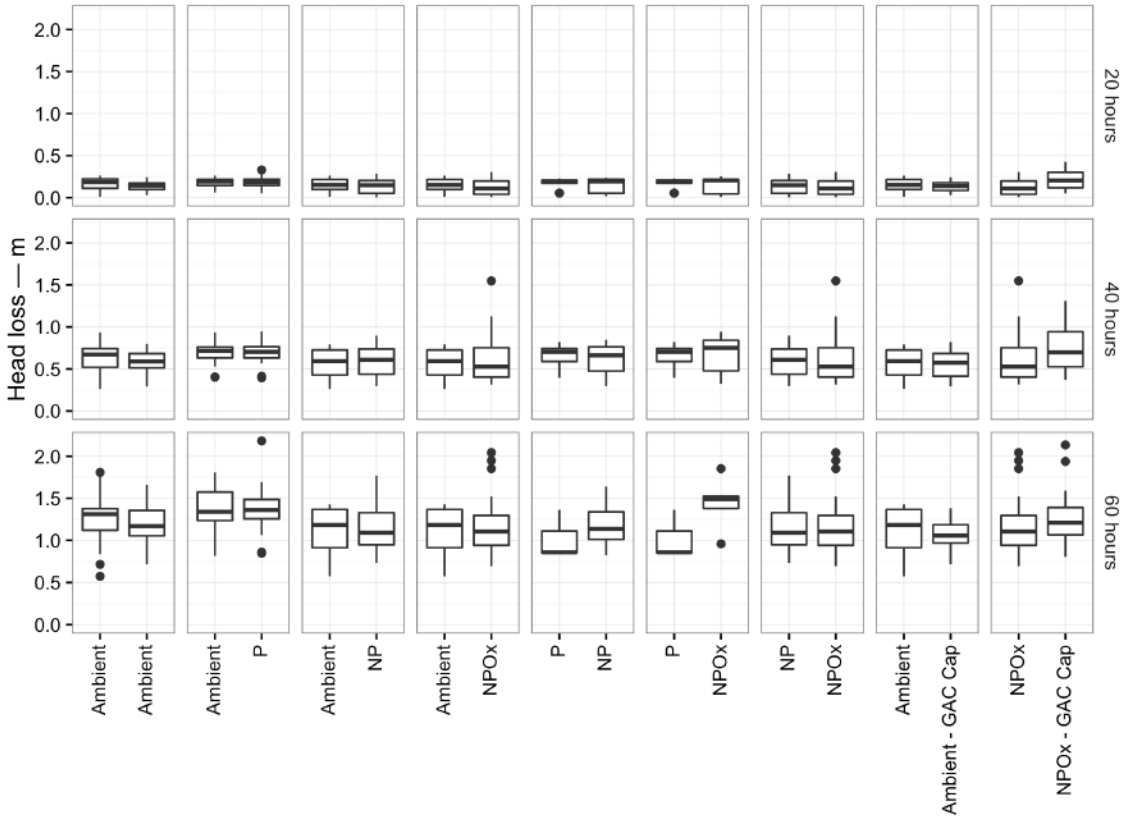

Figure 4.7 Paired comparisons of biofilter head loss following 20, 40 and 60 hours of filter run time at a raw water temperature of ≥15°C

Table 4.7 Paired comparisons of filtered water head loss following 20, 40 and 60 hours of filter run time at raw water temperature ≥15°C

Treatment 1	Treatment 2	Filter Run Time	Head loss			Head loss (at T ≥ 15°C)		
			Mean Difference*	n	p	Mean Difference*	n	p
		—h	*—m*			*—m*		
Ambient	Ambient	20	0.02	97	**0.000**	0.03	48	**0.000**
		40	0.03	88	**0.000**	0.05	46	**0.000**
		60	0.05	59	**0.010**	0.07	37	**0.002**
Ambient	P	20	-0.01	77	0.282	0.00	34	0.592
		40	0.01	63	0.163	0.00	30	0.757
		60	0.03	27	0.355	0.03	21	0.423
Ambient	NP	20	0.00	108	0.721	0.02	35	**0.001**
		40	0.00	77	0.900	0.02	29	0.156
		60	0.05	32	0.176	0.10	19	**0.038**
Ambient	NPOx	20	0.03	102	**0.000**	0.05	34	**0.000**
		40	0.03	72	**0.007**	0.07	29	**0.006**
		60	0.10	28	**0.006**	0.18	17	**0.000**
P	NP	20	0.01	42	0.255	-0.01	9	0.247
		40	-0.02	33	0.085	-0.02	8	0.423
		60	-0.11	4	**0.031**	-0.14	2	0.218
P	NPOx	20	0.02	40	**0.003**	-0.01	9	0.182
		40	-0.03	32	**0.015**	-0.07	8	**0.010**
		60	-0.11	3	**0.031**	NA	NA	NA
NP	NPOx	20	0.03	122	**0.000**	0.02	47	**0.000**
		40	0.01	101	**0.030**	0.01	43	0.542
		60	-0.01	46	0.490	-0.02	24	0.574
Ambient	Ambient (GAC cap)	20	0.00	126	0.338	0.02	37	**0.004**
		40	0.02	100	**0.000**	0.03	34	**0.010**
		60	0.03	42	0.208	0.06	24	0.054
NPOx	NPOx (GAC cap)	20	-0.09	121	**0.000**	-0.10	48	**0.000**
		40	-0.11	104	**0.000**	-0.13	46	**0.000**
		60	-0.16	44	**0.000**	-0.22	21	**0.000**

Mean differences were determined as Treatment 1 – Treatment 2

4.4 CONCLUSIONS

Nutrient, oxidant and media enhancement strategies were applied to pilot-scale biofilters with the objective of enhancing biodegradation to improve effluent water quality (e.g., TOC, DOC, SUVA, THMfp, HAAfp) and filter performance (e.g., effluent turbidity and head loss). While some statistically significant ($\alpha = 0.05$) mean differences in DOC and DBPfp removal were identified with specific enhancement strategies, enhancement strategies did not result in improvements in water quality (as measured by TOC, DOC, SUVA and DBPfp) that could be considered of practical operational importance. Water quality improvements were either operationally inconsistent, small in magnitude and/or within the deviation that would be expected from the biofilters even when operated under equivalent ambient (i.e., not enhanced) conditions. The treatment train did not include ozonation and the biofilter influent water had a low fraction of biodegradable organic matter, which may have contributed to the lack of observed improvement in NOM removal and DBP formation potential with the attempted enhancements.

With respect to filter performance, enhancement strategies occasionally resulted statistically significant increases or decreases in effluent turbidity and head loss. However, increases or decreases in effluent turbidity were deemed not meaningful given the instrument accuracy (i.e., ±0.02 NTU), their relatively small magnitude, and the magnitude of the deviation observed between biofilters operated under equivalent ambient conditions. With respect to head loss, NPOx enhancement resulted in a statistically significant reduction in head loss as compared to the control biofilter operated under ambient conditions, and NPOx combined with media enhancement resulted in a statistically significant increase in head loss as compared to the NPOx-enhanced biofilter. These head loss results were largely consistent with the literature and were considered meaningful given the magnitude of the deviation between ambient biofilters and the accuracy of the pressure transmitters. However, the magnitude of the meaningful mean differences that showed improvements to head loss were small (10 cm at T=1.1-22.5°C and 18 cm at T ≥15°C for a run time of 60 hours), and likely would not

be sufficient to substantially extended filter run times to have practical operational significance for the full-scale plant at this location.

CHAPTER 5 BACTERIAL COMMUNITY STRUCTURE IN NUTRIENT- AND OXIDANT-ENHANCED DRINKING WATER BIOFILTRATION

ABSTRACT

The objective of this full- and pilot-scale study was to investigate the impact of nutrient and oxidant enhancement strategies on the microbial community structure of drinking water biofilters. Three enhanced treatment biofilters were operated at pilot-scale to compare and contrast the microbial community structures. Enhancement strategies included addition of phosphorus alone (P-enhanced), combined addition of nitrogen and phosphorus (NP-enhanced) and combined addition of nitrogen, phosphorus, and hydrogen peroxide (NPOx-enhanced). Two ambient full-scale biofilters were operated in parallel with the three enhanced treatment pilot-scale biofilters and one ambient pilot-scale biofilter. NP-enhancement and NPOx-enhancement resulted in an increase in biomass, as measured by ATP, over the ambient pilot-scale biofilter. Comparatively, P-enhancement alone did not increase biomass as compared to the ambient pilot-scale biofilter. Overall, the results suggested a response in microbial community structure when NP- and NPOx-enhancments were applied as compared to the ambient biofilter, but the P-enhanced and ambient biofilters had similar microbial communities. The abundance of select functionally significant genera varied with respect to biofilter scale (i.e. full- vs. pilot-scale) and enhancement strategy. Most notably, the abundances of *Nitrospira* and *Bradyrhizobium* were greater in the NP- and NPOx-enhanced biofilters than in the full- or pilot-scale ambient biofilters. Despite increases in biomass and changes in microbial community structure, effluent water quality (e.g., total and dissolved organic carbon, UV absorbance at 254 nm, specific UV absorbance at 254 nm and disinfection byproduct formation potential) was similar for full-scale ambient biofilters and pilot-scale ambient and enhanced biofilters.

5.1 INTRODUCTION

Biofiltration, often in conjunction with other treatment steps such as coagulation/flocculation and ozonation, has been used to remove a variety of contaminants from drinking water, including biodegradable organic matter (BOM), manganese (Mn), taste and odour compounds, and disinfection byproduct (DBP) precursors. In drinking water biofiltration, indigenous bacteria from the source water form biofilms on granular filter media and biodegrade certain contaminants.

Recently, studies have investigated strategies to improve the biological ability to control contaminants and/or limit the potentially negative effects of biofilm on biofilter hydraulic performance (e.g., head loss) (Vahala et al., 1998; Sang et al., 2003; Lauderdale et al., 2012; Lauderdale et al., 2014; Azzeh et al., 2014; Granger et al., 2014; McKie et al., 2015; Rahman et al., 2016). Many of these studies have focused on enhancing biofilter performance by adjusting the biofilter influent carbon:nitrogen:phosphorus (C:N:P) molar ratio to approach a C:N:P ratio of 100:10:1, the approximate ratio—derived from the gross composition of microbial biomass ($C_5H_7NO_2P_{1/30}$)—at which carbon, nitrogen and phosphorus are required by microorganisms (Van der Kooij et al., 1982; LeChevallier and McFeters, 1985; LeChevallier et al., 1991).

The effect of nutrient enhancement (i.e., N and P addition) on contaminant removal in biofilters has been variable. Lauderdale et al. (2012) reported improved control of 2-methylisoborneol (MIB), manganese (Mn), and dissolved organic carbon (DOC), as well as reduced terminal head loss with phosphorus (0.02 mg/L) enhancement of pilot-scale GAC biofilters. Similarly, Granger et al. (2014) found that a phosphorus dose of 0.02 or 0.20 mg/L supported increased Mn and DOC removal over a control biofilter. Rahman et al. (2016) found an initial 6% increase in DOC removal with phosphorus enhancement (0.01 mg P/L) of a pilot-scale anthracite-sand biofilter as compared to a control; however, improvement was not sustained past 40 days of operation and did not reoccur following a subsequent increase in phosphorus dose (0.05 mg P/L). Other researchers have found that combined nitrogen and phosphorus enhancement did not significantly improve DOC,

biopolymer or DBP precursor removal in pilot-scale anthracite-sand biofilters (Azzeh et al., 2014; Mckie et al., 2015). Similarly, Vahala et al. (1998) found no improvement in total organic carbon (TOC), assimilable organic carbon (AOC) or UV absorbance at 254 nm (UV_{254}) removal with phosphorus or nutrient cocktail enhancement of pilot-scale GAC biofilters.

While the impact of nutrient enhancement on treatment performance has been variable, the impact of H_2O_2 addition on hydraulic performance of biofilters has been positive thus far (Lauderdale et al., 2012; Azzeh et al., 2014; Lauderdale et al., 2014). Lauderdale et al. (2012) reported a ~60% reduction in terminal head loss of pilot-scale GAC biofilters with 1 mg/L H_2O_2 addition, and Azzeh et al. (2014) found that low doses (0.1-1 mg/L) of H_2O_2 reduced head loss by 9-48% in pilot-scale anthracite-sand biofilters.

Although hydraulic improvements have been observed, previous studies have reported that biomass concentrations (measured as ng ATP/cm^3 dry media) do not correspond to substrate removal as measured by DOC (Pharand et al., 2014). With respect to nutrient enhancement, other researchers have found greater quantities of attached biomass (measured as g ATP/ mL or g of media) in nutrient-enhanced biofilters (Lauderdale et al., 2012; Granger et al., 2014). However, in other cases, nutrient enhancement did not result in significantly increased or decreased biomass concentrations, measured as pg ATP/g media (McKie et al., 2015) and measured as nmol ATP/g dry media (Vahala et al., 1998).

As the literature contains conflicting findings on the impact of nutrient enhancement on contaminant removal in biofilters, a missing component in understanding the connection between nutrient enhancement and biofilter performance might be the structure of the microbial community itself. Further, the microbial community structure might also provide clues as to why substrate removal (e.g., DOC removal) does not necessarily correspond to biomass concentration in biofilters (e.g., Pharand et al., 2014). Additionally, bacterial communities in biofilters have been shown to impact the bacterial communities in filter effluents (Lautenschlager et al., 2014; Pinto et al., 2012), which

makes microbial community structure in biofilters important to downstream water quality.

The objective of this investigation was to understand the impact of nutrient- and oxidant-enhancement strategies on the microbial community structure of drinking water biofilters using DNA sequencing. Two ambient (non-enhanced) full-scale biofilters were operated in parallel for this work. In addition, one ambient and three enhanced pilot-scale biofilters were sampled to compare and contrast the microbial community structures. Enhancement strategies included the addition of phosphorus alone (P-enhanced), combined addition of phosphorus and nitrogen (NP-enhanced) and combined addition of phosphorus, nitrogen, and hydrogen peroxide (NPOx-enhanced). Analysis of biofilters involved monitoring biofilter operational parameters (e.g., hydraulic loading rate, UFRV, head loss), general water quality parameters (e.g., TOC, DOC, specific UV absorbance at 254 nm (SUVA), disinfection byproduct formation potential (DBPfp)) and biomass concentration (ATP).

5.2 MATERIALS AND METHODS

5.2.1 Source Water

Four sampling events were conducted over a period of four months (May-August) at the JD Kline Water Supply Plant and associated pilot plant in Halifax, Canada. Average source water temperature was 8.4°C, 16.3°C, 19.1°C and 22.2°C for the May, June, July and August sampling events, respectively. Source water and average biofilter influent water quality during each sampling event is given in Table 5.1.

Table 5.1 Average raw water and biofilter influent TOC, DOC, UV_{254} and SUVA values. ± represents the standard deviation of two triplicate measures.

Sample Month	TOC—mg/L	DOC—mg/L	UV_{254}—cm^{-1}	SUVA—*L/mg-m*
		Raw Water		

May	3.06 ± 0.09	3.03 ± 0.02	0.130 ± 0.006	4.27 ± 0.17
June	2.81 ± 0.04	2.73 ± 0.04	0.108 ± 0.002	3.95 ± 0.07
July	2.95 ± 0.07	3.15 ± 0.15	0.093 ± 0.001	3.07 ± 0.11
August	2.97 ± 0.08	3.00 ± 0.06	0.086 ± 0.001	2.89 ± 0.08
		Pilot-Scale Train 1 Biofilter Influent		
May	3.07 ± 0.06	2.31 ± 0.04	0.057 ± 0.004	2.95 ± 0.12
June	2.96 ± 0.10	1.72 ± 0.03	0.038 ± 0.003	2.21 ± 0.06
July	3.03 ± 0.05	2.19 ± 0.05	0.038 ± 0.000	1.77 ± 0.01
August	3.24 ± 0.22	2.17 ± 0.16	0.035 ± 0.001	1.74 ± 0.04
		Pilot-Scale Train 2 Biofilter Influent		
May	3.04 ± 0.06	2.29 ± 0.03	0.053 ± 0.003	2.75 ± 0.05
June	2.83 ± 0.04	1.87 ± 0.03	0.043 ± 0.001	2.29 ± 0.03
July	3.03 ± 0.08	2.03 ± 0.10	0.039 ± 0.001	1.88 ± 0.10
August	3.07 ± 0.09	1.89 ± 0.03	0.038 ± 0.002	2.04 ± 0.10
		Full-Scale Biofilter Influent		
May	3.00 ± 0.06	2.30 ± 0.02	0.050 ± 0.004	2.57 ± 0.10
June	2.73 ± 0.11	1.72 ± 0.05	0.039 ± 0.002	2.30 ± 0.07
July	2.71 ± 0.19	2.15 ± 0.10	0.039 ± 0.003	1.83 ± 0.17
August	3.01 ± 0.33	2.05 ± 0.08	0.037 ± 0.001	1.84 ± 0.05

5.2.2 Full- and pilot-scale plant configuration and operation

A schematic of the full- and pilot-scale treatment trains is provided in Figure 5.1. General full-scale biofilter performance and operation is described in detail in Chapters 2 and 3. In brief, at the time of this study, the treatment train prior to biofiltration consisted of withdraw from Pockwock Lake, pH adjustment with lime, potassium permanganate addition for iron and manganese oxidation, pH adjustment with carbon dioxide (CO_2), aluminum sulphate addition for coagulation, three-stage hydraulic flocculation and direct biofiltration through anthracite-sand media.

The pilot plant (Intuitech Inc., Salt Lake City, Utah) was comprised of two identical parallel treatment trains. These were operated to mirror the full-scale treatment train chemical dosages and pH targets for potassium permanganate pre-oxidation and aluminum sulfate coagulation, which varied depending on full-scale plant performance. In the pilot plant configuration, raw water entered the first of three pre-mix tanks where

mechanical mixing occurred for pre-oxidation and chemical addition. Lime was added in the first pre-mix tank to adjust the pH for pre-oxidation with potassium permanganate. In the final pre-mix tank, CO_2 was added to reduce the pH to the coagulation target, and aluminum sulphate was added as the coagulant. The pre-mix process was followed by three-stage flocculation and direct biofiltration through four independent anthracite-sand biofilters.

The pilot-scale biofilters were equipped with continuous monitoring for filter performance parameters including effluent turbidity, particle count, head loss, filter run time and flow to ensure that pilot-scale filter performance mirrored the full-scale treatment train. Previous research at this facility demonstrated that the parallel pilot-scale trains could produce reasonably equivalent water quality to each other (Chapter 4) and to the full-scale plant (Knowles et al., 2012). Pilot-scale biofilters were operated to emulate the full-scale hydraulic conditions to the greatest extent possible. The average hydraulic loading rate, average unit filter run volume (UFRV) and average 48-h terminal head loss for the four monitored filter cycles is provided in Table 5.2. As part of normal plant operation, the hydraulic loading rate of the full-scale biofilters was manually controlled at the beginning and end of each filter cycle to optimize ripening and control turbidity breakthrough, resulting in the lower average hydraulic loading rate and UFRV in the full-scale biofilters as compared to pilot scale biofilters.

Full- and pilot-scale filter cycles were operated in parallel for all monitored filter cycles to ensure comparable source water quality during each of the four sampling events. At the time of first sampling, full-scale filters had operated as biofilters for approximately two years, following a conversion to biofiltration through the removal of pre-chlorination as described in Chapter 2. Pilot-scale biofilters had operated as biofilters for approximately 3 years and under the described enhancement strategies for at least 8 months prior to the first sampling event for this study. The monitored filter cycle length for this study was 48 hours.

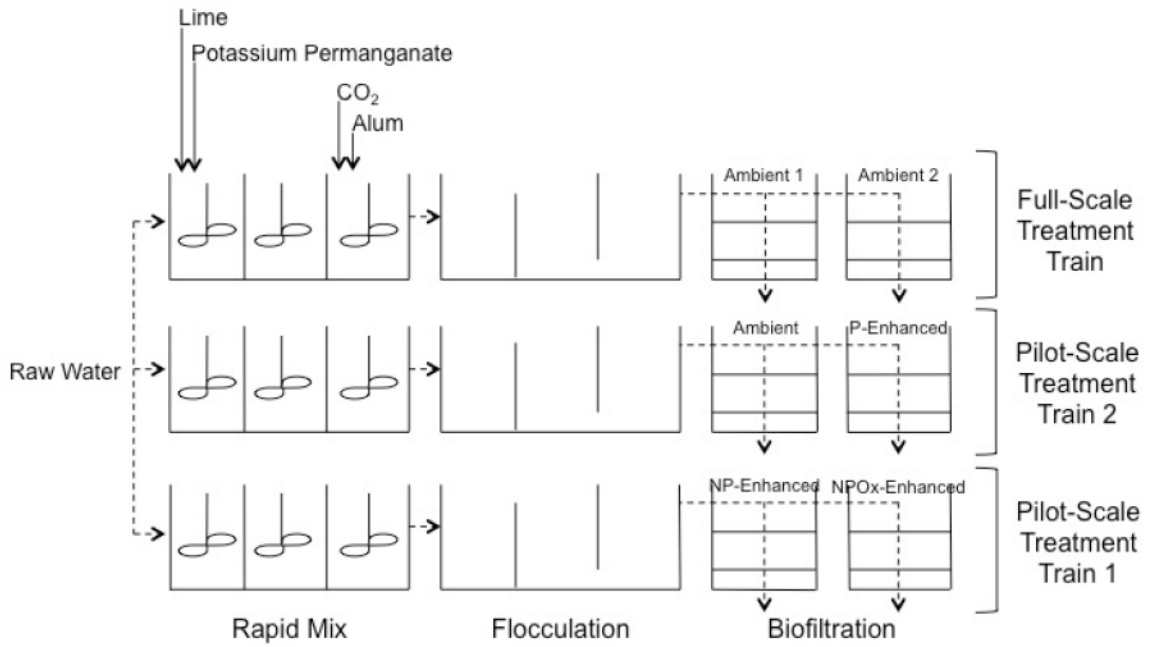

Figure 5.1 Full- and pilot-scale treatment train schematic

Table 5.2 Average hydraulic loading rate, average unit filter run volume (UFRV), average empty bed contact time (EBCT) and average terminal head loss for the four monitored filter cycles. The ± represents the 95% confidence interval with n = 4

Operational Parameter[a]	Full-Scale		Pilot-Scale			
	Ambient 1	Ambient 2	Ambient	P	NP	NPOx
Hydraulic Loading Rate—m/h	3.8±0.2	3.8±0.2	4.4±0.0	4.4±0.0	4.4±0.0	4.4±0.0
Unit Filter Run Volume—m^3/m^2	181±9	181±9	228±0	228±0	228±0	228±0
Empty bed contact time—min	15.3±0.7	15.3±0.7	12.5±0.0	12.5±0.0	12.5±0.0	12.5±0.0
Terminal Head loss—m	1.23±0.12	1.28±0.15	0.79±0.25	0.77±0.29	0.82±0.32	0.81±0.35

[a]All averages determined based on a 48-hour filter cycle
N—Nitrogen enhancement with ammonium chloride addition at a target dose of 0.351 NH_4-N mg/L for a C:N molar ratio of 100:10
P—Phosphorus enhancement with phosphoric acid addition at a target dose of 0.078 mg PO_4-P/L for a C:P molar ratio of 100:1
Ox—Oxidant enhancement with hydrogen peroxide addition at a target dose of 0.4 mg/L

5.2.3 Chemical Methods

5.2.3.1 Enhancement Strategy Application and Monitoring

Nitrogen (N) and phosphorus (P) enhancement strategies were applied to maintain a C:N:P molar ratio of 100:10:1 given a typical influent TOC concentration of ~ 3 mg/L (Table 5.1). As described in Chapter 4, N, P and Ox enhancements were applied at target doses of 0.351 mg NH_4-N/L, 0.078 mg PO_4^{3-}-P/L and 0.4 mg H_2O_2/L as water passed from the last flocculation tank to each pilot-scale biofilter. Concentrations were verified through sample ports directly above the filter media in each biofilter to ensure proper dosing. Stock solutions were prepared every 2-3 days and stored in opaque containers.

Phosphorus (P) enhancement was dosed from stock solutions prepared from concentrated phosphoric acid. Biofilter influent orthophosphate-phosphorus [PO_4^{3-}-P] concentration was verified spectrophotometrically using a DR4000 spectrophotometer (Hach, Loveland, CO) by the ascorbic acid method. Spectrophotometric measurements were used for on-site dose monitoring. Biofilter influent and effluent total phosphorus concentrations were measured for additional verification purposes using inductively coupled plasma mass spectrometry (XSeries 2 ICPMS, Thermo Fisher Scientific, Inc., Waltham, MA).

Nitrogen (N) enhancement was dosed from stock solutions prepared from ammonium chloride (NH_4Cl). Typical analyses of nitrogen species for this source water indicated that ammonia-nitrogen (NH_3-N), nitrate-nitrogen (NO_3^--N) and nitrite-nitrogen (NO_2^--N) concentrations were typically low, at <0.050 mg N/L, 0.057 mg N/L and <0.010 mg N/L, respectively (Halifax Water, 2014). Biofilter influent and effluent total nitrogen (TN) samples were collected headspace-free, in baked (24 hours, 100°C) glass vials, acidified to pH <2 with phosphoric acid and stored at 4°C pending analysis. TN was determined using a Shimadzu Total Nitrogen unit (Shimadzu Corporation, Kyoto, Japan) mounted on a Shimadzu TOC-VCPH (Shimadzu Corporation, Kyoto, Japan).

Hydrogen peroxide (H_2O_2) was dosed from a stock solution prepared from commercial-grade 3% H_2O_2. H_2O_2 concentration was verified spectrophotometrically using a H_2O_2 test kit (Hach, Loveland, CO) according to the manufacturer's instructions.

5.2.3.2 Natural Organic Matter Removal Monitoring

TOC, DOC and UV_{254} were measured after 24 and 48 hours of filter run time during each of the four monitored filter runs. TOC and DOC samples were collected headspace free in baked (24 hours, 100°C) glass vials, acidified to pH <2 with phosphoric acid and stored at 4°C pending analysis using a TOC-V CPH analyzer (Shimadzu Corp, Kyoto, Japan). Samples for DOC analysis were filtered (0.45 µm) prior to collection. UV_{254} was determined spectrophotometrically (DR4000, Hach, Loveland, CO) after filtration at 0.45 µm. TOC, DOC and UV_{254} were measured in triplicate. SUVA was determined by dividing average DOC concentration by average UV_{254}. DBPfp was measured once after 24 hours of filter run time during each monitored filter run. Trihalomethane (THM) and total haloacetic acid (HAA) formation potential were determined using uniform formation conditions as described by Summers et al. (1996). THM and HAA formation potential were measured from a single sample using gas chromatography with electron capture (CP-3800 Gas Chromatograph, Varian, Inc., Walnut Creek, CA) according to US EPA methods 551.1 and 552.2, respectively.

5.2.4 Microbiological Techniques

5.2.4.1 Media Collection

Media samples were collected in 50-mL sterile falcon tubes from the media surface of full- and pilot-scale biofilters at the start of a filter cycle (0 hours of filter run time) and after 48 hours of filter run time. In pilot-scale biofilters, media also was collected from a sample port at a media depth of 150 mm after 48 hours of filter run time.

5.2.4.2 Adenosine Triphosphate

All filter media samples were analyzed for ATP concentration. ATP concentration was measured on-site, immediately after sampling. Samples were measured in triplicate using a commercial test kit (Deposit Surface Analysis, LuminUltra Technologies Ltd., Fredericton, Canada) and luminometer (PhotonMasterTM Luminometer, LuminUltra Technologies Ltd., Fredericton, Canada) according to the manufacturer's instructions using a 1 g sample. ATP concentration was expressed as ng ATP/cm^3 media using a dry weight correction factor and an anthracite density of 0.8 g dry weight/cm^3 (Pharand et al., 2014). Dry weight correction factors were measured in triplicate following drying of three subsamples of each media sample at 105°C for approximately 24 hours.

5.2.4.3 Community Analysis

A subsample of the filter media collected from the media surface of full- and pilot-scale biofilters after a 48-hour filter run time was shipped overnight on ice to the University of Texas at Austin for microbial community analysis. Upon arrival, DNA was extracted directly from media samples using the FastDNA Spin Kit for Soil (MP Biomedicals, Santa Ana, CA) according to the manufacturer's instructions. Approximately one gram of filter media was taken aseptically from homogenized media for DNA extraction. Duplicate DNA extractions were performed for each sample, and DNA from duplicate extractions was combined for further purification using the PowerClean® Pro DNA Clean-up Kit (MO BIO Laboratory, Inc., Carlsbad, CA). The concentration of DNA was measured with a Nanodrop1000 (Thermo Scientific, Wilmington, DE).

Multiplex sequencing of the 16S rRNA gene was carried out at the Genomic Sequencing and Analysis Facility at The University of Texas at Austin. Briefly, the V4 and V5 regions were amplified from all DNA extracts with primer sets 515F/909R (Wang and Qian, 2009) (PCR) and sequenced on the Illumina Miseq® benchtop sequencer (using pair-end 250-bp kits). Sequences were then processed as follows using the QIIME pipeline version 1.8 (Caporaso et al., 2010). Reads were excluded from the analysis if the average quality score was lower than 10 during the split library script. Chimeric

sequences were identified using USEARCH and were then removed. The remaining sequences were clustered into operational taxonomic units (OTU), defined by a 97% sequence similarity, using open-reference-based OTUs with Uclust. A representative sequence from each OTU was selected and, using the RDP classifier (Wang et al., 2007), taxonomies were assigned by comparison with the Greengenes database (DeSantis et al., 2006).

Alpha-diversity metrics (i.e., Chao1, abundance-based coverage estimator (ACE), Shannon index and inverse Simpson), which describe diversity within a given sample, were determined using the R package Phyloseq (McMurdie and Holmes, 2013). Shannon evenness was calculated by dividing the Shannon index by the natural logarithm of observed OTUs. Chao1 and ACE are estimators of species richness (i.e. number of species). The inverse Simpson metric is a species diversity indicator. Beta-diversity, which describes diversity among samples, was assessed using weighted UniFrac-based principal coordinate analysis (PCoA) plots (Lozupone et al., 2011) calculated with the R package Phyloseq (McMurdie and Holmes, 2013) following rarefaction of the data at 3440 sequences per sample using the QIIME pipeline.

5.2.5 Statistical Analysis

Two-tailed paired t-tests (α=0.05) were used to confirm that treatment trains produced equivalent water quality prior to biofiltration (i.e., following coagulation/flocculation) and to determine the impact of enhancement strategies on effluent water quality, biomass concentration and diversity indices.

5.3 RESULTS & DISCUSSION

5.3.1 Water Quality

5.3.1.1 Natural Organic Matter Removal and DBP Formation Potential

As shown in Table 5.1, raw water TOC and DOC were equivalent (p-value > 0.05) over the course of the study, indicating that most of the lake water NOM was in the dissolved form. Raw water UV_{254} decreased with each sample month ($p < 0.05$) and SUVA appeared to follow a similar trend (Table 5.1). SUVA can be an indicator of the aromaticity (Weishaar et al., 2003) and humic fraction (Edzwald and Van Benschoten, 1990) of DOC in water, indicating that a decrease in the aromaticity and humic content of the raw water likely occurred over the study period.

As shown in Figure 5.1, the full-scale biofilters, the pilot-scale ambient and P-enhanced biofilters, and the pilot-scale NP- and NPOx-enhanced biofilters received influent water from different treatment trains, making it necessary to determine if equivalent water quality was achieved among the treatment trains prior to biofiltration. Paired t-tests indicated that pilot-scale treatment trains produced statistically equivalent influent water quality with respect to TOC, DOC, UV_{254} and SUVA. The full-scale treatment train produced statistically equivalent water quality to the pilot-scale treatment trains with respect to DOC and SUVA but differed statistically from pilot train 1 with respect to TOC (p-value < 0.05) and pilot train 2 with respect to UV_{254} (p-value < 0.05). Despite statistical significance, this difference in treatment train performance was small in actual magnitude and within the operationally feasible mean difference determined by Knowles et al. (2012) as discussed in Chapter 4.

Biofilter effluent water quality for full-scale ambient biofilters and pilot-scale ambient and enhanced biofilters is shown in Table 5.3 and Table 5.4. In general, the average effluent TOC, DOC, UV_{254} and SUVA concentrations were higher in the pilot-scale ambient biofilter than in the full-scale ambient biofilters. Paired t-tests indicated that the higher effluent values in the pilot-scale ambient biofilter compared to the full-scale

ambient biofilters were only statistically significant for TOC (p-value = 0.05) and DOC (p-value <0.05). This may have occurred as a result of the higher influent TOC concentration observed at the pilot-scale. Consistent with Chapter 4, enhancement strategies resulted in statistically equivalent effluent TOC, DOC and SUVA concentrations and DBP formation potentials as compared to the ambient pilot-scale biofilter.

Table 5.3 Average effluent TOC, DOC, UV_{254} and SUVA for full- and pilot-scale biofilters. ± represents the standard deviation of the data with n = 8 (TOC, DOC) and n = 6 (UV_{254}, SUVA)

Experiment Scale	Treatment	TOC—mg/L	DOC—mg/L	UV_{254}—cm^{-1}	SUVA—*L/mg-m*
Full-Scale	Ambient 1	1.80 ± 0.16	1.88 ± 0.17	0.040 ± 0.007	2.20 ± 0.33
	Ambient 2	1.82 ± 0.12	1.86 ± 0.14	0.041 ± 0.006	2.21 ± 0.37
Pilot-Scale	Ambient	1.91 ± 0.12	1.98 ± 0.17	0.044 ± 0.010	2.28 ± 0.48
	P	1.92 ± 0.10	1.91 ± 0.08	0.042 ± 0.007	2.21 ± 0.32
	NP	1.87 ± 0.12	1.91 ± 0.21	0.040 ± 0.006	2.17 ± 0.27
	NPOx	1.87 ± 0.13	1.94 ± 0.18	0.036 ± 0.007	1.93 ± 0.40

Table 5.4 Average effluent THMfp and HAAfp for full- and pilot-scale biofilters. ± represents the standard deviation of the data with (n = 4)

Experiment Scale	Treatment	THMfp—µg/L	HAAfp—µg/L
Full-Scale	Ambient 1	73 ± 18	51 ± 9
	Ambient 2	82 ± 12	52 ± 6
Pilot-Scale	Ambient	89 ± 14	61 ± 13
	P	60 ± 27	56 ± 11
	NP	66 ± 22	64 ± 16
	NPOx	77 ± 21	58 ± 11

5.3.2 Microbial Community

5.3.2.1 The effect of enhancement strategies on biomass quantity

Average biomass concentration, as measured by ATP, varied significantly in the six biofilters (Figure 5.2). ATP concentrations for individual samples is provided in Supplementary Figure A.7. Ambient full- and ambient pilot-scale biofilters had statistically equivalent biomass concentrations at the start of the filter cycle (i.e., at 0 hours of filter run time) (p-value >0.05). Pilot-scale biofilters had significantly different biomass concentrations at the start of the filter cycle (p-value < 0.01). Paired t-testing showed that P-enhancement alone did not result in a statistically significant difference in biomass concentration measured at the start of the filter cycle as compared to the ambient pilot-scale biofilter (p-value >0.05); however, NP- (p-value < 0.01) and NPOx-enhancement (p-value < 0.01) increased biomass concentrations measured at the start of the filter cycle over the pilot-scale ambient biofilter. NP-enhancement and NPOx-enhancement also resulted in a statistically significant (p-value <0.05) increase in biomass concentration measured at the start of the filter cycle as compared to the P-enhanced filter, which suggests the addition of nitrogen caused the increase in biomass. Biomass measured at the start of the filter cycle was not statistically different for the NP- and NPOx-enhanced biofilters (p-value >0.05), which indicates that the addition of hydrogen peroxide did not negatively impact biomass concentration.

Biomass concentration also was measured 48 hours into the filter cycle. The 48-h sample time represented the maximum expected biomass concentration at the media surface, based on the previous analyses of full-scale biomass evolution at this study site (Chapter 3). As shown in Figure 5.2 (and Supplementary Figure A.7), both full- and pilot-scale biofilters demonstrated an increase in biomass concentration at the filter surface with filter run time (Figure 5.2). Trends in 48-h biomass were consistent with trends in biomass concentrations measured at the start of the filter cycle; P-enhancement alone did not significantly impact biomass concentration.

Also shown in Figure 5.2, biomass decreased with filter depth. A reduction in biomass with filter depth has been documented in other rapid biofilters (e.g., Wang et al., 1995, Servais et al., 1994) and is typically attributed to a reduction in substrate availability with filter depth. Trends in biomass concentration at a depth of 150 mm after 48 hours of filter run time were consistent with trends in both biomass concentrations measured in the top of the filter at the start of the filter cycle and after 48 hours of filter run time (FRT).

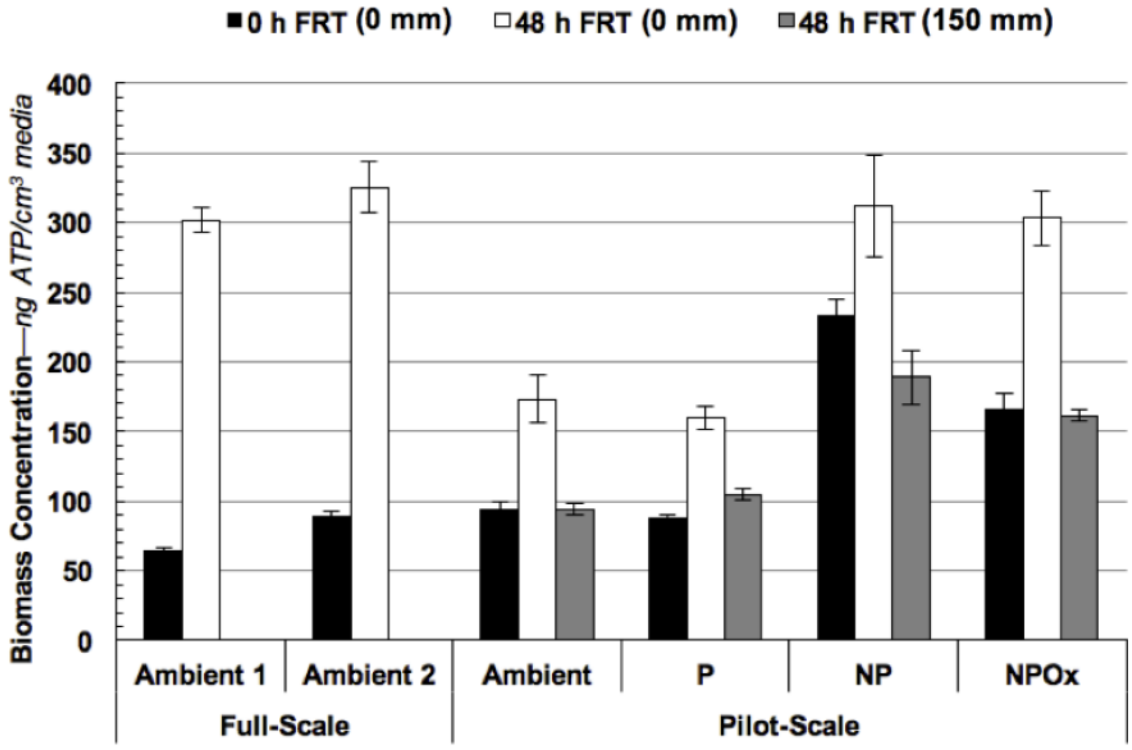

Figure 5.2 Average biomass concentration as measured by ATP for full- and pilot-scale biofilter effluents. Error bars represent the 95% confidence interval of the data with n = 4

5.3.2.2 The effect of enhancement strategies on microbial community structure in biofilters

5.3.2.2.1 Relative abundance in biofilter microbial communities

Proteobacteria, *Bacteriodetes*, *Acidobacteria*, *Planctomycetes*, *Nitrospirae*, and *Chloroflexi* previously have been identified as major phyla in rapid-sand, slow-sand, and GAC biofilters (Lautenschlager et al., 2014; Liao et al., 2015). In the current study, a total of 18 bacterial phyla were identified in 24 samples retrieved from the two full-scale and four pilot-scale biofilters. As shown in Figure 5.3 (and Supplementary Figure A.8), the most abundant phylum in all biofilters was *Proteobacteria*. Of *Proteobacteria*, *Alphaproteobacteria* was the most abundant, followed by *Betaproteobacteria*, *Gammaproteobacteria*, and *Deltaproteobacteria* (Figure 5.4 [and Supplementary Figure A.9]). Changes in *Proteobacteria* abundance among the biofilters was controlled by a decrease in *Alphaproteobacteria* at the pilot-scale, with the lowest *Alphaproteobacteria* abundance in the NP-enhanced biofilter.

Other common phyla identified in the biofilters were *Actinobacteria*, *Bacteroidetes*, *Acidobacteria*, *Plantomycetes*, *Nitrospirae*, and *Chloroflexi* (Figure 5.3). In general, community composition at the phylum level was very similar among full-scale ambient biofilters and pilot-scale ambient and P-enhanced biofilters. Shifts in the full-scale ambient biofilters and the pilot-scale ambient and P-enhanced biofilter microbial community were an increase in *Acidobacteria* and *Bacteroidetes* and decrease in *Planctomycetes* at the pilot-scale. The most notable difference in phylum level community composition that occurred in the NP- and NPOx-enhanced biofilters as compared to the other pilot-scale biofilters was that *Nitrospirae*, *Thermi* and *Chloroflexi* became substantial phyla in the NP and NPOx-enhanced biofilters. The occurrence of *Nitrospirae* in biofilters has been used as an indicator of potential occurrence of biological nitrification (Lautenschlager et al., 2014), suggesting that biological nitrification might have occurred in the biofilters that were supplemented with nitrogen.

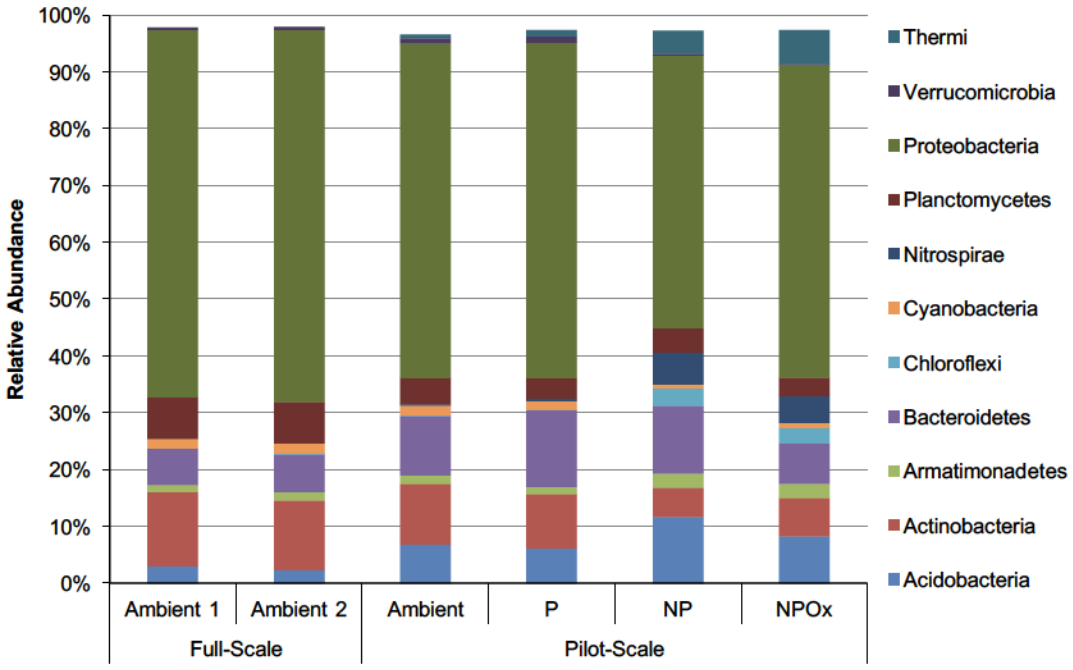

Figure 5.3 Microbial community composition at the phylum level for full- and pilot-scale biofilters. Abundances represent the average of the four sampling events. Unassigned phyla and phyla with abundance < 1% in all samples were excluded.

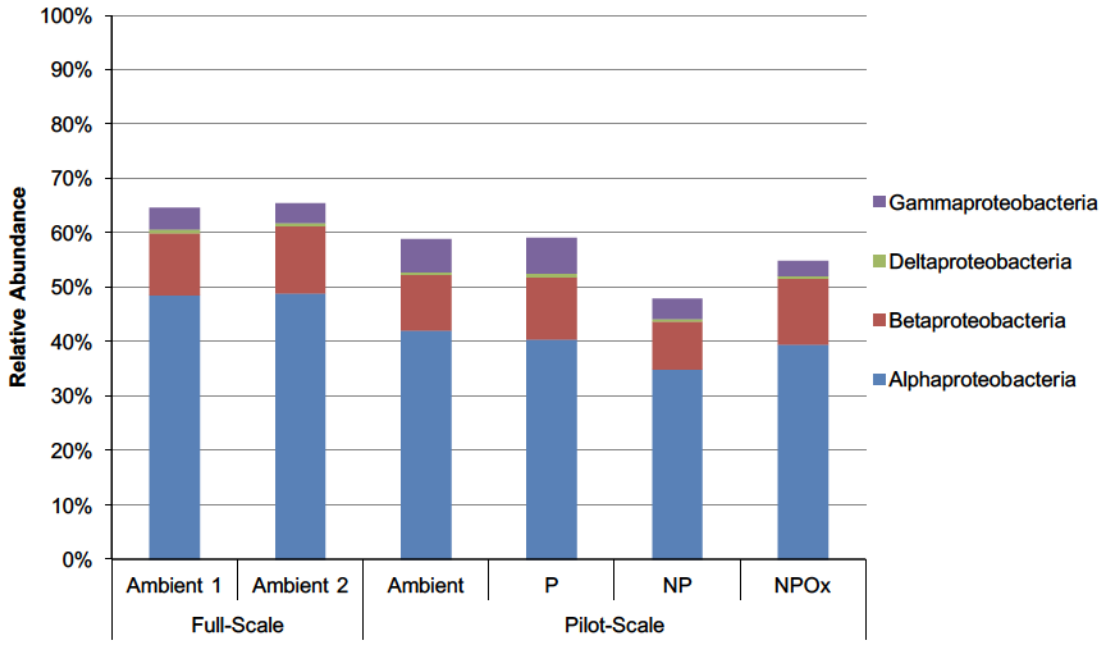

Figure 5.4 Relative abundance of classes of *Proteobacteria* in the microbial communities of full- and pilot-scale biofilters averaged for sampling events in May, June, July and August.

As shown in Figure 5.5 (and Supplementary Figure A.10), *Rhizobiales* was the most abundant order identified in all biofilters. Other orders that were identified and whose abundance was dependent on the scale (i.e., full- vs. pilot-scale) or enhancement strategy (i.e., nitrogen addition and hydrogen peroxide addition) included *Sphingomondales*, *Actinomycetales*, *Saprospirales*, *Burkholderiales, Rhodospirillales*, *Planctomycetales*, *Solibacterales*, *Gallionellales*, *Nitrospirales*, *Methylophilales* and *Deinococcales*.

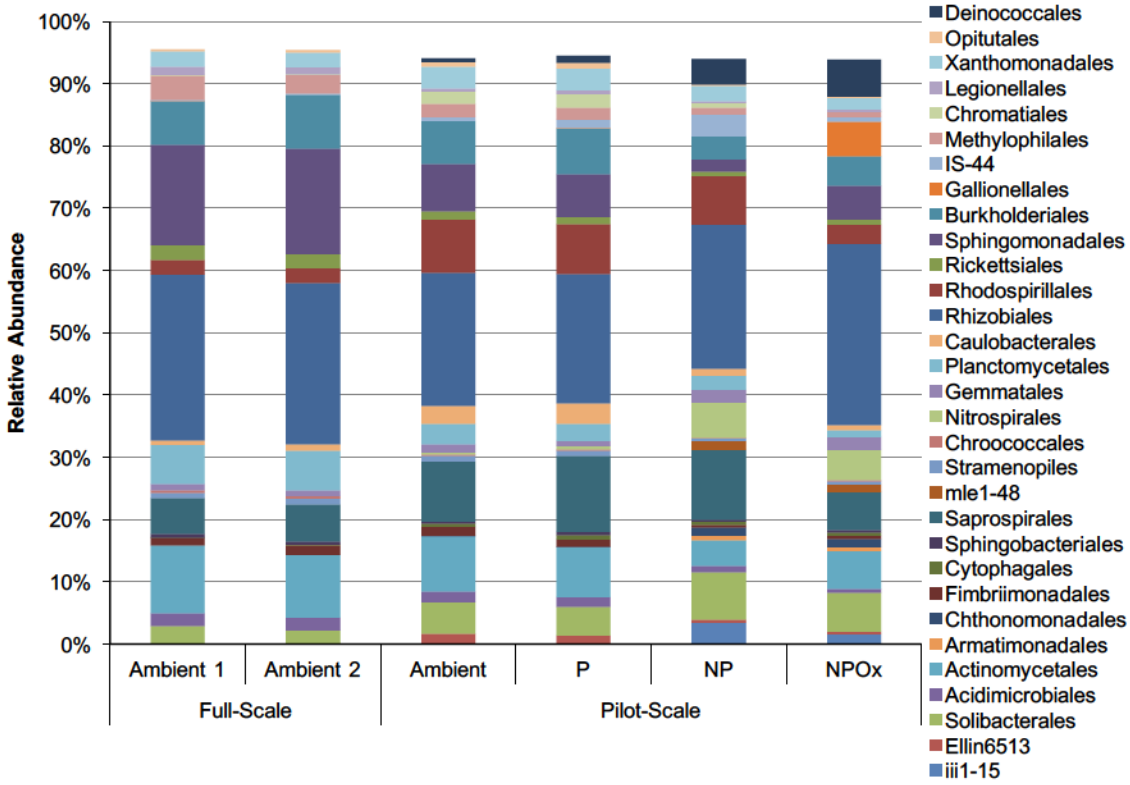

Figure 5.5 Microbial community composition at the order level for full- and pilot-scale biofilters for the four sampling events. Unassigned orders and orders with abundance <1% in all samples were excluded.

As shown in Table 5.5, some bacteria genera were more abundant in the full-scale ambient biofilters than in the pilot-scale ambient biofilter, indicating a difference in microbial community structure between the two scales. Bacteria with notably greater abundance in the full-scale ambient biofilters included *Planctomyces, Hyphomicrobium* and bacteria belonging to unassigned genera in the orders *Actinomycetales* and *Sphingmonadales*. Similarly, some genera were more abundant in the ambient pilot-scale biofilter than in the full-scale biofilters, including the genus *Bradyrhizobium*, CM44, and unassigned genera of the orders *Saprospirales* and *Rhodospirialles*. These findings suggested inherent differences in microbial community structure between full- and pilot-scale biofilters, even when operated under equivalent treatment conditions and influent water quality. An inverse relationship between hydrodynamic shear rate and microbial community diversity has been observed for freshwater biofilms (Rickard et al., 2004).

Hydraulic loading rate has been shown to influence community structure in biofilters treating drinking water (Zhang et al., 2010). On average, hydraulic loading rate in pilot-scale biofilters was 0.6 m/h greater than the hydraulic loading rate of full-scale biofilters (Table 5.2) which may have influenced this difference in microbial community structure. Increasing hydrodynamic shear can also increase substrate diffusion, biofilm density and EPS production (Zhu et al., 2010).

Some genera were found in greater abundance in NP- and NPOx-enhanced biofilters than in ambient pilot- and full-scale biofilters. *Nitrospira*, a genus of bacteria in the order *Nitrospirales*, had an average relative abundance of 5.6% and 4.7% for NP and NPOx-enhanced biofilters, respectively (Table 5.5). In contrast, *Nitrospira* was not detected in full-scale ambient biofilters and had an average relative abundance of ≤0.5% in ambient and P-enhanced pilot-scale biofilters. Liao et al. (2013) also found higher *Nitrospira* abundance in a biofilter receiving higher influent ammonia-nitrogen concentration.

The genus *Bradyrhizobium* also was detected in greater abundance in the NP and NPOx-enhanced biofilters. *Bradyrhizobium* was detected at low abundance the full-scale ambient biofilters (0-0.4%), the ambient pilot-scale biofilter (0.9-2.8%), and the P-enhanced pilot-scale biofilter (0.8-2.0%). *Bradyrhizobium* was more abundant in the NP-enhanced and NPOx-enhanced pilot-scale biofilters at abundances of 2.5-5.9% and 7.1-11.4%, respectively. This indicated that the H_2O_2 added in this study did not inhibit its growth. Lauderdale et al. (2011) also found that H_2O_2 enhancement did not inhibit *Bradyrhizobium* abundance over a control without peroxide (i.e., 15% abundance in control and 31% abundance in peroxide enhanced biofilter). However, Lauderdale et al. (2011) found that operating biofilters at a C:N:P molar ratio of 100:14:2 resulted in a large decrease in the abundance of *Bradyrhizobium* as compared to biofilters operated under nitrogen-limited (i.e., a C:N:P molar ratio of 100:7:1) and combined nitrogen- and phosphorus-limited conditions (i.e., a C:N:P: molar ratio of 100:7:0), which is in contrast with the findings in the current study. In that study, the reduction in *Bradyrhizobium* was hypothesized to influence an improvement in biofilter hydraulic performance, as *Bradyrhiziobium* are known to produce substantial amounts of extracellular polymeric

substances. The addition of hydrogen peroxide to biofilters has been associated with improved hydraulic performance (Azzah et al., 2014; Lauderdale et al., 2012). As discussed in Chapter 4, NPOx enhancement at target C:N:P molar ratio of 100:10:1 was the only enhancement strategy observed to reduce head loss in the pilot-scale biofilters. Therefore, the increase in *Bradyrhizobium* in the NP- and NPOx-enhanced biofilters relative to the ambient pilot-scale biofilter in the current study is notable.

Gallionella, a genus of bacteria in the order *Gallionellales*, associated with iron oxidation, was only detected in the NPOx-enhanced pilot-scale biofilter at an average relative abundance of 5.6% for the four sampling events. The presence of *Gallionella* suggests that biological iron oxidation occurred in this biofilter (De Vet et al., 2011). This indicated the apparent selection of this genus with the addition of hydrogen peroxide. Similarly, bacteria in the order *Deinococcales* were not identified in the full-scale biofilters, were detected at low abundance in the pilot-scale ambient and P- and NP-enhanced biofilters and showed greatest abundance in the NPOx-enhanced biofilter. Some *Deinococcus* species require nutrient-rich conditions for cell replication and can be resistant to oxidative stress (Slade and Radman, 2011), which might explain the increase in abundance in the NPOx-enhanced biofilter.

Table 5.5 Average relative abundance at the genus level for the four sampling events. Genera were selected for this table if relative abundance was >5% in any given biofilter in at least one of the sampling events. Values in parentheses represent the range of the data.

Phylum	Order	Genus	Full Scale		Pilot-Scale			
			Ambient 1	Ambient 2	Ambient	P	NP	NPOx
Acidobacteria	*Solibacteriales*	Unassigned	1.2 (0.4-2.1)	1.4 (0.4-2.6)	2.9 (1.7-4.2)	2.5 (1.3-4.1)	7.1 (5.7-8.7)	6.1 (4.8-7.6)
Actinobacteria	*Actinomycetales*	Unassigned	9.9 (5.9-16.0)	9.3 (4.4-19.2)	7.6 (5.7-12.2)	6.9 (5.3-10.7)	3.9 (2.6-6.5)	4.9 (3.2-8.5)
Bacteroidetes	*Saprospirales*	Unassigned	2.4 (1.8-3.0)	2.6 (1.7-4.0)	8.1 (4.8-10.6)	11.0 (7.4-12.9)	10.7 (9.6-11.9)	5.4 (4.8-6.1)
Nitrospirae	*Nitrospirales*	*Nitrospira*	0.0 (0.0-0.0)	0.0 (0.0-0.0)	0.3 (0.0-0.6)	0.5 (0.3-0.6)	5.6 (2.9-7.9)	4.7 (1.9-6.6)
Planctomycetes	*Planctomycetales*	*Planctomyces*	6.3 (3.4-9.6)	6.3 (5.1-7.6)	3.3 (1.6-5.3)	2.8 (1.7-3.6)	2.3 (1.6-3.5)	1.1 (0.9-1.6)
Proteobacteria	*Rhizobiales*	*Bradyrhizobium*	0.2 (0.0-0.4)	0.2 (0.1-0.4)	2.0 (0.9-2.8)	1.5 (0.8-2.0)	4.3 (2.5-5.9)	8.8 (7.1-11.4)
		Unassigned	2.0 (0.5-3.6)	1.8 (0.7-3.1)	3.3 (2.0-5.1)	3.1 (1.5-4.7)	5.4 (3.7-7.4)	3.6 (2.6-4.7)
		Hyphomicrobium	14.3 (8.6-22.4)	13.6 (5.0-24.7)	8.8 (6.1-11.8)	7.4 (5.7-9.0)	5.3 (4.0-7.0)	5.8 (4.4-8.2)
	Rhodospirillales	Unassigned	2.1 (1.9-2.3)	2.1 (1.4-3.0)	8.1 (6.6-9.4)	7.7 (5.5-9.7)	7.4 (5.6-8.1)	2.8 (1.6-4.2)
	Sphingmonadales	Unassigned	15.9 (10.9-18.9)	16.7 (9.8-27.4)	7.1 (3.5-9.7)	6.4 (2.6-9.4)	1.9 (1.3-2.5)	5.3 (2.9-7.8)
	Gallionellales	*Gallionella*	0.0 (0.0-0.1)	0.0 (0.0-0.0)	0.0 (0.0-0.0)	0.0 (0.0-0.0)	0.0 (0.0-0.0)	5.6 (1.9-9.2)
Thermi	*Deinococcales*	CM44	0.0 (0.0-0.0)	0.0 (0.0-0.0)	0.7 (0.1-1.7)	1.1 (0.3-2.1)	4.1 (3.2-4.9)	6.0 (5.1-7.4)

5.3.2.2.2 Microbial richness and diversity in biofilters

Richness, diversity and evenness metrics are provided in Table 5.6. No statistically significant differences in species richness were observed among the biofilters ($p > 0.05$). All richness metrics showed a large spread in the observed and estimated number of species in the samples. This was because the samples collected in May had greater richness compared to samples collected at other time points, based on observed OTUs, and the richness based estimators, Chao1 and ACE (Supplementary Figure A.11). The August samples also appeared to have greater richness than the June and July samples, which appeared similar. Similar separation of May and August samples from June and July samples was apparent in rarefaction curves (Supplementary Figure A.12). This was perhaps in response to a shift in raw and biofilter influent water quality from more hydrophobic and aromatic material (i.e., higher SUVA, higher UV_{254}) in May to more hydrophilic, less aromatic material (i.e., lower SUVA, lower UV_{254}) in June, July and August. Low molecular weight hydrophilic material is typically considered more amenable to biofiltration. A more amenable substrate during the June, July and August samples might have allowed specific species to proliferate and out-compete rare species, leading to a reduction in richness in these samples. Water temperature also has been linked to changes in microbial community structure (Fonseca et al., 2002). Raw water temperature was much lower in May (i.e, 8.6°C as compared to 16.3°C, 19.1°C and 22.2°C for the June, July and August sampling events, respectively), possibly contributing to the greater richness in the May samples. Li et al. (2010) observed a decrease in richness (Chao1 index) following the addition of phosphorus to bench- and pilot-scale bioreactors. However, in a more similar investigation to the current study, Lauderdale et al. (2014) found no significant difference in the richness (Chao) in pilot-scale control, nutrient- or peroxide-enhanced biofilters in optimization studies for two water sources.

Diversity and evenness metrics did not appear to be impacted by sample month (Supplementary Figure A.11). As shown in Table 5.6, on average, full-scale ambient biofilters had less diverse communities than did the pilot-scale biofilters. At the pilot-

scale, diversity was similar in the ambient and P-enhanced biofilters. There was a slight increase in average diversity in the NP-enhanced filter and a decrease in diversity in the NPOx-enhanced biofilter as compared to the ambient pilot-scale biofilter, indicating that combined nutrient enhancement had a positive impact on diversity while oxidant enhancement negatively impacted diversity. Conflicting findings have been reported related to the impact nutrient and oxidant addition have on diversity. Similar to the current study, Lauderdale et al. (2014) observed an increase in diversity in nutrient-enhanced biofilters in two pilot-scale optimization studies and a decrease in diversity in oxidant-enhanced biofilters in one of two pilot-scale optimization studies. In contrast, Liao et al. (2013) found a decrease in diversity in a biofilter receiving ammonia (1 mg/L) supplementation.

It has been hypothesized that a decrease in evenness, and the subsequent indication of the dominance of few bacterial taxa, may increase biofilter susceptibility to process failures and limit the range of pollutants that can be removed by biofilters (Lauderdale et al., 2014). As shown in Table 5.6, similar evenness was calculated for all biofilters, regardless of scale or enhancement, indicating that enhancement strategies did not cause significant changes in relative species dominance.

Table 5.6 Average richness, diversity and evenness for the four sampling events. Error bars indicate the 95% confidence interval of the data.

Scale	Biofilter	Richness			Diversity	Evenness
		Observed	Estimated		Inverse Simpson	Shannon Evenness
			Chao1	ACE		
Full-Scale	Ambient 1	1051 ± 491	1913 ± 946	2071 ± 1159	41 ± 10	0.70 ± 0.02
	Ambient 2	1475 ± 885	2441 ± 1188	2562 ± 1436	45 ± 22	0.68 ± 0.04
Pilot-Scale	Ambient	1218 ± 938	2119 ± 1521	2243 ± 1731	64 ± 8	0.74 ± 0.04
	P	1458 ± 970	2517 ± 1500	2637 ± 1765	63 ± 9	0.72 ± 0.03
	NP	1266 ± 862	2152 ± 1307	2314 ± 1497	68 ± 8	0.74 ± 0.05
	NPOx	1435 ± 1072	2257 ± 1451	2412 ± 1652	50 ± 6	0.72 ± 0.04

A weighted unifrac principle coordinate analysis (PCoA) plot is provided in Figure 5.6. Full-scale samples clustered together indicating that they were distinct from pilot-scale

biofilters, which is consistent with abundance observations previously discussed. Pilot-scale ambient and P-enhanced samples clustered together indicating that limited changes in microbial community structure occurred with P-enhancement. NP-enhanced and NPOx-enhanced samples appeared distinct from each other and the other pilot-scale samples, indicating that both NP-enhancement and NPOx-enhancement resulted in a change in the microbial community structure. The sample month also influenced the microbial community structure, with May and June samples clustering and July and August samples clustering for each biofilter

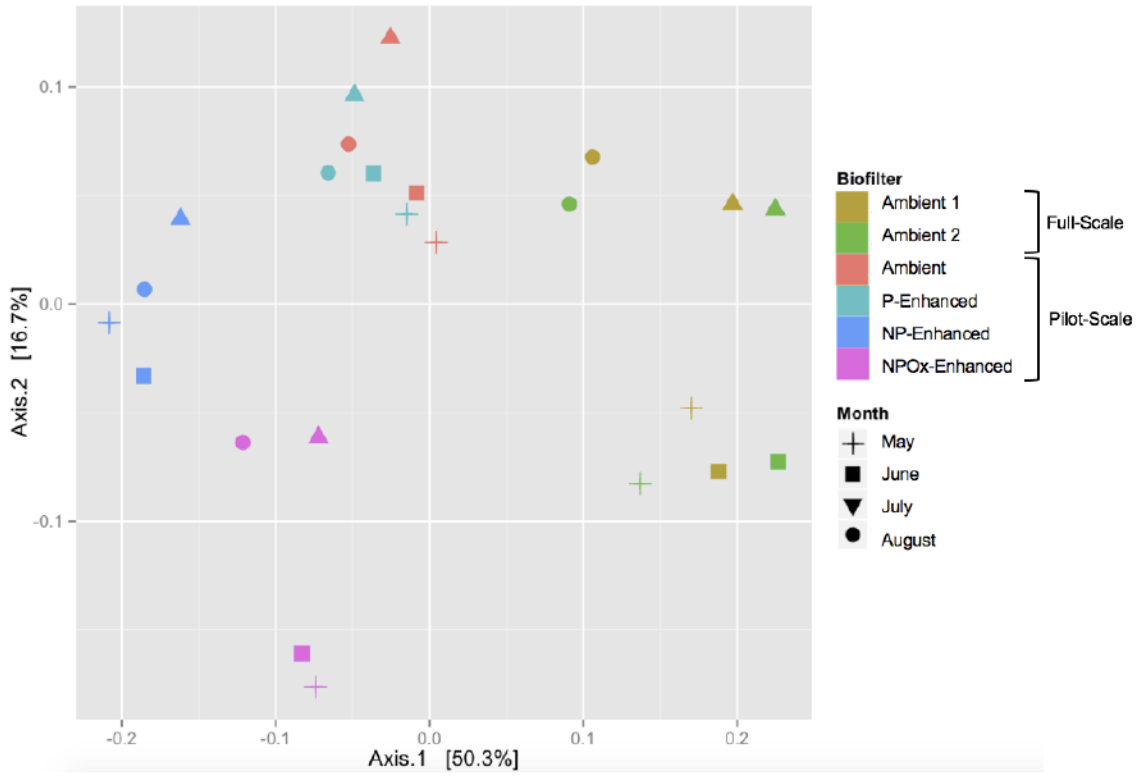

Figure 5.6 Weighted Unifrac PCoA plot for examining the impact of different enhancement strategies and seasonal variation in full- and pilot-scale biofilters for the four sampling events

5.4 CONCLUSIONS

Combined nutrient-enhancement (nitrogen and phosphorus), and combined nutrient- and oxidant-enhancement (nitrogen, phosphorus, and hydrogen peroxide) resulted in an increase in biomass, as measured by ATP, in pilot-scale drinking water biofilters. Comparatively, phosphorus enhancement alone did not increase biomass quantity as compared to an ambient pilot-scale biofilter.

Some bacterial genera were more abundant in the full-scale ambient biofilters than in the pilot-scale ambient biofilter, suggesting inherent differences in microbial community structure between full- and pilot-scale biofilters, even when operated under equivalent influent water quality conditions. Genera with notably greater abundance in the full-scale ambient biofilters included *Planctomyces, Hyphomicrobium*, and bacteria belonging to unassigned genera in the orders *Actinomycetales* and *Sphingmonadales.* In contrast, *Bradyrhizobium*, CM44, and unassigned genera of the orders *Saprospirales* and *Rhodospirialles* were more abundant in the pilot-scale ambient biofilter.

Enhancements resulted in clear shifts in the microbial community structure when nitrogen and phosphorus (NP), and nitrogen, phosphorus, and hydrogen peroxide (NPOx) were applied in combination. However, a similar microbial community structure to the ambient pilot-scale biofilter was observed when phosphorus (P) enhancement alone was applied. In particular, the abundance of *Nitrospira* and *Bradyrhizobium* was greater in the biofilter enhanced with nitrogen and phosphorus than in the full- or pilot-scale ambient biofilters. Oxidant addition also had an impact on particular genera; the abundance of *Gallionella*, CM44 and unassigned genera in the order *Sapropirales* and *Rhodospirillales* were increased or decreased in abundance when hydrogen peroxide was applied.

All richness metrics showed a large spread in the observed and estimated number of species in the samples due to greater richness in the May sample set, potentially resulting from changes in influent water quality and temperature. On average, the microbial communities of full-scale ambient biofilters were less diverse than those in the pilot-scale ambient biofilters. At the pilot-scale, alpha diversity was similar in the ambient and

phosphorus (P) enhanced biofilters. There was a slight increase in average diversity in the nitrogen and phosphorus (NP) enhanced pilot-scale biofilter and a decrease in diversity in the nitrogen, phosphorus and oxidant (NPOx) enhanced pilot-scale biofilter as compared to the ambient pilot-scale biofilter. With respect to beta diversity, full- and pilot-scale ambient biofilters had distinct community composition. At the pilot-scale, ambient and phosphorus (P) enhanced biofilters had similar community compositions while the NP and NPOx had more distinct community compositions.

Despite increases in biomass and differences in microbial community structure, effluent water quality (e.g., TOC, DOC, UV_{254}, SUVA, DBPfp) for full-scale ambient biofilters and pilot-scale ambient and enhanced biofilters was similar.

CHAPTER 6 APPLICATION OF PHOTOELECTROCHEMICAL CHEMICAL OXYGEN DEMAND TO DRINKING WATER

6.1 ABSTRACT

This study investigated the use of a photoelectrochemical chemical oxygen demand (peCOD) analyzer for the detection of model organic compounds and natural organic matter (NOM) from four drinking water treatment plants in Nova Scotia, Canada. Most model organic compounds showed reasonable correlation between peCOD and theoretical oxygen demand (ThOD), indicating that peCOD was a reasonable predictor of chemical oxygen demand (COD). Results also showed that peCOD/TOC (total organic carbon) ratios followed predicted values from stoichiometry, when peCOD was a good predictor of ThOD. peCOD determination for surface water showed that peCOD was measurable in the raw and treated drinking water range and trended with other organic matter surrogates. Finally, pooling of raw water, finished drinking water and water sampled throughout the treatment process at these four utilities showed that peCOD was correlated with specific ultraviolet absorbance at 254 nm (SUVA).[4]

---

[4] Note: A version of this chapter is published in *Journal American Water Works Association.*

Stoddart, A. K., & Gagnon, G. A. (2014). Application of photoelectrochemical chemical oxygen demand to drinking water. *Journal American Water Works Association*, *106* (9), E383-E390.

6.2 INTRODUCTION

Natural organic matter (NOM) in surface waters can be produced through many pedogenic and aquagenic processes (Krasner et al, 1996). NOM in drinking water source water is of specific concern because it has been identified as a precursor to regulated and unregulated disinfection by-products (DBPs) with both known and unknown health effects (Krasner et al, 1989; Krasner et al, 2006; Nieuwenhuijsen et al, 2000; Villanueva et al, 2000). As summarized in the literature by Matilainen et al (2011), NOM can be characterized using several spectroscopic, chromatographic and mass spectrometric methods to provide very specialized information on NOM character. Of these methods, high performance size exclusion chromatography (SEC), UV absorption at different wavelengths and resin fractionation are common (Cabaniss et al, 2000; Krasner et al, 1996; Edzwald et al, 1985). For non-selective and efficient NOM monitoring, tools such as total organic carbon (TOC), dissolved organic carbon (DOC) and UV absorption at a wavelength of 254 nm (UV_{254}) are often used to provide rapid assessment of NOM in water. Although these are widely used tools, there are continuing needs to develop new monitoring tools to better understand and efficiently manage NOM in drinking water processes.

Chemical oxygen demand (COD) is the amount of oxygen required to fully oxidize organic matter, as determined by using a strong oxidant (Droste, 1997). COD is often measured using Method 5220 of *Standard Methods* (APHA, 2012), which involves oxidation of organic matter at high temperatures with sulfuric acid, dichromate and a catalyst for 2 to 3 hours, followed by indirect determination of COD through unreacted dichromate. This method involves the use of hazardous chemicals (i.e. mercury, hexavalent chromium, sulfuric acid and silver) and is suitable for COD concentrations > 50 mg/L with alterations to allow for COD detection from 5 to 50 mg/L. Adjustments to the COD procedure for the lower detection range are at the expense of accuracy and precision (APHA, 2012). The method can also be altered to reduce wastes, but again at the expense of accuracy (APHA, 2012). Although these alterations can allow for the

detection of COD in surface waters, the dichromate method is typically not sensitive enough for treated drinking waters (Rittman and Huck, 1989).

COD can also be measured using a photoelectrochemical method (Zhao et al, 2004). Recently, a commercial COD analyzer using this photoelectrochemical method has been developed. With a calculated method detection limit of 0.5 mg/L, it was anticipated that this tool could be a useful surrogate parameter (much like TOC, DOC and specific absorbance at 254 nm [SUVA]) for assessing NOM in raw and treated drinking water that could overcome challenges with traditional COD methods through improved detection limit and reduction in hazardous wastes.

The hypothesis of this study was that photoelectrochemical chemical oxygen demand, or peCOD, could provide analysis of NOM removal that would be applicable to the drinking water industry. To address this hypothesis, the study was structured into the following research tasks: (1) evaluate the ability to detect and quantify COD from model organic compounds (e.g., amino acids and carboxylic acids) in a concentration range relevant for drinking water; (2) compare peCOD analysis to traditional NOM detection techniques (e.g., TOC analysis); and (3) evaluate peCOD concentration range in source water and during subsequent treatment from surface water treatment plants in Nova Scotia, Canada. Because COD is a measure of oxidizable organic matter, relationships between peCOD and traditional NOM surrogates were also studied.

6.3 MATERIALS AND METHODS

6.3.1 Model Compound Preparation

Three amino acids (tyrosine, tryptophan, phenylalanine), three carboxylic acids (sodium acetate, sodium oxalate and sodium formate), and two reference standards (potassium hydrogen phthalate [KHP] and caffeine) were used as model organic compounds. These model organic compounds are summarized in Table 6.1.

Table 6.1 Model organic compound descriptions

Compound	Chemical Formula	Description	Molecular Weight–*g/mol*
Potassium Hydrogen Phthalate (KHP)	$C_8H_5KO_4$	Reference Standard	204.22
Caffeine	$C_8H_{10}N_4O_2$	Reference Standard	194.19
Phenylalanine	$C_9H_{11}NO_2$	Amino Acid	165.19
Tyrosine	$C_9H_{11}NO_3$	Amino Acid	181.19
Tryptophan	$C_{11}H_{12}N_2O_2$	Amino Acid	204.23
Sodium Formate	HCOONa	Carboxylic Acid	68.01
Sodium Acetate	$C_2H_3O_2Na$	Carboxylic Acid	82.03
Sodium Oxalate	$Na_2C_2O_4$	Carboxylic Acid	134.00

Carboxylic acids and amino acids are found in natural waters and can make up 8% and 2-3% of COD in natural waters, respectively (Langlais et al, 1991). Relative proportions of amino acids to organic matter surrogates, such as DOC, can vary considerably from source to source. In a survey of 16 utilities across the United States, Dotson and Westerhoff (2009) found that raw water total amino acid concentration accounted for between 0.19 and 11.6%, or 3.5% on average, of raw water DOC. As summarized by Dotson and Westerhoff (2009), amino acids are precursors to regulated and unregulated DBPs, and amino acids with aromatic side chains, such as tryptophan and tyrosine, can have the highest DBP yields on a carbon basis. KHP was chosen since it is commonly used as a reference standard for TOC determination. Finally, caffeine was chosen as it is commonly used as a marker for human contamination.

Model compound stock solutions (100 mg C/L) were prepared by diluting chemical in deionized (DI) water (Millipore, Billerica, Massachusetts). Stock solutions were then further diluted with DI water to 0.25, 0.5, 1, 3, 5 mg C/L as TOC in the range of 1.5 – 5 mg/L represents common raw and treated water TOC content in surface water in Nova Scotia. Model compounds were prepared for TOC and COD.

6.3.2 Surface Water Collection

Samples were collected from four surface water treatment plants in Nova Scotia. Treatment trains included one biofiltration plant (Pockwock Lake), one ultrafiltration/nanofiltration membrane plant (Fletcher Lake) and two conventional filtration plants (Lake Major and Bennery Lake). Details of the treatment process for each plant are described in Table 6.2.

Table 6.2 Treatment train descriptions for four surface water treatment plants in Halifax, Nova Scotia, Canada

Source	Treatment
Pockwock Lake	Lime, potassium permanganate, carbon dioxide, aluminum sulfate coagulation, seasonal polymer*, three-stage hydraulic flocculation, direct anthracite-sand biofiltration, chlorination, sodium hydroxide, zinc-orthopolyphosphate, fluoride
Bennery Lake	Lime, potassium permanganate, carbon dioxide, aluminum sulfate coagulation, three-stage hydraulic flocculation, sedimentation, anthracite-sand filtration, chlorination, sodium hydroxide, zinc-orthopolyphosphate
Fletcher Lake	Ultrafiltration, nanofiltration, ultraviolet, chlorination
Lake Major	Lime, carbon dioxide, aluminum sulfate coagulation, polymer, flocculation, up-flow clarification, pre-chlorination, anthracite-sand filtration, chlorination, sodium hydroxide, zinc-orthopolyphosphate, fluoride

*The treatment plant at Pockwock Lake was not using seasonal polymer when sampling was conducted.

Samples included raw water, pre-filtered water, filtered water, and finished water from each location, with the exception of pre-filtered water and finished water from Fletcher Lake. Raw water samples were taken from the plant's raw water intake at all locations. Pre-filtered water was taken from the final flocculation tank for the Pockwock and Bennery Lake samples, and from the top of the clarifier, prior to pre-chlorine addition, for the Lake Major sample. A pre-filtered sample was not taken at Fletcher Lake since no additional chemicals were added between the raw water intake and ultrafiltration step. Filtered samples were taken immediately following filtration and before the addition of any finish chemicals at all locations. For Fletcher Lake, this included a sample immediately after ultrafiltration and another sample immediately after nanofiltration. Finished water samples were taken from finished water compliance taps in all locations, with the exception of Fletcher Lake where no finished water sample was taken. Samples

were collected in clean 1 L plastic bottles. Samples were stored on ice during transport to the laboratory and stored at 4°C in the laboratory. Samples were analyzed for TOC, DOC, UV_{254} and peCOD.

6.3.3 Determination of Organic Carbon and UV Absorbance

TOC and DOC samples were prepared headspace free in baked (100°C for 24 h) 40 mL borosilicate glass vials, preserved with three drops of phosphoric acid to pH < 2 and analyzed using a TOC analyzer (TOC-V CPH analyzer, Shimadzu Corp, Kyoto, Japan). Samples for DOC were filtered through a 0.45 µm filter paper that was rinsed with 500 mL deionized water prior to preparation. Samples were analyzed for UV_{254} using a spectrophotometer (DR/4000 U Spectrophotometer and DR 5000™ UV-Vis Laboratory Spectrophotometer, Hach Company, Mississauga, Ontario, Canada). SUVA was determined by dividing the UV_{254} (cm^{-1}) by the DOC (mg/L) and multiplying by 100. Model compound TOC and peCOD samples were prepared immediately after the compounds were diluted. Surface water sample preparation was completed within eight hours of sample collection.

6.3.4 peCOD Analysis

Samples were analyzed for peCOD using a commercial COD analyzer (PeCOD® L100 AssayPlus™ analyzer, MANTECH INC., Guelph, Ontario, Canada) with an autosampler (AutoMax™ 73 autosampler, MANTECH INC., Guelph, Ontario, Canada) and associated automation software (PC-Titrate™ software, MANTECH INC., Guelph, Ontario, Canada). This method has a manufacturer reported calculated method detection limit of 0.5 mg/L and sample analysis time ranging from 5-10 minutes. To measure COD, the analyzer measures the current generated from the photocatalytic oxidation of organic matter using a titanium dioxide catalyst irradiated with UV light from a light emitting diode (LED). The analyzer performs a direct count of the electrons transferred during the oxidation of the sample. This method of COD determination does not include a digestion step and is therefore considered a measure of soluble COD.

Samples were measured after a single point calibration with 20 mg/L COD calibrant (Blue range (<25 mg/L) calibrant, MANTECH INC., Guelph, Ontario, Canada) and calibration verification with calibrant standards of 20, 15, 10, 5, 3, 1, 0.5 and 0.25 mg/L for model organic compounds and of 20, 15, 10, 5, 3 and 1 mg/L for surface waters. The system was operated with a sample-to-electrolyte ratio of 3:1, in which the electrolyte is used to determine the background photocurrent generated by the oxidation of water. Calibration was accepted when the COD-to-charge generated ratio was between 0.02 and 0.06 COD/μC, the terminal photocurrent generated was >90% of the 20 μA baseline and the R^2 of the calibration verification was ≥ 0.99. A COD-to-charge generated ratio in this range ensured that the charge generated from the oxidation reaction was adequate for the expected calibrant concentration (20 mg/L). A terminal photocurrent near the baseline photocurrent ensured that the calibrant was oxidized completely.

6.3.5 Determination of Theoretical Oxygen Demand (ThOD)

ThOD is the amount of oxygen required to oxidize a given compound based on stoichiometry (Droste, 1997). ThOD was determined according to the equation described by Baker et al. (1999):

$$C_nH_mO_eX_kN_jS_iP_h + bO_2 \rightarrow$$

$$nCO_2 + \frac{m-k-3j-2i-3h}{2}H_2O + kHX + jNH_3 + iH_2SO_4 + hH_3PO_4 \qquad (1)$$

where X is the sum of halogens and

$$b = n + \frac{m-k-3j-2i-3h}{4} - \frac{e}{2} + 2i + 2h \qquad (2)$$

ThOD for sodium acetate, sodium oxalate and sodium formate dilutions were calculated on the basis of the acid form for each; acetic acid, oxalic acid and formic acid.

6.4 RESULTS AND DISCUSSION

6.4.1 Correlation between peCOD and ThOD

The model organic compounds were used to determine peCOD correlation to ThOD. In this case, a value of unity demonstrated that peCOD was a complete predictor of ThOD. Overall, model compound peCOD measurements showed reasonable correlation with ThOD, with the exception of the reference standards.

The reference standards, caffeine and KHP, had slopes of 0.69 ($R^2 = 0.96$) and 1.92 ($R^2 = 0.99$), respectively (Figure 6.1). The value of unity was not contained in the 95% confidence interval of the regression slope for either reference compound indicating that peCOD was not a good predictor of ThOD for these compounds.

Oxalate, formate and acetate had slopes of 1.47 ($R^2 = 0.99$), 0.96 ($R^2 = 0.98$) and 0.79 ($R^2 = 0.94$), respectively (Figure 6.2). Formate and acetate peCOD correlated well with ThOD as the 95% confidence intervals of both regression slopes contained the expected value of unity. Oxalate gave a statistically higher peCOD/ThOD response than expected. Esler et al. (2010) found a similar result where the COD/ThOD ratio for oxalic acid was greater with peCOD than dichromate COD. Esler et al. (2010) attributed this to current doubling (one UV photon yielding two photocurrent electrons) during the photocatalytic reaction. This photocatalytic reaction behavior was unique to oxalic acid among the 34 compounds investigated by Esler et al. (2010).

Phenylalanine, tyrosine and tryptophan had slopes of 1.14 ($R^2 = 0.98$), 1.01 ($R^2 = 0.97$) and 1.01 ($R^2 = 0.99$), respectively (Figure 6.3). Regressions for all three amino acids had slopes with 95% confidence intervals containing the expected value of unity, demonstrating excellent correlation between amino acid peCOD and ThOD.

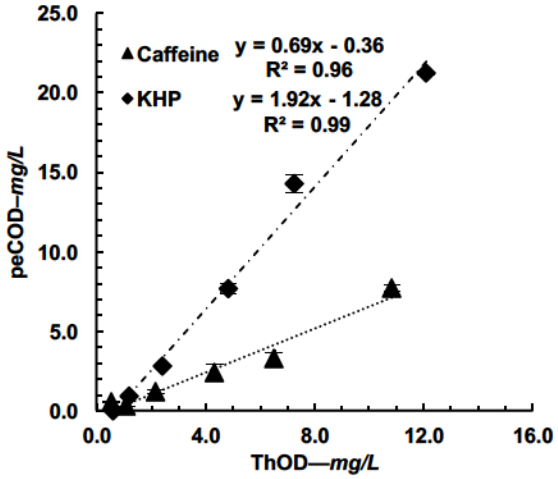

Figure 6.1 Relationship between ThOD and peCOD for reference model compounds. Error bars represent the 95% confidence interval of the data with n = 3

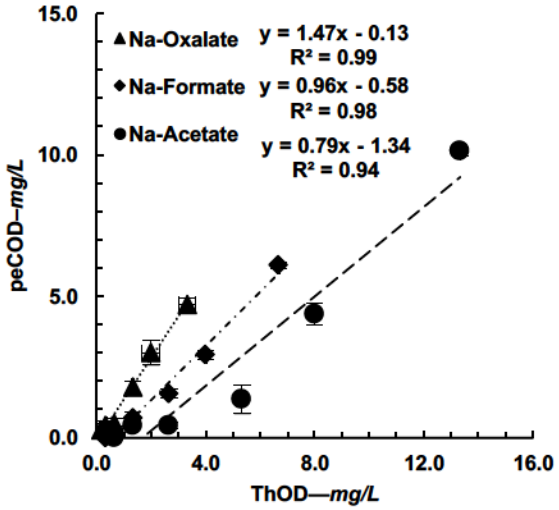

Figure 6.2 Relationship between ThOD and peCOD for carboxylic acid model compounds. Error bars represent the 95% confidence intervals with *n* = 3

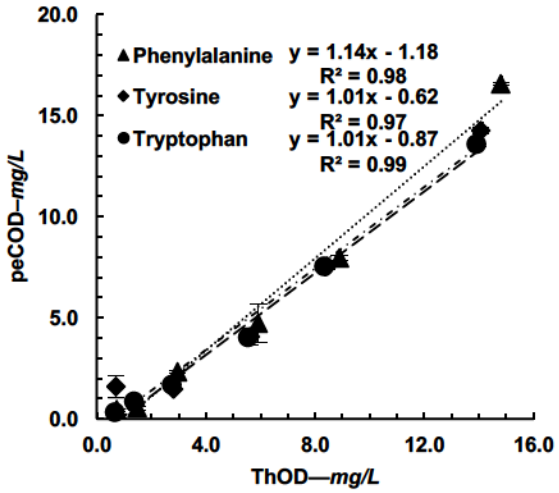

Figure 6.3 between ThOD and peCOD for amino acid model compounds. Error bars represent the 95% confidence intervals with $n = 3$

6.4.2 Model Compounds

peCOD-to-TOC relationships were observed for model compounds. On the basis of the stoichiometry of the oxidation reactions, the theoretical COD/TOC ratios (molecular ratio of oxygen to carbon) for caffeine and KHP are 2.17 and 2.5, respectively. Measured slopes for caffeine and KHP were 1.53 ($R^2 = 0.97$) and 5.04 ($R^2 = 0.99$) (Figure 6.4). Theoretical COD/TOC ratios were not contained in the 95% confidence interval of the regression slope for either reference compound. This is likely a result of poor correlation of peCOD to ThOD for these compounds as noted earlier.

The theoretical COD/TOC values for oxalate, formate and acetate are 0.67, 1.33 and 2.67, respectively. The carboxylic acid group had measured slopes of 1.03 ($R^2 = 0.99$), 1.33 ($R^2 = 0.98$) and 2.14 ($R^2 = 0.94$) for oxalate, formate and acetate, respectively (Figure 6.5). The intercepts were not statistically different from zero ($p>0.05$) for two of the three carboxylic acids with formate being the exception ($p = 0.019$). Regressions for formate and acetate had slopes with 95% confidence intervals containing the theoretical COD/TOC ratio. The 95% confidence interval for the COD/TOC ratio for oxalate did not

contain the theoretical COD/TOC value of 0.67. This difference is likely a result of the peCOD overestimation of oxalate ThOD.

Theoretical COD/TOC relationships for phenylalanine, tyrosine and tryptophan are 2.96, 2.81 and 2.79, respectively. The amino acid group had measured slopes of 3.24 (R^2 = 0.99), 3.05 (R^2 = 0.96), and 3.11 (R^2 = 0.99) for phenylalanine, tyrosine and tryptophan, respectively (Figure 6.5). The intercepts were statistically different from zero ($p<0.05$) for phenylalanine and tryptophan but not for tyrosine ($p = 0.219$). Regressions for all three amino acids had slopes with 95% confidence intervals containing the theoretical COD/TOC ratio.

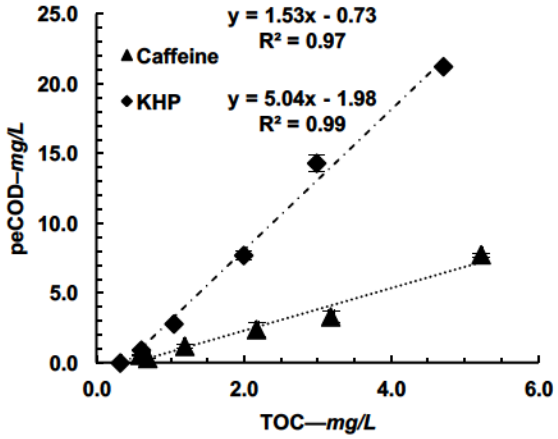

Figure 6.4 Relationship between TOC and peCOD for reference compounds. Error bars represent the 95% confidence intervals with *n* = 3

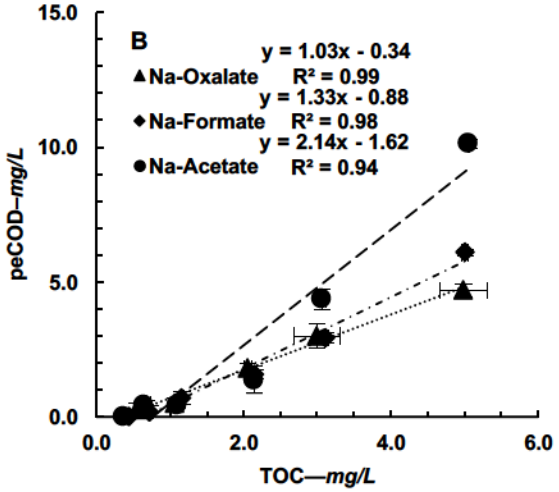

Figure 6.5 Relationship between TOC and peCOD for carboxylic model compounds. Error bars represent the 95% confidence intervals with $n = 3$

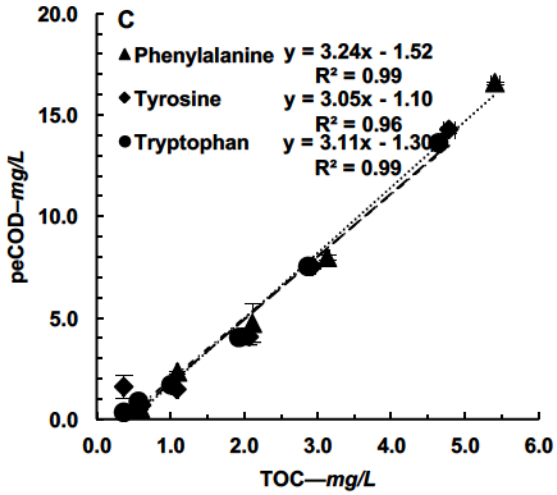

Figure 6.6 Relationship between TOC and peCOD amino acid model compounds. Error bars represent the 95% confidence intervals with $n = 3$

6.4.3 Surface and Treated Waters

Recognizing the potential for peCOD to evaluate NOM in water, four surface waters were analyzed during the course of treatment. peCOD, TOC, DOC, UV_{254}, and peCOD/TOC ratio results are provided in Table 6.3.

Table 6.3 peCOD , TOC, DOC, UV_{254} and peCOD/TOC ratio for four surface water treatment trains. All values are average with $n = 3$.

Surface Water	Sample Location	peCOD–*mg/L*	TOC–*mg/L*	DOC–*mg/L*	UV_{254}–*/cm*	peCOD/TOC
Fletcher Lake	Raw	15.1	4.60	4.37	0.19	3.3
	Ultrafilter	14.4	4.29	4.25	0.17	3.4
	Nanofilter	0.1	0.26	0.38	0.00	0.5
Lake Major	Raw	17.6	5.30	5.25	0.25	3.3
	Clarifer	4.7	2.11	2.05	0.04	2.2
	Filter	4.0	1.93	1.88	0.03	2.1
	Finish	4.0	2.05	2.00	0.03	1.9
Bennery Lake	Raw	20.5	5.91	5.92	0.23	3.5
	Floc	6.5	6.48	2.87	0.05	1.0
	Filter	6.2	2.83	2.81	0.05	2.2
	Finish	6.2	2.75	2.74	0.04	2.3
Pockwock Lake	Raw	7.4	2.73	2.71	0.09	2.7
	Floc	5.6	2.83	1.97	0.04	2.0
	Filter	4.1	1.68	1.71	0.03	2.4
	Finish	3.8	1.70	1.66	0.03	2.2

Results show that raw water peCOD for all locations was < 50 mg/L, preventing use of COD standard methods 5220Ba, 5220C and 5220D (APHA, 2012). Standard Method 5220B can be altered (5220Bb) at the expense of precision and accuracy to allow COD determination from 5 to 50 mg/L. The use of this method would allow for COD determination of raw water from the four locations. However, peCOD decreased with treatment progression for all treatment trains, resulting in filtered water peCOD concentrations less than 5 mg/L for three of the four treatment systems investigated.

As with model compounds, peCOD/TOC ratios were calculated for each surface water sample location (Table 6.3). Measured and compared on a regular basis, these ratios could provide utilities with insight into the relative proportions of oxidizable organic matter, as increases in COD/TOC ratios over reaction times have been attributed to the formation of degradation products and subsequent increase in easily oxidizable organic matter (Balcioglu and Arslan, 1998). Additionally, previous studies with Nova Scotia

surface water have shown that TOC was strongly correlated with DBP formation (Waller et al, 1996).

Overall, reductions in peCOD during the course of treatment at all utilities mirrored reductions in TOC and DOC, demonstrating the ability of peCOD to function as a treatment-performance indicator similar to TOC and DOC.

As shown in Table 6.3, the DOC in Pockwock Lake was reduced from 2.71 mg/L to 1.66 mg/L, or a total of 1.05 mg/L, from raw to finished water. Comparatively, the peCOD reduction from raw to finished water was much greater at 3.6 mg/L. This expanded scale of resolution noted with peCOD could allow for easier detection of subtle changes in treatment performance and subsequent water quality. This expanded scale could be especially important for biofiltration monitoring because the biodegradable fraction of DOC typically represents between 10 and 30% of the total DOC (Joret et al, 1991), often putting DOC reductions across biofilters in the µg/L range. For example, reduction in DOC across the filter was similar to values reported elsewhere (Lauderdale et al, 2012), but, as illustrated in Figure 6.7, Pockwock Lake had a much larger peCOD reduction (1.5 mg/L) than DOC reduction (0.26 mg/L) across the biofilter.

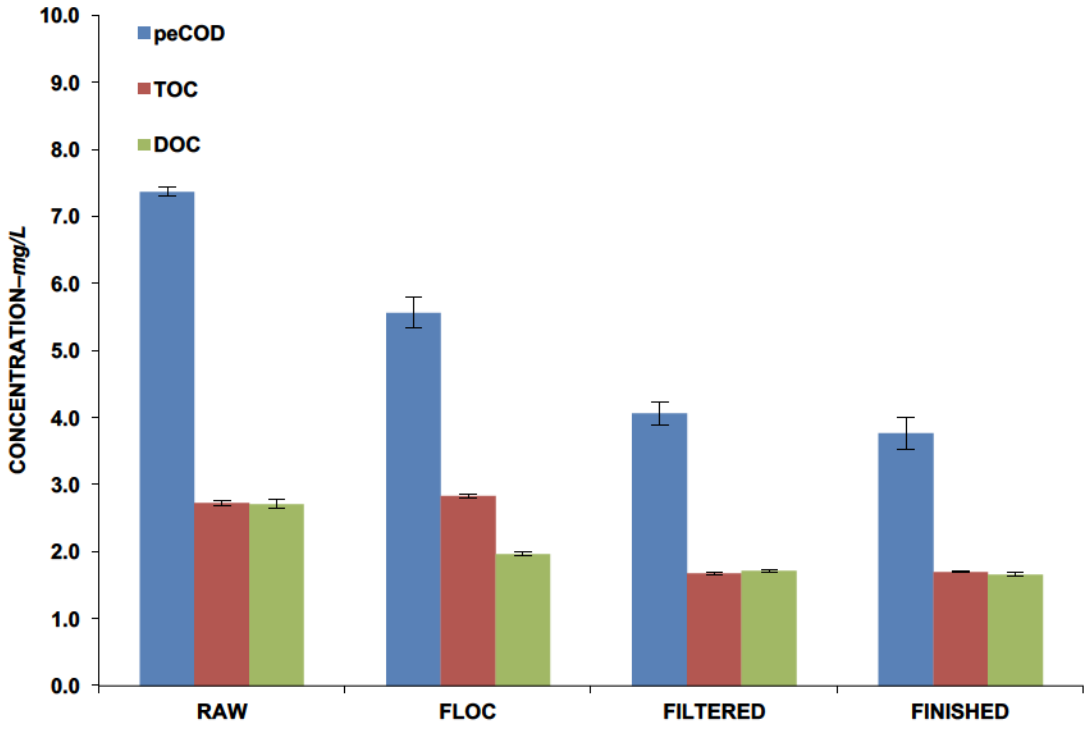

Figure 6.7 Comparison of Pockwock Lake peCOD, TOC and DOC during treatment. Error bars represent 95% confidence intervals with $n = 3$

COD is common in monitoring wastewater treatment processes; it has not been used frequently for drinking water because method detection limitations have prevented application in drinking water treatment. The use of TOC to replace COD in the wastewater treatment industry has been cautioned because TOC does not actually represent the electron-donating capacity of a compound (Mara and Horan, 2003). When assessing the performance of drinking water biological treatment, this has led to the use of slower, more labor-intensive measurement techniques such as assimilable organic carbon (AOC) and biodegradable dissolved organic carbon (BDOC) (Huck, 1990). With biological treatment gaining popularity in the drinking water industry, rapid assessment tools are required, and determination of COD in the treated drinking water concentration range is increasingly important. Measurable reductions in peCOD across the biofilter at Pockwock Lake show the potential for peCOD use as a biofiltration performance indicator. Measurement of COD at drinking water concentrations would also be

beneficial for monitoring oxidation processes proceeding biofiltration because COD can distinguish between compounds with the same number of carbon atoms at different oxidation states.

In the Fletcher Lake raw water sample, 95% of TOC was in the dissolved form and therefore there was very little reduction of TOC and DOC with ultrafiltration at this facility. As a result, the majority of TOC and DOC removal at this facility is through nanofiltration causing significant NOM loading to the nanofilter and increasing fouling rates. The difficulties with the membrane process at this treatment facility have been documented elsewhere (Lamsal et al, 2012). As shown in Figure 6.8, similar to TOC and DOC removal, reduction in peCOD with ultrafiltration was also limited, with the majority of peCOD removed with nanofiltration demonstrating the ability of peCOD to provide similar treatment performance information as TOC and DOC.

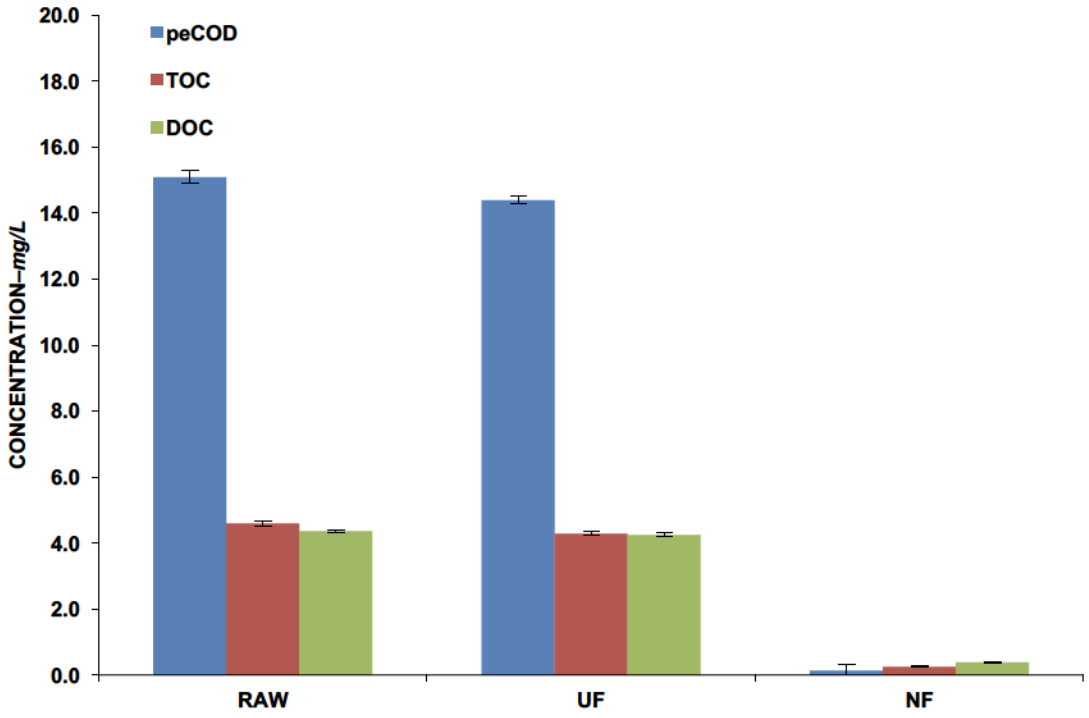

Figure 6.8 Comparison of Fletcher Lake peCOD, TOC and DOC during treatment. Error bars represent 95% confidence intervals with $n = 3$

The analysis of surface waters showed that peCOD was correlated with TOC and DOC in four raw and treated surface waters which is consistent with the model organic compounds studied in this paper. The correlations peCOD = 2.69TOC + 0.49 ($R^2 = 0.64$) and peCOD = 3.91DOC – 3.08 ($R^2 = 0.97$) were identified. The slopes of both correlations were significant at $p < 0.01$. The intercept was only significant for the DOC relationship ($p < 0.01$). It was anticipated that peCOD would be better correlated with DOC than TOC since, as previously mentioned, peCOD does not include a digestion step and is thus a measure of soluble COD.

SUVA was also determined over the course of treatment for the four surface waters. SUVA is considered an indicator of aromaticity (Weishaar et al, 2003), which is often associated with reactivity of NOM. The relationship peCOD = 4.27SUVA – 2.26 ($R^2 = 0.84$) was identified for pooled data for samples taken at the source, during treatment and after treatment at the four locations (Figure 6.9). The slope of the correlation was

significant at $p < 0.01$ and the intercept was not statistically different from zero with $p = 0.131$. This relationship shows that peCOD has a relationship with SUVA for the waters tested and could provide additional insight into reactivity of organic matter for these sites. A relationship could be useful in a practical sense, as SUVA determination typically involves the use of two analytical tools (spectrophotometer for UV_{254} determination and TOC analyzer for DOC determination), whereas peCOD can be determined rapidly with a single analytical tool.

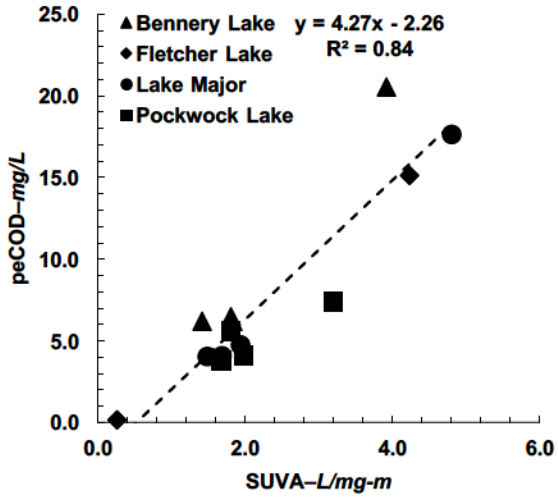

Figure 6.9 Relationship between SUVA and peCOD for four surface water sources pre-, during and post-treatment

Overall, it is noteworthy that this work was conducted in oligotrophic Canadian waters, and further work would be required for its suitability to other water matrixes. Although not an issue for the waters investigated in this study, Zhang and Zhao (2008) found that peCOD was sensitive to chloride concentrations above 26.6 ppm. To address conductivity concerns, the authors reported that measurement error could be reduced to acceptable levels (i.e., < 5%) with a chloride-to-organics ratio smaller than 5:1. Similarly, the current study provides evidence for the development of peCOD as a useful drinking water NOM surrogate.

6.4.4 peCOD as a Biofiltration Performance Indicator

Removal of NOM is often a critical target for drinking water biofiltration. However, traditional NOM surrogates may not be suitable to understand NOM removal in biofilters. Parameters such as assimilable organic carbon (AOC) and biodegradable dissolved organic carbon (BDOC) normally require several days to weeks to process and therefore do not provide a rapid indication of substrate removal. Additionally, removal of TOC across biofilters directly following coagulation/flocculation processes can be confounded by particle removal. More recently, studies have shown poor connection between DOC removal across biofilters and bioactivity as measured by ATP (Pharand et al., 2014; Chapter 2), making it difficult to routinely and meaningfully assess substrate removal/transformation across biofilters. As biological oxidation of organic matter yields ATP and simpler organic compounds (Jurtshuk, 1996), this preliminary study hypothesized that DOC may not provide information on biodegradation of NOM due to transformation of NOM through incomplete oxidation reactions. As a result, additional sampling was conducted over a period of nine months at the JD Kline Water Supply Plant treating water from Pockwock Lake as a short validation study to compare peCOD to TOC and DOC. Average TOC, DOC and peCOD concentrations for raw water, post-coagulation/flocculation and post-biofiltration are provided in Table 6.4. Percentage removals for coagulation/flocculation and biofiltration are provided in Figure 6.10.

Table 6.4 Average raw water, post-coagulation/flocculation and post-biofiltration TOC, DOC and peCOD concentration. +/- represents the standard deviation of the data

Parameter	Raw Water	Coagulation/Flocculation		Biofiltration	
	Mean	Mean	Removal	Mean	Removal
TOC—*mg/L*	3.16 ± 0.13	3.00 ± 0.16	0.16	2.06 ± 0.07	0.94
DOC—*mg/L*	3.04 ± 0.34	2.07 ± 0.06	0.97	2.09 ± 0.12	-0.05
peCOD—*mg/L*	8.51 ± 0.55	5.90 ± 0.46	2.61	4.64 ± 0.42	1.26

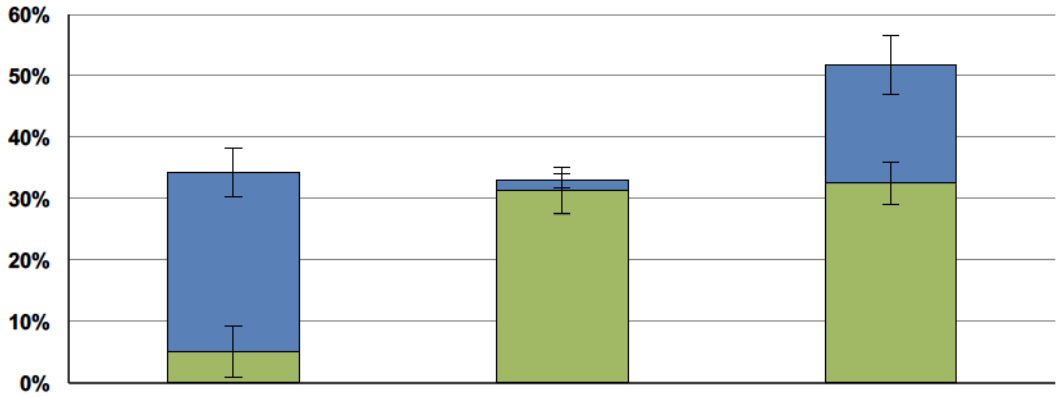

Figure 6.10 TOC, DOC and peCOD percentage removals for coagulation/flocculation and biofiltration

As shown in Table 6.4, peCOD removal for both coagulation/flocculation and biofiltration was greater than TOC and DOC removal on a mass basis. This was anticipated based on the TOC/peCOD and DOC/peCOD correlations identified previously (i.e., peCOD = 2.69TOC + 0.49 (R^2 = 0.64) and peCOD = 3.91DOC – 3.08 (R^2 = 0.97)). As shown in Figure 6.10, TOC removal primarily occurred during biofiltration, likely as a result of physical removal of flocculated material. DOC removal primary occurred following coagulation/flocculation, corroborating the assumption that the substantial TOC removal across the biofilter was physical-chemical. Given that the TOC removal observed across the filter was likely physical-chemical removal, peCOD removal as a result of coagulation/flocculation was similar to that of TOC and DOC at approximately 30%, indicating that the TOC:peCOD and DOC:peCOD ratios remained largely unchanged through physical-chemical treatment. However, peCOD removal across the biofilter was considerably greater than DOC removal across the biofilter indicating a large shift in the peCOD:DOC ratio with biofiltration. This result indicated that the use of peCOD to monitor biofiltration may provide additional information on NOM removal and subsequent biofilter performance to compliment traditional NOM surrogates.

A comparison of total peCOD and dissolved peCOD (filtered at 0.45 µm), TOC and DOC was also conducted with respect to filter run time. peCOD, TOC and DOC measurements were taken in conjunction with ATP testing conducted on full-scale filter 1 and filter 2 (Figure 3.4). As shown in Figure 6.11, effluent TOC and DOC concentration remained constant over the course of the each filter run, while total and dissolved peCOD decreased with respect to filter run time. When compared with the ATP results from these filter cycles (Figure 3.4), the decrease in effluent peCOD also corresponded with an increase in filter media biomass. This result again demonstrates that peCOD may detect NOM transformation or removal that is not evident with DOC measurements.

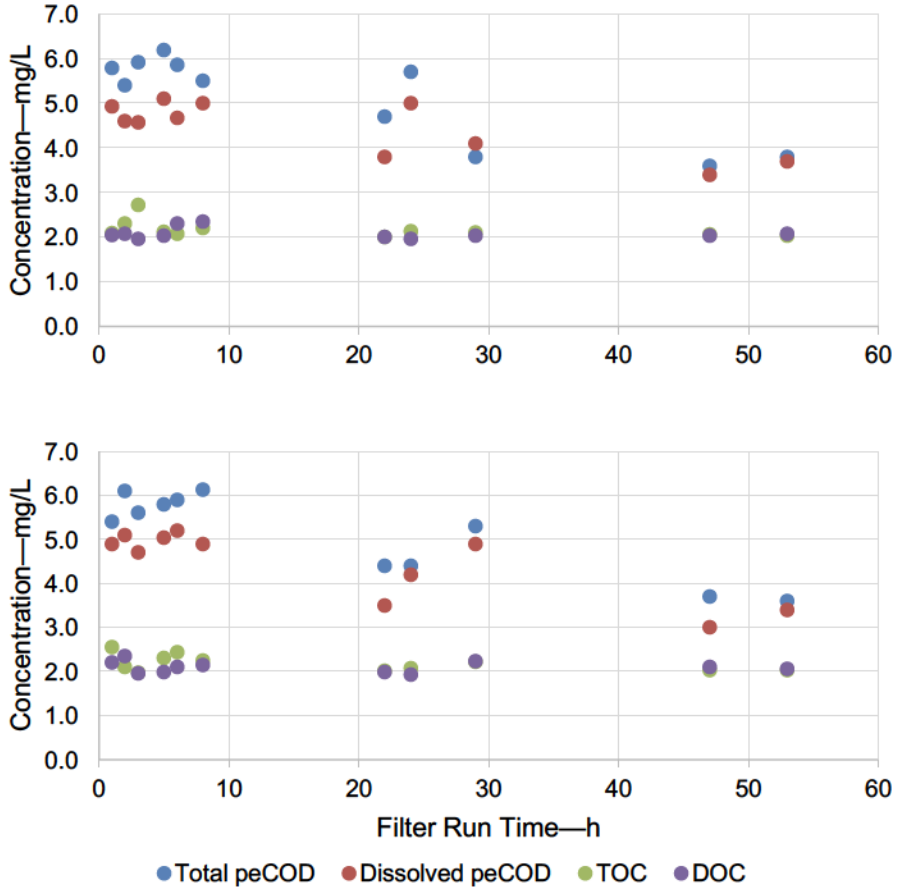

Figure 6.11 Filter 1 (top) and filter 2 (bottom) total peCOD, dissolved peCOD, TOC and DOC effluent concentration with respect to filter run time.

6.5 CONCLUSIONS

This paper demonstrated the potential for photoelectrochemical determination of COD in the drinking water industry. Analysis with eight reference compounds was reproducible and followed a predictable trend with ThOD and TOC for most compounds. peCOD was also used to monitor NOM at four surface water treatment plants. It was found that the removal of peCOD followed a trend that was similar to other NOM surrogate parameters, such as TOC and DOC. When compared with other surrogate parameters, peCOD had an expanded scale of resolution, highlighting its ability to provide information on treatment performance even when NOM removal is small (e.g., in the µg C/L range across a biofilter). Given the need for rapid response time in treatment plant analysis, it is conceivable that this tool could be accepted for inline analysis or for analysis of water treatment processes that require more understanding of NOM removal such as biofiltration and advanced oxidation.

CHAPTER 7 CONCLUSIONS AND RECOMMENDATIONS

7.1 Conclusions

This research used pilot- and full-scale studies to investigate conversion from direct filtration (chemical coagulation-flocculation-filtration) to biofiltration (chemical coagulation-flocculation-biofiltration) in a drinking water treatment plant. As part of this work there was a need to address a knowledge gap surrounding process monitoring tools for optimizing biofilter enhancements.

The research was guided by two research questions:

1. Can direct filters be converted to direct biofilters without negatively impacting filter performance?
2. What process monitoring tools can be used to understand and enhance biofiltration performance?

These research questions were addressed through the following research objectives:

1. Determine if conversion from direct filtration to biofiltration can increase NOM removal and decrease DBP formation without negatively impacting filter performance;
2. Understand how converted biofilters acclimate biologically following conversion from direct filtration to biofiltration;
3. Investigate the use of nutrient, oxidant and media enhancement strategies to increase NOM removal and decrease DBP formation in biofilters;
4. Examine the effect of nutrient and oxidant enhancement strategies on the biomass quantity and microbial community structure in biofilters;
5. Assess the use of photoelectrochemical chemical oxygen demand as a drinking water treatment and biofiltration performance indicator.

7.1.1 Research Question 1: Conversion to Biofiltration

Prechlorination was removed from a full-scale direct filtration drinking water treatment process to implement a direct biofiltration process (Objective 1). Water quality and filter performance parameters before and after the conversion were compared under both warm and cold water conditions. Once prechlorine was removed, biomass concentration, as measured by ATP on the filter media at the end of an individual filter cycle, increased to levels observed in other drinking water biofilters. Average daily finished water production, filter run times, filter loading rates, unit filter run volumes and clean-bed head loss were not affected by the conversion to biofiltration. Effluent turbidity increased with conversion; however, 95th percentile effluent turbidity remained $\leq$ 0.3 NTU (i.e., the Health Canada *guideline* value for direct and conventional filtration) under both warm and cold water conditions. The 95th percentile effluent turbidity was 0.081 NTU under warm water conditions and 0.107 NTU for cold water conditions. Floc carryover under cold water conditions was a historical challenge for the study site, consequently the increased winter turbidity was not seen as a deterrent for biofiltration. On an average quarterly basis, effluent TOC and DOC removals remained unchanged before and after conversion. Limited DOC removal across the biofilters was observed; however, THM and HAA formation was reduced by 10-20 µg/L and 6-10 µg/L, respectively, in the immediate plant effluent, as well as at most points in the distribution system after conversion. This prompted the research program to identify NOM metrics other than DOC for biofilter monitoring.

Based on these findings, it was concluded that direct filters can be converted to direct biofilters to decrease DBP formation without negatively impacting filter performance.

7.1.2 Research Question 2: Biofiltration Process Monitoring Tools

7.1.2.1 NOM Monitoring

Photoelectrochemical chemical oxygen demand (peCOD) was optimized for use in a drinking water matrix and used to evaluate NOM removal (Objective 5). This was the

first application of this NOM metric to the drinking water industry. Results showed that peCOD had an expanded scale of resolution as compared to other NOM metrics, highlighting its potential to provide information on treatment performance, even when NOM removal measured by other metrics was small. The tool detected NOM transformation or removal with respect to filter run time that was not detectable with TOC or DOC. It was therefore concluded that peCOD was identified as a viable process monitoring tool for biofiltration.

7.1.2.2 Biomass Monitoring

Full-scale filter media biomass concentration was tracked during conversion to biofiltration in order to understand biofilter acclimation (Objective 2). ATP was measured at the start and end of select filter cycles for a period of nearly two years. Following start-up and despite the dynamic process of frequent backwashing, ATP measured on the filter media at both the beginning and end of the filter cycle increased with operational day. This indicated a change in biomass concentration with respect to operational day, and demonstrated ATP as a key indicator for biofiltration start-up. The length of the ATP monitoring program showed that ATP ultimately reached a steady-state with respect to operational day at both reference points after approximately 220 days; however, the accumulation pattern to reach these steady-states was somewhat dissimilar.

The ATP concentration measured at the start of the filter cycle increased from approximately 10 ng ATP/cm^3 media to a steady-state of approximately 60 ng ATP/cm^3 media, while ATP concentration measured at the end of the filter cycle increased from approximately 40 ng ATP/cm^3 media to an apparent steady-state of 270 ng ATP/cm^3 media. Values reported in the literature typically range from 100-1000 ng ATP/cm^3 media. Once the steady-states were reached, additional and focused ATP monitoring within two individual filter cycles showed the pattern of ATP accumulation on the filter media over the course of an individual filter cycle. Within both individual filter cycles,

ATP accumulated with respect to filter run time before reaching a steady-state 8 hours into the 53-hour filter cycle.

A unique growth model was used to understand this ATP accumulation in biofilters. This was the first application of this model for ATP in drinking water biofilters. Using this tool, specific accumulation rates for ATP were determined. A specific ATP accumulation rate of 0.008 d^{-1} was determined for biofilter start-up at this study site. Once biomass concentration at both the start and end of the filter cycles reached steady-state, a specific accumulation rate of 1.96-4.46 d^{-1} was identified for the individual filter cycles. Thus it was concluded that site specific benchmarks for biomass accumulation and steady-state can be established for biofiltration using ATP and this model.

7.1.2.3 DNA Sequencing

DNA sequencing was conducted to gain further insight into the microbial community within the full- and pilot-scale biofilters (Objective 4). Results showed that some bacterial genera were more abundant in the full-scale ambient condition biofilters than in the pilot-scale ambient condition biofilter, suggesting inherent differences in microbial community structure between full- and pilot-scale biofilters, even when operated under equivalent influent water quality conditions.

At the pilot-scale, nutrient addition (i.e., phosphorus [P] or combined nitrogen and phosphorus [NP]), oxidant addition (i.e., hydrogen peroxide [Ox]) and filter media configuration (i.e., addition of a GAC cap) were investigated as strategies to potentially improve biofilter effluent water quality and operational performance (Objective 3). Both the NP and NPOx enhancements increased media biomass concentrations (i.e., ATP) as compared to the ambient condition, while P enhancement alone did not. Increases in filter media biomass again did not correspond to an increase in NOM removal (i.e., effluent TOC, DOC or SUVA) or a reduction in THM or HAA formation potential as compared to an ambient condition biofilter. Operationally, enhancements did not significantly impact effluent turbidity; however, mixed outcomes were identified for head loss, with combined nitrogen, phosphorus and oxidant addition resulting in a reduction in head loss.

Use of DNA sequencing revealed clear differences in the microbial community structure when nitrogen and phosphorus (NP), and nitrogen, phosphorus, and hydrogen peroxide (NPOx) were applied in combination; however, a similar microbial community structure to the ambient pilot-scale biofilter was observed when phosphorus (P) enhancement alone was applied. Thus, DNA sequencing was a useful tool to identify impacts to biomass that were not evident with effluent water quality metrics.

7.2 Recommendations

Based on the findings and limitations of this work, there are several recommendations for future research.

7.2.1 Conversion from Direct Filtration to Direct Biofiltration

The full-scale conversion to biofiltration investigated in this study represents a specific set of conditions where conversion did not result in any immediate unintended consequences. However, biofiltration has been associated with a number of operational challenges (e.g., rapid head loss development, underdrain clogging) and should be implemented with caution. Biofiltration was piloted at this full-scale location for approximately one year before conversion was attempted.

Additionally, while the focus of this study was NOM removal and potential unintended consequences to filter operational performance, maintenance of a free chlorine residual in filter influent can promote manganese oxidation and precipitation on filter media and removal of prechlorination to convert to biofiltration can result in manganese release from filter media (Lauderdale et al., 2016). The potential for manganese desorption and release should be considered during conversion studies (Lauderdale et al., 2016).

7.2.2 Tools to Evaluate Biofiltration Performance

7.2.2.1 Adenosine Triphosphate

Biomass concentrations in aqueous samples (i.e., raw water, biofilter effluent and biofilter interstitial water) and on filter media (i.e., anthracite and GAC) were assessed using ATP throughout this study. With respect to process control, fitting the ATP data collected during filter acclimation following the removal of prechlorination to the Baranyi and Roberts model allowed for the estimation of growth rate (increase in ATP concentration at the start of the filter cycle with respect to operational day), accumulation rate (increase in ATP over the course of an individual filter cycle), and steady-state. Within an individual water treatment plant, these parameters could be used for benchmarking purposes. For example, with respect to the JD Kline Water Supply Plant, it is recommended that plant staff revisit the results in Chapter 2 when the filter media at the JD Kline Water Supply Plant is replaced in 2017.

A limitation of measuring ATP in biofilters operated in direct filtration mode is that flocculated material is retained in the biofilter. It is recommended the filter surveillance be performed at the JD Kline Water Supply Plant to understand how floc material and biomass interact within the filter bed. Filter surveillance should also include the quantification of extracellular polymeric substances (EPS) since it is likely that the increase in ATP observed as a result of conversion to biofiltration was also accompanied by an increase in EPS. EPS has been linked to the failure of filter underdrains and rapid head loss development in biofilters.

7.2.2.2 Photoelectrochemical Chemical Oxygen Demand

This study developed a new procedure for measuring peCOD in source and treated drinking waters. The 3:1 sample to electrolyte ratio used to measure peCOD in this study is recommended for source and drinking water with peCOD concentration <25 mg/L. Source and treated drinking water tends to have low peCOD and a more concentrated sample is needed to reliably measure peCOD at low concentrations. For best results, it is

recommended that other operational parameters for the peCOD analyzer be as described in Section 6.3.4 and that the user verify the linearity of the calibration before analyzing samples. It is recommended that a consensus-based standard operating procedure (SOP) be developed for measuring peCOD in source and treated drinking waters based on the measurement conditions outlined in Section 6.3.4. Samples collected for peCOD in this study were analyzed immediately, if a consensus-based SOP is developed, it should address sample hold time and preservation.

To the authors' knowledge, this study was the first to use peCOD as a tool to evaluate biofiltration performance. It was found that peCOD had an expanded scale of resolution as compared to other bulk NOM indicators, which could make it a useful tool for (1) researchers to use to more effectively study and evaluate biofiltration optimization strategies for NOM removal and (2) plant operators to use to make process adjustments to optimize treatment train performance for NOM removal. It is also anticipated that peCOD use could be expanded to optimize other oxidation processes in drinking water treatment, such as ozonation, which is complimentary to biofiltration. It is recommended that future research test peCOD in more drinking water treatment plants to understand how it responds to source water type and various treatment processes. In addition, since peCOD was shown to be an effective NOM indicator, its ability to predict DBP formation should be evaluated. Furthermore, in the current study peCOD measurements were conducted from grab samples; however, at-line peCOD units are now available and should be investigated further for process monitoring.

As a biofiltration performance indicator, the peCOD parameter appeared to correspond well with filter media biomass concentration as measured by ATP. This relationship should be investigated further.

7.2.2.3 Microbial Community Structure

This type of analysis generates a significant amount of data and provides valuable information on the type of bacteria present. The data was analyzed with the objective of identifying differences/similarities in community structure as a result of nutrient and

oxidant additions. Further analysis of the bacteria genera present in the biofilters is recommended to determine the presence of bacteria that may be exploited for specific treatment goals (e.g., head loss control, geosmin removal) or the presence of potentially harmful bacteria.

7.2.3 Tools to Enhance Biofiltration Performance

The nutrient, oxidant and media enhancement strategies investigated in this study were tested at only one dose or configuration and were not evaluated using peCOD. If optimization of nutrient- oxidant- and/or media enhancement strategies is investigated further at this location, it is recommended that peCOD also be used as a performance indicator. Additionally, the nutrient doses investigated in this study resulted in detectable nitrogen and phosphorus in the biofilter effluent. Future nutrient enhancement studies should consider the potential downstream impacts nutrient breakthrough could have on the distribution system. Furthermore, NPOx enhancement reduced 60 hour run time head loss in pilot-scale biofilters. Should head loss become an issue for the full-scale biofilters at this location, it would be beneficial to investigate oxidant addition in the absence of nutrient addition. It is also recommended that the addition of oxidants be investigated further to address NOM removal for this study site.

REFERENCES

Ahmad, R., Amirtharajah, A., Al-Shawwa, A., & Huck, P. M. (1998). Effects of backwashing on biological filters. *Journal – American Water Works Association, 90*(12), 62-73.

American Public Health Association (APHA), American Water Works Association (AWWA), and Water Environment Federation (WEF). (2012). *Standard Methods for the Examination of Water and Wastewater, (22nd ed.).*, Washington, D.C.

Anderson, W. B., Douglas, I. P., Van Den Oever, J., Jasim, S. Y., Fraser, J. C., & Huck, P. M. (1993). Experimental techniques for pilot plant evaluation. In Proceedings, AWWA Water Quality Technology Conference, Miami, Florida.

Andrews, R. C., Alam, Z., Hofmann, R., Lachuta, L., Cantwell, R., Andrews, S., Moffet, E., Gagnon, G. A., Rand, J. & Chauret, C. (2005). Impact of Chlorine Dioxide on Transmission, Treatment, and Distribution System Performance. *Water Research Foundation* and *US Environmental Protection Agency*, Denver, Colorado.

Azzeh, J., Taylor-Edmonds, L., & Andrews, R. C. (2015). Engineered biofiltration for ultrafiltration fouling mitigation and disinfection by-product precursor control. *Water Science & Technology: Water Supply, 15*(1), 124-133.

Baker, J. R., Milke, M. W., & Mihelcic, J. R. (1999). Relationship between chemical and theoretical oxygen demand for specific classes of organic chemicals. *Water Research, 33*(2), 327-334.

Balcioglu, I. A., & Arslan, I. (1998). Application of photocatalytic oxidation treatment to pretreated and raw effluents from the Kraft bleaching process and textile industry. *Environmental Pollution*, *103*(2), 261-268.

Baranyi, J., & Roberts, T. A. (1994). A dynamic approach to predicting bacterial growth in food. *International Journal of Food Microbiology*, *23*, 277-294

Bell-Ajy, K., Abbaszadegan, M., Ibrahim, E., Verges, D., & LeChevallier, M. (2000). Conventional and optimized coagulation for NOM removal. *American Water Works Association. Journal*, *92*(10), 44.

Berney, M., Vital, M., Hülshoff, I., Weilenmann, H. U., Egli, T., & Hammes, F. (2008). Rapid, cultivation-independent assessment of microbial viability in drinking water. *Water Research, 42*(14), 4010-4018.

Blanck, C. A., (1979). Trihalomethane Reduction in Operating Water Treatment Plants. *Journal – American Water Works Association, 71*(9), 525-528.

Cabaniss, S. E., Zhou, Q., Maurice, P. A., Chin, Y. P., & Aiken, G. R. (2000). A log-normal distribution model for the molecular weight of aquatic fulvic acids. *Environmental Science & Technology*, *34*(6), 1103-1109.

Caporaso, J. G., Kuczynski, J., Stombaugh, J., Bittinger, K., Bushman, F. D., Costello, E. K., Fierer, N., Peña, A. G., Goodrich, J. K., Gordon, J. I., Huttley, G. A., Kelley, S. T., Knights D., Koenig, J. E., Ley, R. E., Lozupone, C. A., McDonald, D., Muegge, B. D., Pirrung, M., Reeder, J., Sevinsky, J.R., Turnbaugh, P.J., Walters, W.A., Widmann, J., Yatsunenko, T., Zaneveld, J., & Knight, R. (2010). QIIME allows analysis of high-throughput community sequencing data. *Nature Methods, 7*(5), 335-336.

Carlson, K. H., & Amy, G. L. (2001). Ozone and biofiltration optimization for multiple objectives. Journal *American Water Works Association*, *93*(1), 88.

Christensen, B. E., Trønnes, H. N., Vollan, K., Smidsrød, O., & Bakke, R. (1990). Biofilm removal by low concentrations of hydrogen peroxide. *Biofouling*, *2*(2), 165-175.

Coffey, B. M., Krasner, S. W., Sclimenti, M. J., Hacker, P. A., & Gramith, J. T. (1995). A comparison of biologically active filters for the removal of ozone by-products, turbidity, and particles. In Proceedings, AWWA Water Quality Technology Conference, New Orleans, Louisianna.

ComBase (2015). DMFit web edition. https://browser.combase.cc/DMFit.aspx

De Vet, W. W. J. M., Dinkla, I. J. T., Rietveld, L. C., & Van Loosdrecht, M. C. M. (2011). Biological iron oxidation by *Gallionella* spp. in drinking water production under fully aerated conditions. *Water Research, 45*(17), 5389-5398.

DeSantis, T. Z., Hugenholtz, P., Larsen, N., Rojas, M., Brodie, E. L., Keller, K., Huber, T., Dalevi, D., Hu, P., & Andersen, G. L. (2006). Greengenes, a chimera-checked 16S rRNA gene database and workbench compatible with ARB. *Applied and Environmental Microbiology, 72*(7), 5069-5072.

Dotson, A., & Westerhoff, P. (2009). Occurrence and removal of amino acids during drinking water treatment. *Journal – American Water Works Association*, *101*(9), 101-115.

Droste, R. L. (1997). Theory and Practice of Water and Wastewater Treatment. *Wiley*, New York, New York.

Edzwald, J. K., & Tobiason, J. E. (1999). Enhanced coagulation: US requirements and a broader view. *Water Science and Technology*, *40*(9), 63-70.

Edzwald, J. K., & Van Benschoten, J. E. (1990). Aluminum coagulation of natural organic matter. In Chemical water and wastewater treatment (pp. 341-359). *Springer*, Heidelberg, Germany.

Edzwald, J. K., Becker, W. C. & Wattier, K. L. (1985). Surrogate parameters for monitoring organic matter and THM precursors. *Journal – American Water Works Association*, *77(*4), 122-132

Elhadi, S. L., Huck, P. M., & Slawson, R. M. (2006). Factors Affecting the Removal of Geosmin and MIB in Drinking Water Biofilters. *Journal – American Water Works Association, 98*(8), 108-119.

Emelko, M. B., Huck, P. M., Coffey, B. M., & Smith, E. F. (2006). Effects of Media, Backwash, and Temperature on Full-Scale Biological Filtration. *Journal – American Water Works Association, 98*(12), 61-73.

Esler, M., Chinen, K., Higginbotham, H., & Reddy, P. (2010). Systematic comparison of PeCOD® and dichromate methods of COD measurement for a suite of 34 organic species. Application Note 005 v02, Aqua Diagnostic, Melbourne, Australia.

Evans, P. J., Optiz, E. M., Daniel, P. A., & Schulz, C. R. (2010). Biological Drinking Water Treatment Perceptions and Actual Experiences in North America. *Water Research Foundation*, Denver, Colorado.

Evans, P. J., Smith, J. L., LeChevallier, M. W., Schneider, O. D., Weinrich, L. A., & Jjemba, P. K. (2013a). A Monitoring and Control Toolbox for Biological Filtration. *Water Research Foundation,* Denver, Colorado.

Evans, P. J., Smith, J. L, LeChevallier, M. W., Schneider, O. D., Weinrich, L. A., & Jjemba, P.K., (2013b). Biological Filtration Monitoring and Control Toolbox: Guidance Manual. *Water Research Foundation*, Denver, Colorado.

Fang, W., Hu, J. Y., & Ong, S. L. (2009). Influence of phosphorus on biofilm formation in model drinking water distribution systems. *Journal of Applied Microbiology*, *106*(4), 1328-1335.

Fonseca, A. C., Summers, R. S., & Hernandez, M. T. (2002). Comparative measurements of microbial activity in drinking water biofilters. *Water Research, 35*(16), 3817-3824.

Ginn, B. K., Cumming, B. F., & Smol, J. P. (2007). Assessing pH Changes Since Pre-industrial Times in 51 Low-Alkalinity Lakes in Nova Scotia, Canada. *Canadian Journal of Fisheries and Aquatic Sciences, 64*(8), 1043-1054.

Goldgrabe, J. C., Summers, R. S., & Miltner, R. J. (1993). Particle Removal and Head Loss Development in Biological Filters. *Journal – American Water Works Association, 85*(12), 94-106.

Granger, H. C., Stoddart, A. K., & Gagnon, G. A. (2014). Direct Biofiltration for Manganese Removal from Surface Water. *Journal of Environmental Engineering,* 140(4). 04014006-1- 04014006-8.

Halifax Water. (2013). *Seventeenth Annual Report.* Retrieved from www.halifax.ca/hrwc/documents/Finalprooflowresweboct282013

Halifax Water. (2014). *Eighteenth Annual Report*. Retrieved from www.halifax.ca/hrwc/documents/AnnualReportFinal-2014.

Hammes, F., Goldschmidt, F., Vital, M., Wang, Y., & Egli, T. (2010). Measurement and interpretation of microbial adenosine tri-phosphate (ATP) in aquatic environments. *Water Research, 44*(13), 3915-3923.

Hargesheimer, E. E., McTigue, N. E., Mielke, J. L., Yee, P., & Elford, T. (1998). Tracking filter performance with particle counting. *Journal - American Water Works Association*, *90*(12), 32–41.

Harms, L. L. & Looyenga, R. W. (1977). Chlorination Adjustment to Reduce Chloroform Formation. *Journal – American Water Works Association, 69*(5), 258-263.

Health Canada (2014). *Guidelines for Canadian Drinking Water—Summary Table.* Water and Air Quality Bureau, Healthy Environments and Consumer Safety Branch, Health Canada, Ottawa, Canada. http://hc-sc.gc.ca/ewh-semt/pubs/ water-eau/sum_guide-res_recom/index-eng.php (accessed Oct. 2, 2015).

Hozalski, R. M. & Bouwer, E. J. (1998). Deposition and retention of bacteria in backwashed filters. *Journal – American Water Works Association, 90*(1), 71-85.

Hozalski, R. M., Bouwer, E. J., & Goel, S. (1999). Removal of natural organic matter (NOM) from drinking water supplies by ozone-biofiltration. *Water Science and Technology*, *40*(9), 157-163.

Hozalski, R. M., Esbri-Amador, E., & Chen, C. F. (2005). Comparison of stannous chloride and phosphate for lead corrosion control. *Journal – American Water Works Association*, *97*(3), 89.

Huck, P. M. (1990). Measurement of biodegradable organic matter and bacterial growth potential in drinking water. *Journal – American Water Works Association*, *82*(7), 78-86.

Huck, P. M., Coffey, B. M., Amirtharajah, A., & Bouwer, E. (2000). Optimizing Filtration in Biological Filters, Report 90793. *AWWA Research Foundation* and *AWWA*, Denver, Colorado.

Huck, P. M., Peldszus, S., Haberkamp, J., & Jekel, M. (2009). Assessing the performance of biological filtration as pretreatment to low pressure membranes for drinking water. *Environmental Science & Technology*, *43*(10), 3878-3884.

Jacangelo, J. G., DeMarco, J., Owen, D. M., & Randtke, S. J. (1995). Selected processes for removing NOM: an overview: Natural organic matter. *Journal - American Water Works Association*, *87*(1), 64-77.

Joret, J. C., Levi, Y., & Volk, C. (1991). Biodegradable dissolved organic carbon (BDOC) content of drinking water and potential regrowth of bacteria. *Water Science & Technology*, *24*(2), 95-101.

Juhna, T., & Rubulis, J. (2004). Problem of DOC removal during biological treatment of surface water with a high amount of humic substances. *Water Science and Technology: Water Supply*, *4*(4), 183-187.

Jurtshuk P. Jr. (1996). Bacterial Metabolism. In: Baron S, editor. Medical Microbiology. 4th edition. Galveston (TX): University of Texas Medical Branch at Galveston. Chapter 4. Available from: https://www.ncbi.nlm.nih.gov/books/NBK7919

Kent, F. C., Montreuil, K. R., Stoddart, A. K., Reed, V. A., & Gagnon, G. A. (2014). Combined Use of Resin Fractionation and High Performance Size Exclusion Chromatography for Characterization of Natural Organic Matter. *Journal of Environmental Science and Health, Part A, 49*(14), 1615-1622.

Kim, J. G., Kim, J. H., Moon, H. S., Chon, C. M., & Ahn, J. S, (2002). Removal capacity of water plant alum sludge for phosphorus in aqueous solutions. *Chemical Speciation & Bioavailability*, *14*(1-4), 67-73.

Knowles, A. D. (2011) Optimizing the removal of natural organic matter in drinking water while avoiding unintended consequences following coagulation. PhD. Thesis, Dalhousie University, Halifax, Nova Scotia.

Knowles, A. D., MacKay, J., & Gagnon, G. A. (2012). Pairing a Pilot Plant to a Direct Filtration Water Treatment Plant. *Canadian Journal of Civil Engineering, 39*(6), 689-700.

Kohl, P. M. & Dixon, D. (2012). Occurrence, Impacts, and Removal of Manganese in Biofiltration Processes. *Water Research Foundation*, Denver, Colorado.

Krasner, S. W., Croué, J. P., Buffle, J., & Perdue, E. M. (1996). Three approaches for characterizing NOM. *Journal – American Water Works Association*, *88(*6), 66-79.

Krasner, S. W., McGuire, M. J., Jacangelo, J. G., Patania, N. L., Reagan, K. M., & Aieta, E. M. (1989). The occurrence of disinfection by-products in US drinking water. *Journal – American Water Works Association*, *81*(8), 41-53.

Krasner, S. W., Weinberg, H. S., Richardson, S. D., Pastor, S. J., Chinn, R., Sclimenti, M. J., Onstad, G. D., & Thruston, A. D. (2006). Occurrence of a new generation of disinfection byproducts. *Environmental Science & Technology*, *40*(23), 7175-7185.

Kwon, B., Lee, S., Cho, J., Ahn, H., Lee, D., & Shin, H. S. (2005). Biodegradability, DBP formation, and membrane fouling potential of natural organic matter: Characterization and controllability. *Environmental Science & Technology*, *39*(3), 732-739.

Lamsal, R.; Chaulk, M.; Zevenhuizen, E.; Walsh, M. E.; & Gagnon, G. A., (2012a). Integrating bench-and full-scale nanofiltration testing for two surface waters. *Journal of Water Supply: Research and Technology—AQUA*, *61*(5), 291-305.

Langlais, B.; Reckhow, D. A.; & Brink, D. R. (editors), (1991). Ozone in water treatment: Application and engineering. *CRC Press LLC*, Boca Raton, Florida.

Lauderdale, C. V. (2011). Engineered biofiltration for enhanced hydraulic and water treatment performance. PhD. Thesis, University of Florida, Gainesville, Florida.

Lauderdale, C. V., Brown, J. C., Chadik, P. A., & Kirisits, M. J. (2011). Engineered Biofiltration for Enhanced Hydraulic and Water Treatment Performance. *Water Research Foundation*, Denver, Colorado.

Lauderdale, C. V., Scheitlin, K., Nyfennegger, J., Upadhyaya, G., & Brown, J. C. (2014). Optimizing Engineered Biofiltration. *Water Research Foundation*, Denver, Colorado.

Lauderdale, C., Chadik, P., Kirisits, M. J., & Brown, J. (2012). Engineered Biofiltration: Enhanced Biofilter Performance through Nutrient and Peroxide Addition. *Journal-American Water Works Association, 104*(5), E298-E309.

Lauderdale, C. V., Pope, G., Scheitlin, K., Zwerneman, J., Kirisits, M., and Bae, S. (2016). Optimizing filter conditions for improved manganese control during conversion to biofiltration. *Water Research Foundation*, Denver, Colorado.

Lautenschlager, K., Hwang, C., Ling, F., Liu, W. T., Boon, N., Köster, O., Egli, T. & Hammes, F. (2014). Abundance and composition of indigenous bacterial communities in a multi-step biofiltration-based drinking water treatment plant. *Water Research, 62*, 40-52.

LeChevallier, M. W., Schulz, W., & Lee, R. G. (1991). Bacterial nutrients in drinking water. *Applied and environmental microbiology*, *57*(3), 857-862.

LeChevallier, M. W., Becker, W. C., Schorr, P., & Lee, R. G. (1992). Evaluating the performance of biologically active rapid filters. *Journal - American Water Works Association*, *84*(4), 136-146.

LeChevallier, M. W., & McFeters, G. A. (1985). Interactions between heterotrophic plate count bacteria and coliform organisms. *Applied and environmental microbiology*, *49*(5), 1338-1341.

Lehtola, M. J., Miettinen, I. T., & Martikainen, P. J. (2002). Biofilm formation in drinking water affected by low concentrations of phosphorus. *Canadian Journal of Microbiology*, *48*(6), 494-499.

Li, X., Upadhyaya, G., Yuen, W., Brown, J., Morgenroth, E., & Raskin, L. (2010). Changes in the structure and function of microbial communities in drinking water treatment bioreactors upon addition of phosphorus. *Applied and Environmental Microbiology*, *76*(22), 7473-7481.

Liang, L., & Singer, P. C. (2003). Factors influencing the formation and relative distribution of haloacetic acids and trihalomethanes in drinking water. *Environmental Science & Technology*, *37*(13), 2920-2928.

Liao, X., Chen, C., Wang, Z., Wan, R., Chang, C. H., Zhang, X., & Xie, S. (2013). Pyrosequencing analysis of bacterial communities in drinking water biofilters receiving influents of different types. *Process Biochemistry*, *48*(4), 703-707.

Liao, X., Chen, C., Zhang, J., Dai, Y., Zhang, X., & Xie, S. (2015). Operational performance, biomass and microbial community structure: impacts of backwashing on drinking water biofilter. *Environmental Science and Pollution Research*, *22*(1), 546-554.

Liu, X., Huck, P. M. & Slawson, R. M. (2001). Factors affecting drinking water biofiltration. *Journal – American Water Works Association*, 93(12), 90-101

Lozupone, C., Lladser, M. E., Knights, D., Stombaugh, J., & Knight, R. (2011). UniFrac: an effective distance metric for microbial community comparison. *The ISME Journal*, *5*(2), 169.

MacLean, R. G., Prevost, M., & Niquette, P. (1996). Evaluating the performance of continuous flow biofilm reactors for the rapid determination of biodegradable dissolved organic carbon in drinking water. *Environmental Technology*, *17*(8), 807-817.

Magic-Knezev, A., & Van Der Kooij, D. (2004). Optimisation and significance of ATP analysis for measuring active biomass in granular activated carbon filters used in water treatment. *Water Research, 38*(18), 3971-3979.

Mara, D., & Horan, N. J. (editors)., (2003). Handbook of water and wastewater microbiology. *Academic press*, Cambridge, Massachusetts.

Matilainen, A., Gjessing, E. T., Lahtinen, T., Hed, L., Bhatnagar, A., & Sillanpää, M. (2011). An overview of the methods used in the characterisation of natural organic matter (NOM) in relation to drinking water treatment. *Chemosphere*, *83*(11), 1431-1442.

Matilainen, A., Vepsäläinen, M., & Sillanpää, M. (2010). Natural organic matter removal by coagulation during drinking water treatment: a review. *Advances in colloid and interface science*, *159*(2), 189-197.

McBean, E.; Zhu, Z.; & Zeng, W. (2010). Modeling Formation and Control of Disinfection Byproducts in Chlorinated Drinking Waters. *Water Science & Technology: Water Supply, 10*(5), 730-739.

McKie, M. J., Taylor-Edmonds, L., Andrews, R. C., & Andrews, S. A. (2015). Engineered Biofiltration for the Removal of Disinfection By-Product Precursors and Genotoxicity. *Water Research, 81*, 196-207.

McMurdie, P. J., & Holmes, S. (2013). Phyloseq: An R Package for Reproducible Interactive Analysis and Graphics of Microbiome Census Data. *Plos One 8*(4), E61217.

Miltner, R. J., Summers, R. S. & Wang, J. Z. (1995). Biofiltration performance: Part 2, effect of backwashing. *Journal – American Water Works Association 87*(12), 64-70.

Montreuil, K. R. (2011). Natural organic matter characterization in drinking water. MASc. Thesis, Dalhousie University, Halifax, Nova Scotia.

Morris, J.K. & Knocke, W.R. (1984). Temperature Effects on the Use of Metal-Ion Coagulants for Water Treatment. *Journal – American Water Works Association, 76*(3), 74-79.

Mouchet, P. (1992). From Conventional to Biological Removal of Iron and Manganese in France. *Journal – American Water Works Association,* 84(4), 158-167.

Nerenberg, R., Rittmann, B. E., & Soucie, W. J. (2000). Ozone/biofiltration for removing MIB and geosmin. Journal - *American Water Works Association*, *92*(12), 85.

Nieuwenhuijsen, M. J., Toledano, M. B., Eaton, N. E., Fawell, J., & Elliott, P. (2000). Chlorination disinfection byproducts in water and their association with adverse reproductive outcomes: a review. *Occupational and Environmental Medicine*, *57*(2), 73-85.

O'Leary, K. C., Eisnor, J. D., & Gagnon, G. A. (2003). Examination of Plant Performance and Filter Ripening With Particle Counters at Full-scale Water Treatment Plants. *Environmental Technology, 24*(1), 1-9.

Owen, D. M., Amy, G. L., Chowdhury, Z. K., Paode, R., McCoy, G., & Viscosil, K. (1995). NOM characterization and treatability. *Journal-American Water Works Association*, *87*(1), 46-63.

Persson, F., Heinicke, G., Uhl, W., Hedberg, T., & Hermansson, M. (2006). Performance of direct biofiltration of surface water for reduction of biodegradable organic matter and biofilm formation potential. *Environmental technology*, *27*(9), 1037-1045.

Pharand, L., Van Dyke, M. I., Anderson, W. B., & Huck, P. M. (2014). Assessment of Biomass in Drinking Water Biofilters by Adenosine Triphosphate. *Journal – American Water Works Association, 106*(10), E433-E444.

Pharand, L., Van Dyke, M. I., Anderson, W. B., Yohannes, Y., & Huck, P. M. (2015). Full-Scale Ozone–Biofiltration: Seasonally Related Effects on NOM Removal. *Journal – American Water Works Association 107*(8), E425-E435.

Pharand, L., Van Dyke, M. I., Halevy, P. Z., Anderson, W.B. & Huck, P. M. (2013). Effects of Seasonal Changes and Nutrient Availability on the Performance of Full-Scale Drinking Water Biofilters. *In Proceedings, AWWA Water Quality Technology Conference, Long Beach, California USA.*

Pinto, A. J., Xi, C., & Raskin, L. (2012). Bacterial community structure in the drinking water microbiome is governed by filtration processes. Environmental science & technology 46(16), 8851-8859.

Rahman, I., Van Dyke, M. I., Anderson, W. B., Jin, X., Ndiongue, S., & Huck, P. M. (2016). Effect of phosphorus addition on biofiltration pre-treatment to reduce ultrafiltration membrane fouling. *Desalination and Water Treatment*, 1-13.

Richardson, S. D., Plewa, M. J., Wagner, E. D., Schoeny, R., & DeMarini, D. M. (2007). Occurrence, genotoxicity, and carcinogenicity of regulated and emerging disinfection by-products in drinking water: a review and roadmap for research. *Mutation Research/Reviews in Mutation Research*, *636*(1), 178-242.

Rittmann, B. E. & P. M. Huck (1989). Biological treatment of public water supplies. *CRC Critical Reviews in Environmental Control*, *19*(2), 119-184.

Sang, J., Zhang, X., Li, L., and Wang, Z. (2003). Improvement of organics removal by bio-ceramic filtration of raw water with addition of phosphorus. *Water Research*, *37*(19), 4711-4718

Seredyńska-Sobecka, B., Tomaszewska, M., Janus, M., & Morawski, A. W. (2006). Biological activation of carbon filters. *Water Research, 40*(2), 355-363.

Servais, P., Anzil, A., & Ventresque, C. (1989). Simple method for determination of biodegradable dissolved organic carbon in water. *Applied and Environmental Microbiology*, *55*(10), 2732-2734.

Servais, P., Billen, G., & Bouillot, P. (1994). Biological colonization of granular activated carbon filters in drinking-water treatment. *Journal of Environmental Engineering, 120*(4), 888–899.

Siebel, E., Wang, Y., Egli, T., & Hammes, F. (2008). Correlations between total cell concentration, total adenosine tri-phosphate concentration and heterotrophic plate counts during microbial monitoring of drinking water. *Drinking Water Engineering and Science, 1*(1), 1-6.

Slade, D., & Radman, M. (2011). Oxidative stress resistance in *Deinococcus radiodurans*. *Microbiology and Molecular Biology Reviews*, *75*(1), 133-191.

Soh, Y. C., Roddick, F., & van Leeuwen, J. (2008). The impact of alum coagulation on the character, biodegradability and disinfection by-product formation potential of reservoir natural organic matter (NOM) fractions. *Water Science and Technology*, *58*(6), 1173-1179.

Speitel Jr, G. E., Symons, J. M., Diehl, A. C., Sorensen, H. W., & Cipparone, L. A. (1993). Effect of ozone dosage and subsequent biodegradation on removal of DBP precursors. *Journal – American Water Works Association*, *85*(5), 86-95.

Summers, R. S., Hooper, S. M., Shukairy, H. M., Solarik, G., & Owen, D. (1996). Assessing DBP yield: uniform formation conditions. *Journal – American Water Works Association, 88*(6), 80-93.

Suthaker, S., Smith, D. W., & Stanley, S. J., (1995). Evaluation of Filter Media for Upgrading Existing Filter Performance. *Environmental Technology*, *16*(7), 625-643.

Switzer, J. A., Rajasekharan, V. V., Boonsalee, S., Kulp, E. A., & Bohannan, E. W. (2006). Evidence that monochloramine disinfectant could lead to elevated Pb levels in drinking water. *Environmental Science & Technology*, *40*(10), 3384-3387.

Urfer, D., & Huck, P. M. (1997). Effects of hydrogen peroxide residuals on biologically active filters. *Ozone: Science & Engineering: The Journal of the International Ozone Association, 19*(4), 371-386.

U.S.EPA Method 551.1. (1995). Determination of Chlorination Disinfection By-products, Chlorinated Solvents, and Halogenated Pesticides/herbicides in Drinking Water by Liquid–liquid Extraction and Gas Chromatograph with Electron-capture Detection (Revision 1.0). Much, J.W., Hautman, D.P. Office of Research and Development, Washington, DC.

US EPA (1995) Method 552.2: determination of haloacetic acids and dalapon in drinking water by liquid–liquid extraction, derivatization and gas chromatography with electron capture detection. Environmental Monitoring and System Laboratory, Cincinnati, OH.

Vadasarukkai, Y. S., Gagnon, G. A., Campbell, D. R., & Clark, S. C. (2011). Assessment of hydraulic flocculation processes using CFD. *Journal – American Water Works Association,* 103(11), 66-80.

Vahala, R., Moramarco, V., Niemi, R. M., Rintala, J., & Laukkanen, R. (1998). The effects of nutrients on natural organic matter (NOM) removal in biological activated carbon (BAC) filtration. *Acta hydrochimica et hydrobiologica*, *26*(3), 196-199.

Van der Kooij, D., Vrouwenvelder, H. S., & Veenendaal, H. R. (1995). Kinetic aspects of biofilm formation on surfaces exposed to drinking water. *Water Science and Technology, 32*(8), 61-65.

Van der Kooij, D., Vrouwenvelder, J. S., & Veenendaal, H. R. (2003). Elucidation and control of biofilm formation processes in water treatment and distribution using the unified biofilm approach. *Water Science & Technology, 47*(5), 83-90.

Velten, S., Boller, M., Koster, O., Helbing, J., Weilenmann, H.U. & Hammes, F. (2011). Development of Biomass in a Drinking Water Granular Activated Carbon (GAC) Filter. *Water Research, 45*(19), 6347-6354.

Velten, S., Hammes, F., Boller, M., & Egli, T. (2007). Rapid and direct estimation of active biomass on granular activated carbon through adenosine tri-phosphate (ATP) determination. *Water Research*, *41*(9), 1973-1983.

Villanueva, C. M., Cantor, K. P., Cordier, S., Jaakkola, J. J., King, W. D., Lynch, C. F., Porru, S., & Kogevinas, M. (2004). Disinfection byproducts and bladder cancer: a pooled analysis. *Epidemiology*, *15*(3), 357-367.

Volk, C., Bell, K., Ibrahim, E., Verges, D., Amy, G., & LeChevallier, M. (2000). Impact of enhanced and optimized coagulation on removal of organic matter and its biodegradable fraction in drinking water. *Water Research*, *34*(12), 3247-3257.

Waines, P. L., Moate, R., Moody, A. J., Allen, M., & Bradley, G. (2011). The effect of material choice on biofilm formation in a model warm water distribution system. *Biofouling, 27*(10), 1161-1174.

Waller, D. H., MacPhee, M. J., Prendiville, P. W., McCurdy, R. F., Gates, A. W., & D'Eon, W. J. (1996). Characterization of Nova Scotia surface waters and treatment options for removal of colour and trihalomethane precursors. *Canadian Journal of Civil Engineering*, *23(*6), 1316-1325.

Wang, J. Z., Summers, R. S., & Miltner, R. J. (1995). Biofiltration performance: part 1, relationship to biomass. *Journal – American Water Works Association*, *87*(12), 55-63

Wang, Q., Garrity, G. M., Tiedje, J. M., & Cole, J. R. (2007). Naive Bayesian classifier for rapid assignment of rRNA sequences into the new bacterial taxonomy. *Applied and Environmental Microbiology, 73*(16), 5261-5267.

Wang, Y., & Qian, P. Y. (2009). Conservative Fragments in Bacterial 16S rRNA Genes and Primer Design for 16S Ribosomal DNA Amplicons in Metagenomic Studies. *Plos One, 4*(10), E7401.

Weishaar, J. L., Aiken, G. R., Bergamaschi, B. A., Fram, M. S., Fujii, R., & Mopper, K. (2003). Evaluation of specific ultraviolet absorbance as an indicator of the chemical composition and reactivity of dissolved organic carbon. *Environmental Science & Technology, 37*(20), 4702-4708.

Weishaar, J. L., Aiken, G. R., Bergamaschi, B. A., Fram, M. S., Fujii, R., & Mopper, K. (2003). Evaluation of specific ultraviolet absorbance as an indicator of the chemical composition and reactivity of dissolved organic carbon. *Environmental Science & Technology*, *37*(20), 4702-4708.

White, M. C., Thompson, J. D., Harrington, G. W., & Singer, P. C. (1997). Evaluating criteria for enhanced coagulation compliance. *Journal - American Water Works Association*, *89*(5), 64.

Woszczynski, M., J. Bergese & G.A. Gagnon. (2013). Comparison of chlorine and chloramines on lead release from copper pipe rigs. *ASCE – J. Environ Engrg.* 139(8), 1099–1107.

Zhang, X. X., Zhang, Z. Y., Ma, L. P., Liu, N., Wu, B., Zhang, Y., Li A. M. & Cheng, S. P. (2010). Influences of hydraulic loading rate on SVOC removal and microbial community structure in drinking water treatment biofilters. *Journal of hazardous materials*, *178*(1), 652-657.

Zhang, S. & Zhao, H. (2008). A new approach prevailing over chloride interference in the photoelectrochemical determination of chemical oxygen demand. *Analyst, 133*(12), 1684-1691.

Zhao, H., Jiang, D., Zhang, S., Catterall, K. & John, R. (2004). Development of a direct photoelectrochemical method for determination of chemical oxygen demand. *Analytical Chemistry*, *76*(1), 155-160.

APPENDIX A – Supplementary Figures

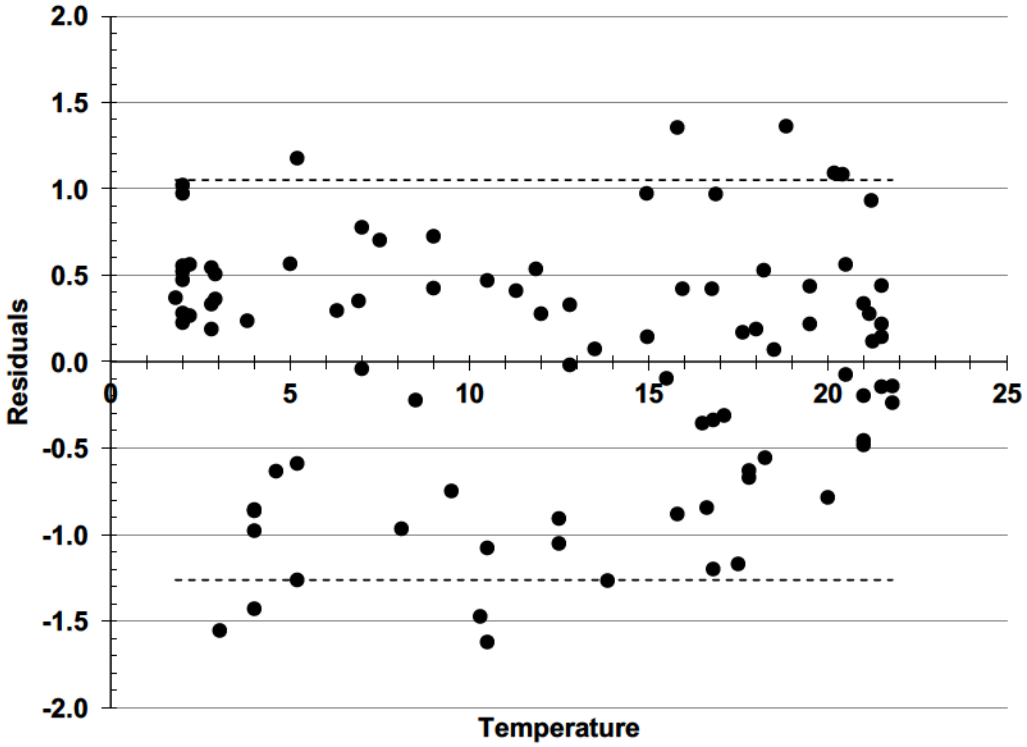

Figure A.1 Residuals analysis of natural log-transformed end-of-filter-cycle biomass concentration (ng ATP/cm^3 media) against temperature. Dashed lines represent the 5th and 95th percentiles of the data.

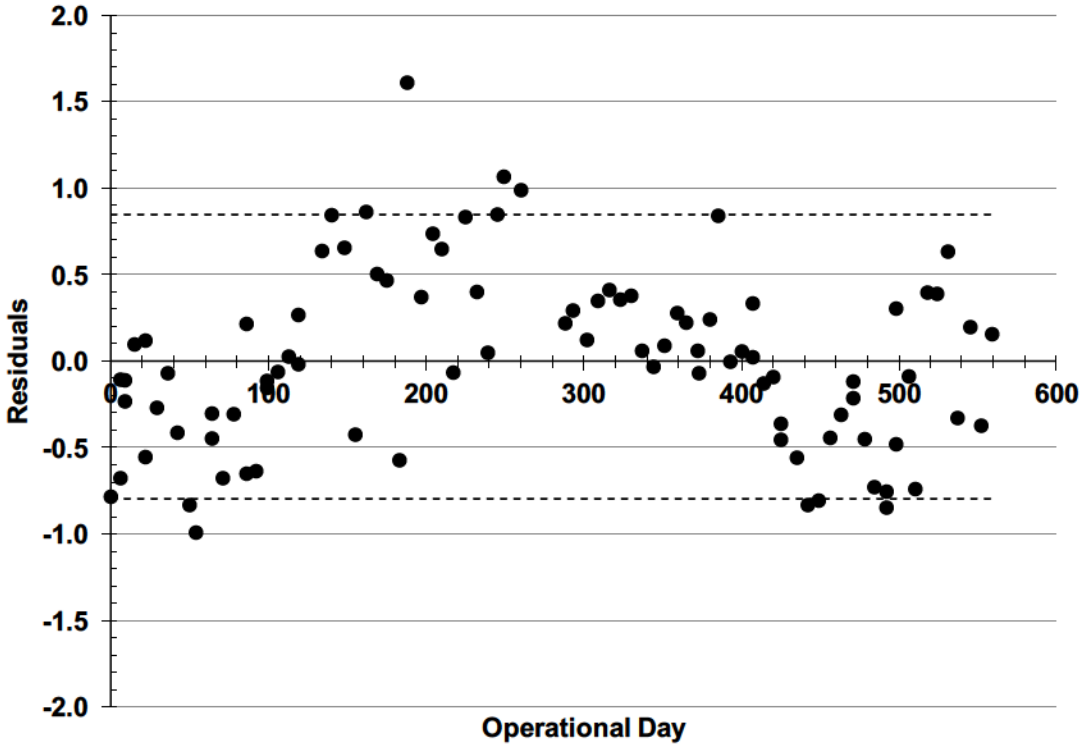

Figure A.2 Residuals analysis of natural log-transformed start-of-filter-cycle biomass (ng ATP/cm^3 media) against operational day. Dashed lines represent the 5th and 95th percentiles of the data.

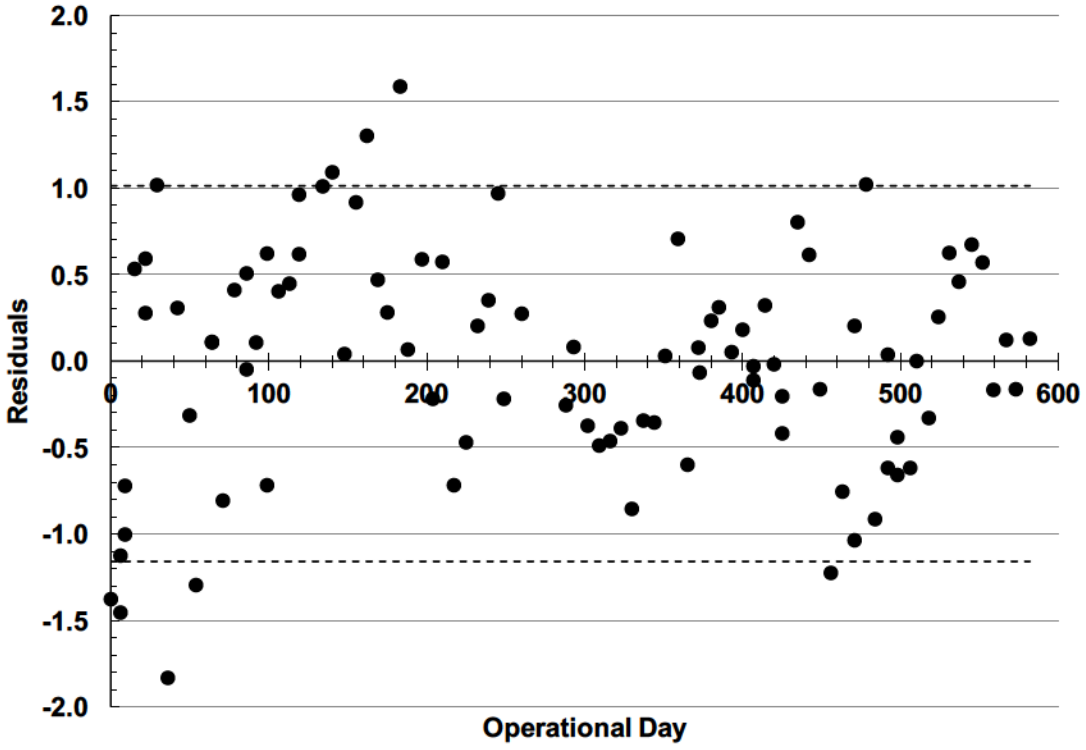

Figure A.3 Residuals analysis of natural log-transformed end-of-filter-cycle biomass concentration (ng ATP/cm^3 media) against operational day. Dashed lines represent the 5th and 95th percentiles of the data.

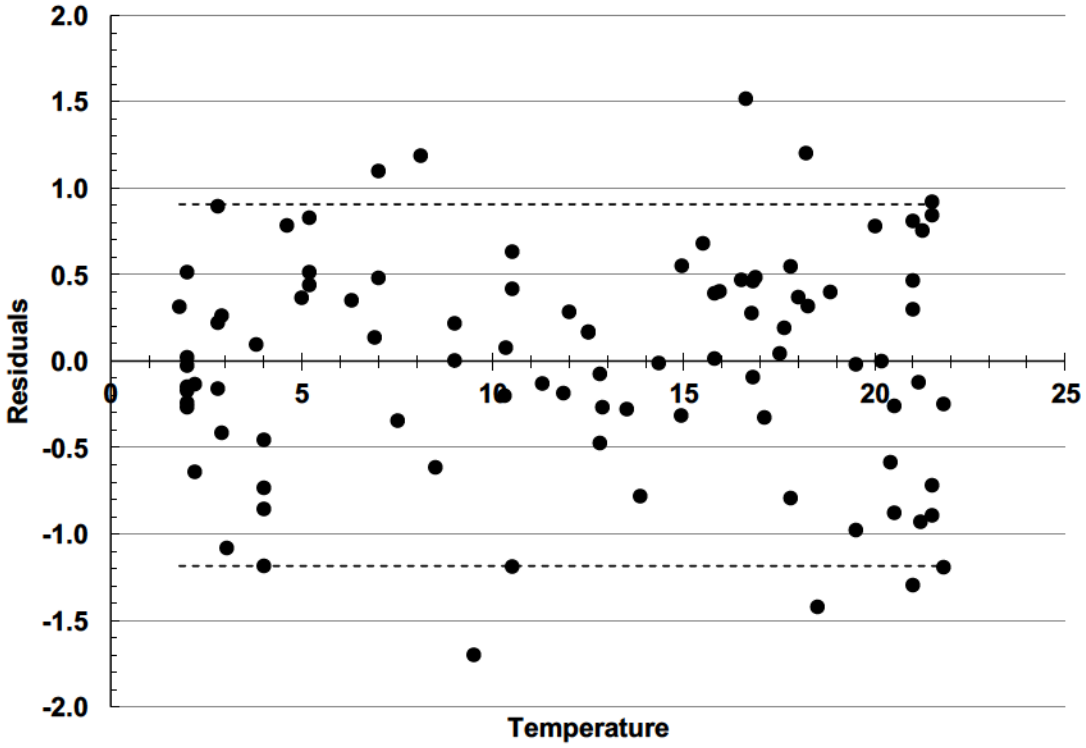

Figure A.4 Residuals analysis of natural log-transformed end-of-filter-cycle biomass (ng ATP/cm^3 media) against temperature. Dashed lines represent the 5th and 95th percentiles of the data.

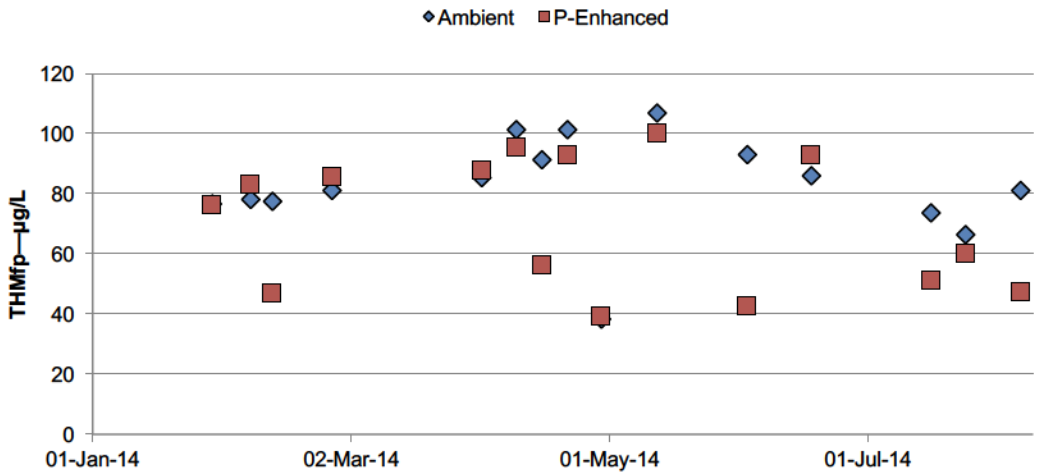

Figure A.5 THMfp in ambient and P-enhanced biofilters over time.

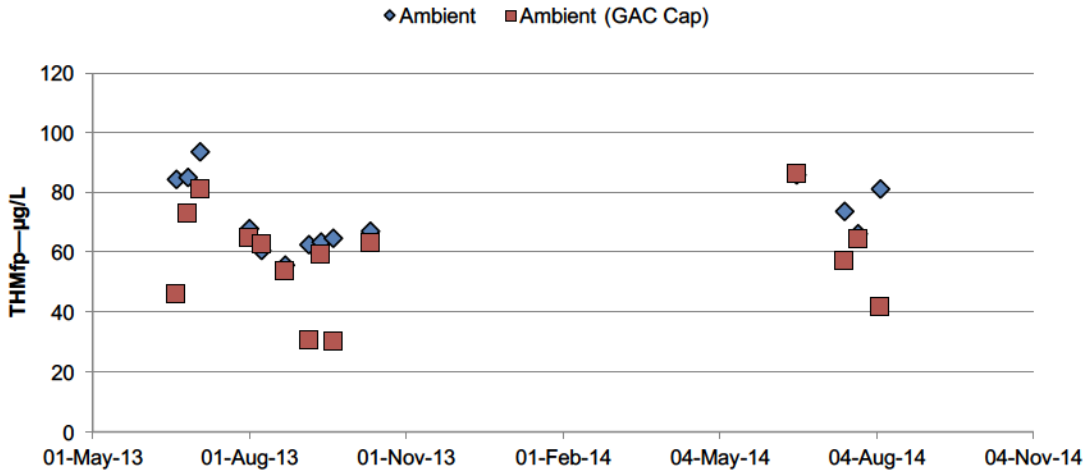

Figure A.6 THMfp in ambient and ambient (GAC-Cap) biofilters over time (T≥15°C)

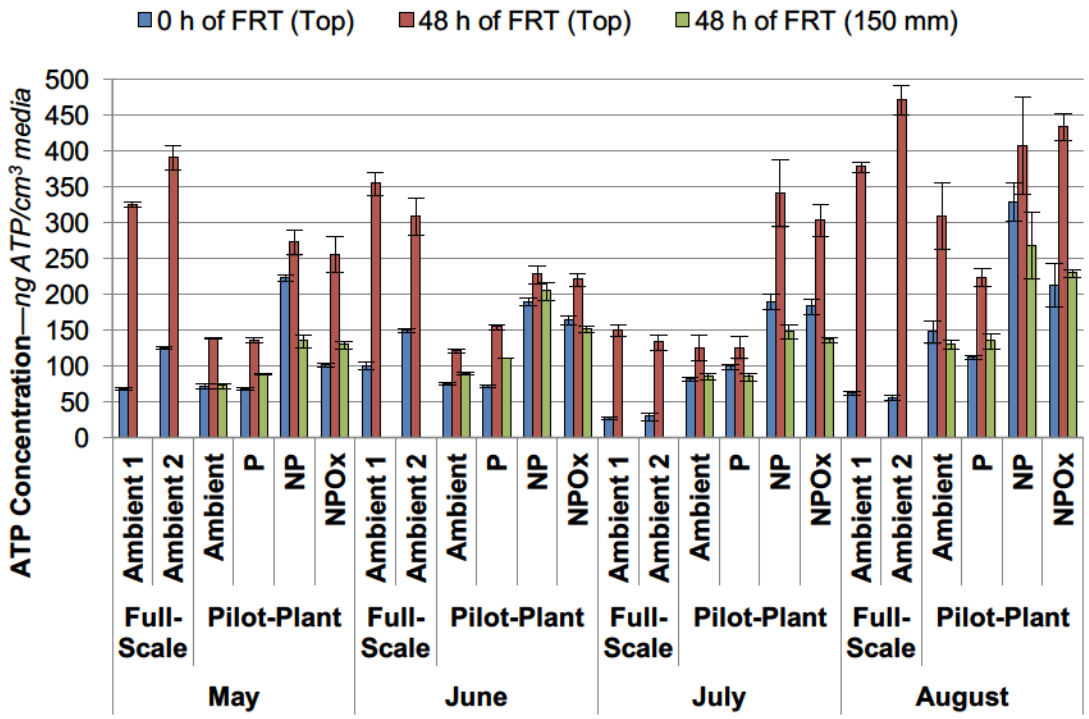

Figure A.7 ATP concentration in ambient, P-enhanced, PN-enhanced and PNOx-enhanced anthracite-sand biofilters at the start of a filter cycle and at 48 hours into a filter cycle at the surface of the media (0 mm) and 150 mm into the media. Error bars represent the standard deviation of triplicate measures.

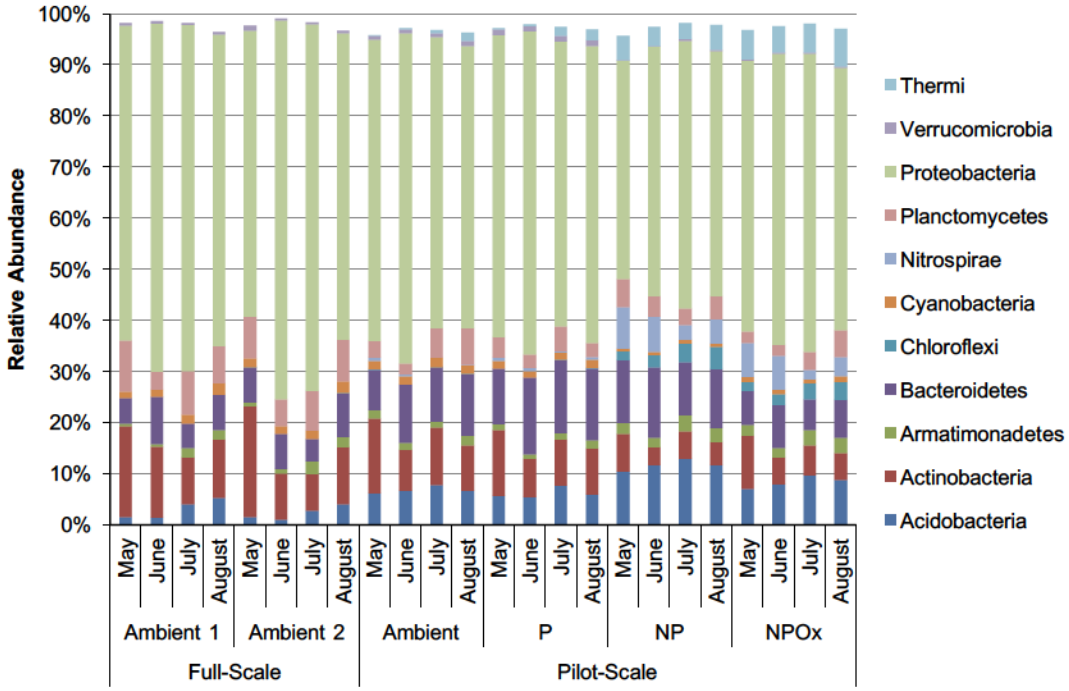

Figure A.8 Microbial community composition at the phylum level of full- and pilot-scale biofilters for sampling events in May, June, July and August. Unassigned phyla and phyla with abundance <1% in all samples were excluded.

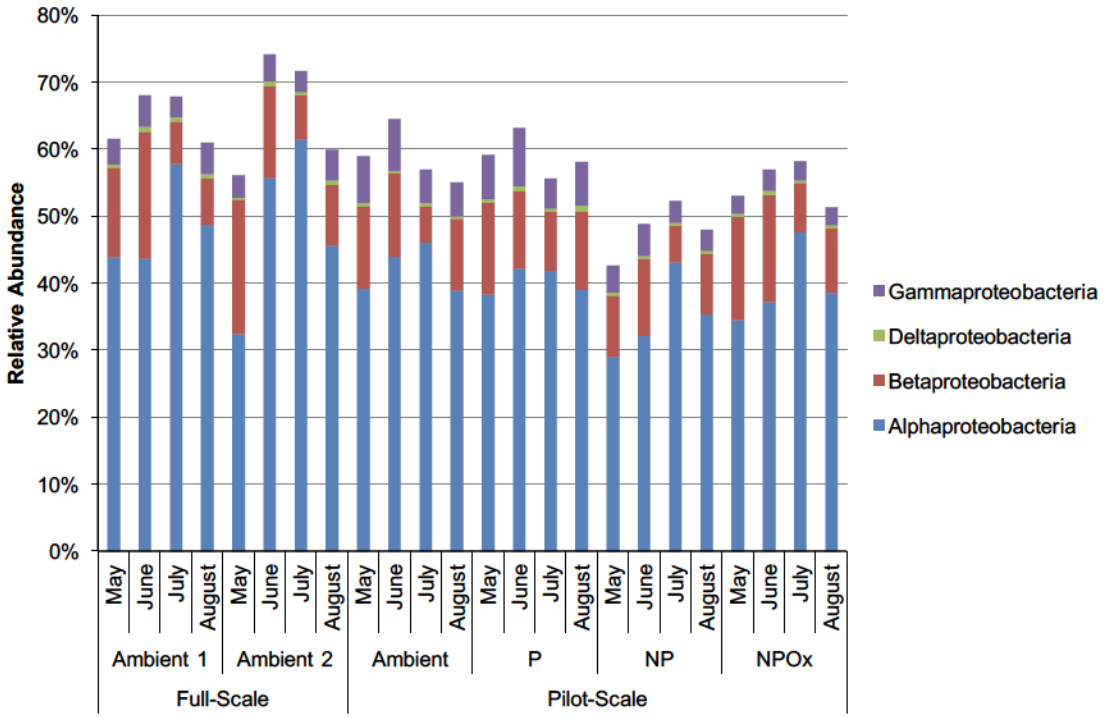

Figure A.9 Relative abundance of classes of *Proteobacteria* in the microbial communities of full- and pilot-scale biofilters for sampling events in May, June, July and August.

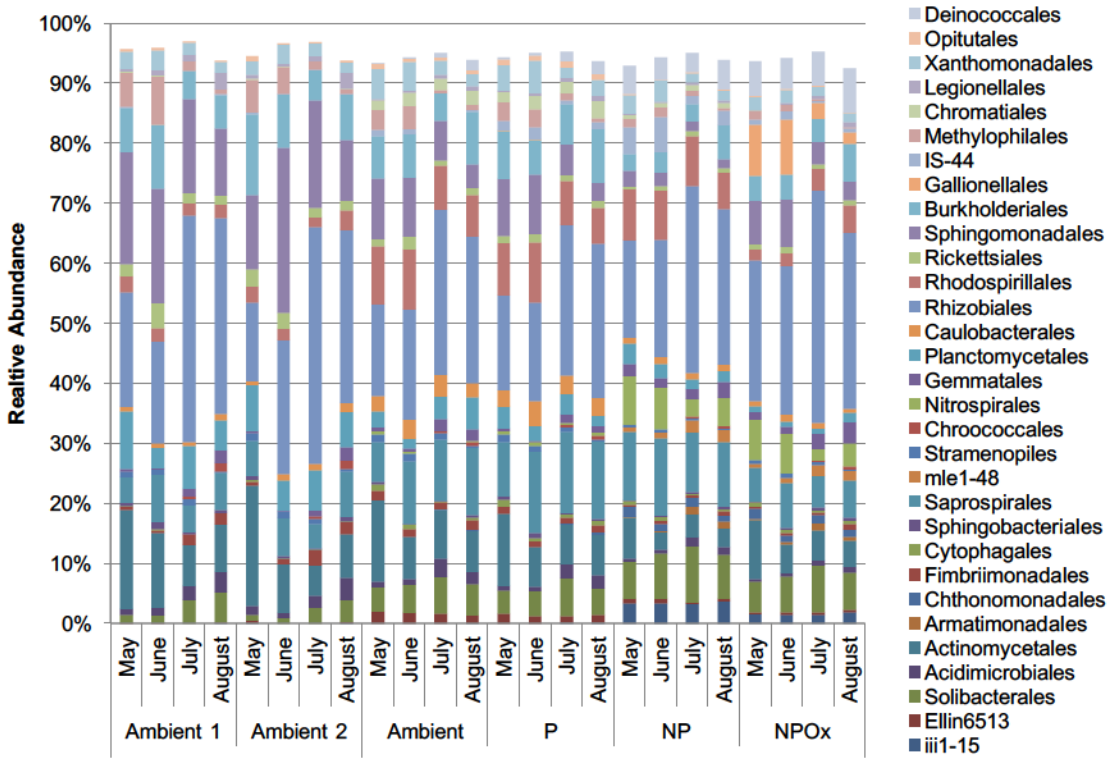

Figure A.10 Microbial community composition at the order level for full- and pilot-scale biofilters for sampling events in May, June, July and August. Unassigned orders and orders with abundance <1% in all samples were excluded.

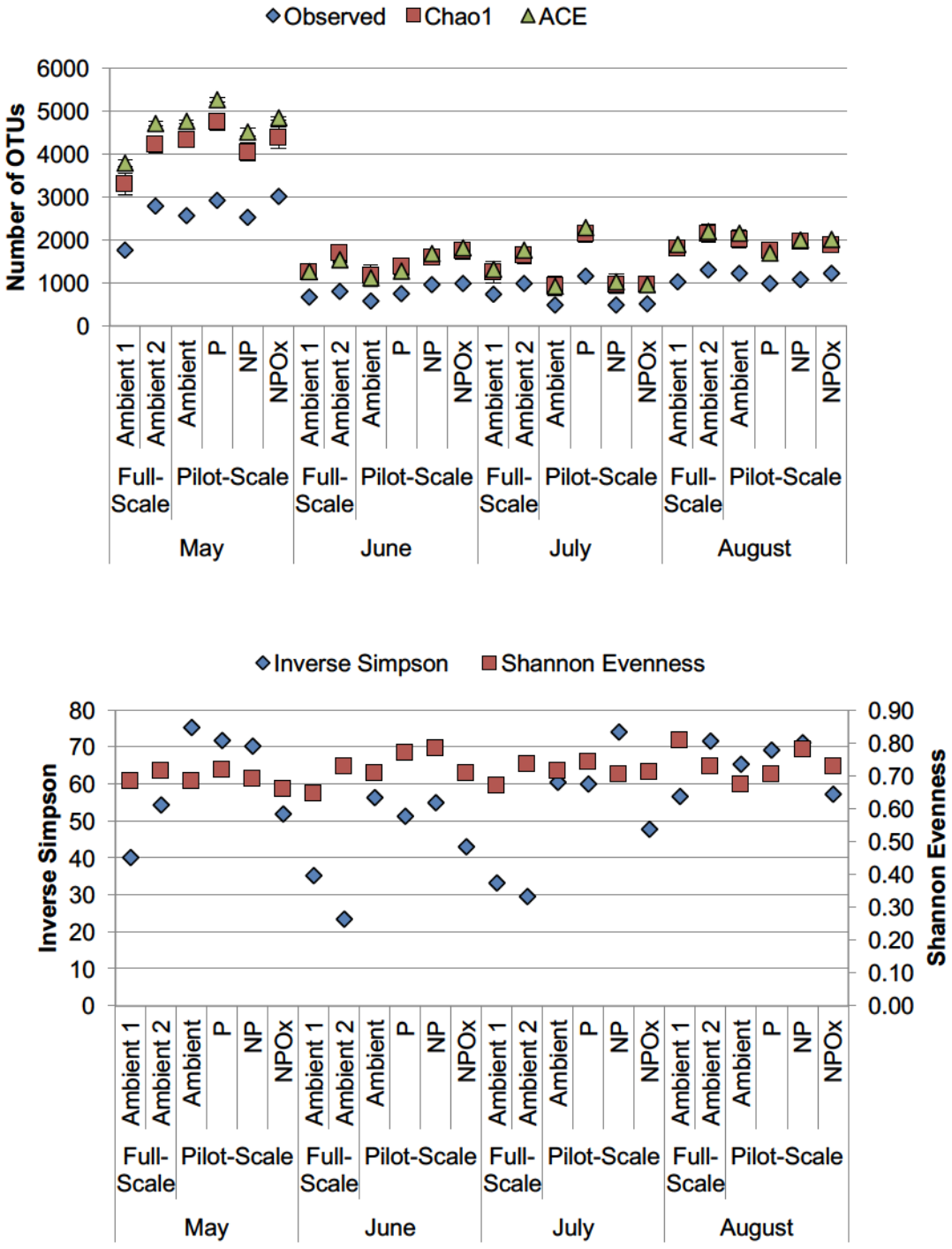

Figure A.11 Observed OTUs, Chao1 Index, and ACE for full- and pilot-scale biofilters. Indicators were calculated using the R package, Phyloseq without rarefaction.

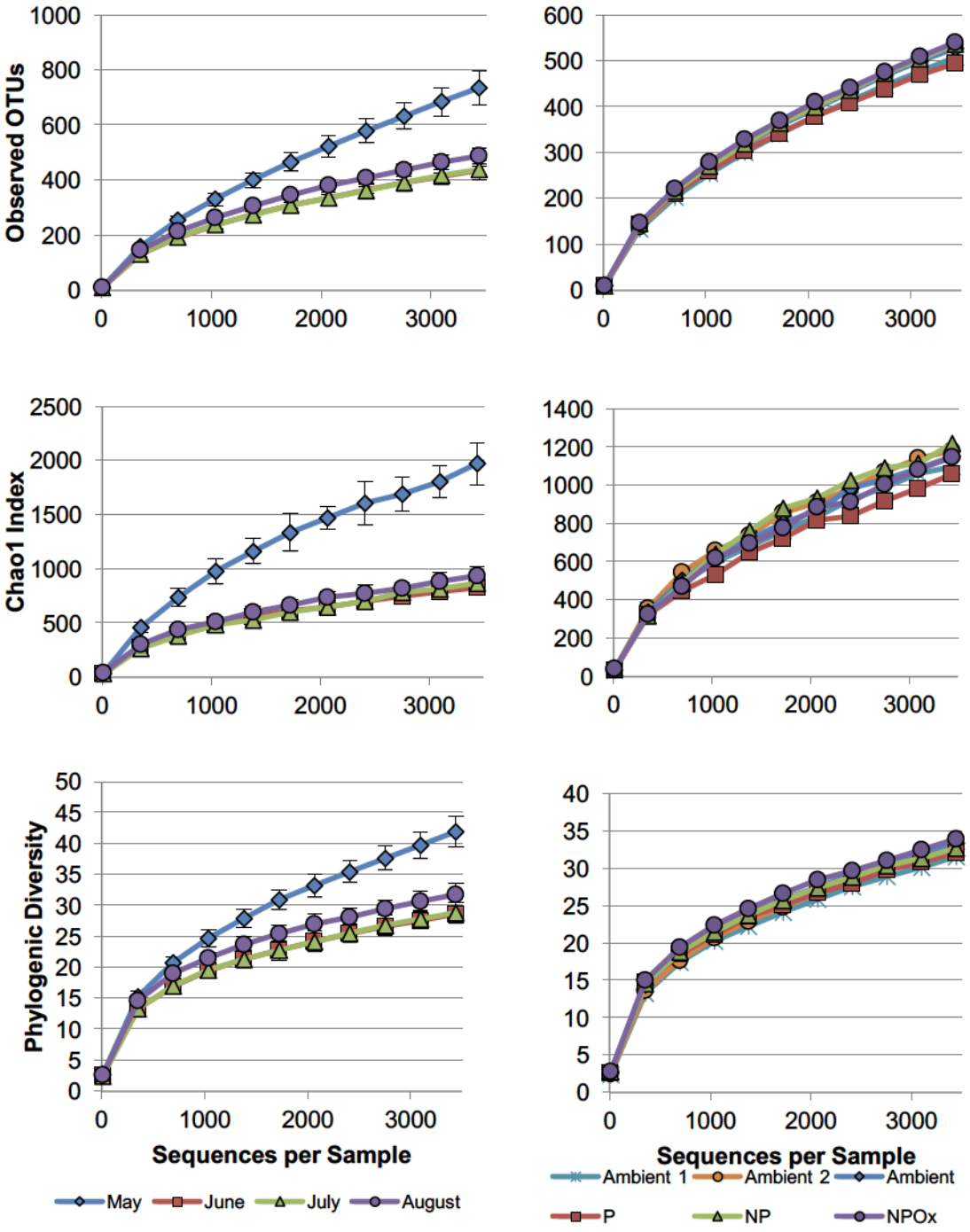

Figure A.12 Rarefaction curves for pilot-scale biofilters for a) observed OTUs, b) Chao1 index and c) phylogenic diversity. The rarefaction depth was set at 3440 sequences per sample.

APPENDIX B – Copyright Permission Letters

Chapter 2

American Water Works Association

Dedicated to the World's Most Important Resource™

December 1, 2015

Amina Stoddart
Dalhousie University
Halifax, Nova Scotia
Canada

Dear Ms. Stoddart:

We are pleased to grant a one-time, English-only use permission to reproduce the following AWWA material:

> "Full-Scale Pre-Chlorine Removal: Impact on Filter Performance and Water Quality" from *Journal AWWA* 107(12) (Dec. 2015) published by the American Water Works Association.

Reproduction is authorized for the following stated purpose:

> Inclusion in thesis for the Dalhousie University, Halifax, NS.

Please use the following citation when you credit AWWA:

> Reprinted from *Journal AWWA* 107:12 by permission. Copyright © 2015 the American Water Works Association.

Thank you for your attention to this matter.

Sincerely,

Director of Publishing
ZS/ng

6666 West Quincy Avenue
Denver, CO 80235-3098
T 303.794.7711
www.awwa.org

Chapter 3

American Water Works Association
Dedicated to the World's Most Important Resource™

6666 West Quincy Avenue
Denver, CO 80235-3098
T 303.794.7711
www.awwa.org

June 24, 2016

Amina Stoddart
Dalhousie University
Halifax, Nova Scotia
Canada

Dear Ms. Stoddart:

We are pleased to grant a one-time, English-only use permission to reproduce the following AWWA material:

> "Biomass evolution in full-scale anthracite-sand drinking water biofilters" from *Journal AWWA* (In press) published by the American Water Works Association.

Reproduction is authorized for the following stated purpose:

> Inclusion in PhD thesis for the Dalhousie University, Halifax, NS.

Please use the following citation when you credit AWWA:

> Reprinted from *Journal AWWA* by permission. Copyright © 2016 the American Water Works Association.

Thank you for your attention to this matter.

Sincerely,

Director of Publishing
ZS/ng

Chapter 4

Author reusing their own work published by the Royal Society of Chemistry

You do not need to request permission to reuse your own figures, diagrams, etc, that were originally published in a Royal Society of Chemistry publication. However, permission should be requested for use of the whole article or chapter except if reusing it in a thesis. If you are including an article or book chapter published by us in your thesis please ensure that your co-authors are aware of this.

Reuse of material that was published originally by the Royal Society of Chemistry must be accompanied by the appropriate acknowledgement of the publication. The form of the acknowledgement is dependent on the journal in which it was published originally, as detailed in 'Acknowledgements'.

Retrieved from: http://www.rsc.org/journals-books-databases/journal-authors-reviewers/licences-copyright-permissions/#reuse-permission-requests

Chapter 6

American Water Works Association
Dedicated to the World's Most Important Resource™

6666 West Quincy Avenue
Denver, CO 80235-3098
T 303.794.7711
www.awwa.org

October 16, 2014

Amina Stoddard
Dalhousie University
Halifax, Nova Scotia
Canada

Dear Ms. Stoddard:

We are pleased to grant a one-time, English-only use permission to reproduce the following AWWA material:

> "Application of Photoelectrochemical Chemical Oxygen Demand to Drinking Water" from *Journal AWWA* 106(9) (Sept. 2014) published by the American Water Works Association.

Reproduction is authorized for the following stated purpose:

> Inclusion in thesis for the Dalhousie University, Halifax, NS.

Please use the following citation when you credit AWWA:

> Reprinted from *Journal AWWA* 106:9 by permission. Copyright © 2014 the American Water Works Association.

Thank you for your attention to this matter.

Sincerely,

Director of Publishing

LH/mv